Technische Universität München
Wissenschaftszentrum Weihenstephan
Lehrstuhl für Molekulare Ernährungsmedizin

Metabolic actions of secretin

A novel non-adrenergic regulator of brown adipose tissue

Sarah-Madeleine Gabler

Vollständiger Abdruck der von der Fakultät Wissenschaftszentrum Weihenstephan für Ernährung, Landnutzung und Umwelt der Technischen Universität München zur Erlangung des akademischen Grades eines

Doktors der Naturwissenschaften

genehmigten Dissertation.

Vorsizender:		Univ.-Prof Angelika Schnieke, Ph.D.
Prüfer der Dissertation:	1.	Univ.-Prof. Dr. Martin Klingenspor
	2.	Univ.-Prof. Dr. Michael Schemann

Die Dissertation wurde am 15.09.2016 bei der Technischen Universität München eingereicht und durch die Fakultät Wissenschaftszentrum Weihenstephan für Ernährung, Landnutzung und Umwelt am 11.01.2017 angenommen.

Contents

Abbreviations

129/S1	mouse strain 129S1/SvEvTac
129/S6	mouse strain 129S6/SvEvTac
4-AAP	4-aminoantipyrine
AC	adenylyl/adenylate cyclase
ACOD	acyl-CoA-oxidase
ACS	acyl-CoA-sythetase
ADP	adenosine diphosphate
ANOVA	analysis of variance
anti A	antimycin A
AR	adrenergic receptor
ARC	arcuate nucleus of hypothalamus
ATGL	adipose triglyceride lipase
ATP	adenosine triphosphate
AUC	area under the curve
β-3-AR	β-3-adrenergic receptor
BAT	brown adipose tissue
BMI	body mass index
BMR	basal metabolic rate
bp	base pairs
BSA	bovine serum albumin
BW	body weight
C57BL/6J	mouse strain C57BL/6J
$CaCl_2$	calcium chloride
cAMP	cyclic adenosine monophosphate
cAMP-RE/CRE	cAMP-response element
CD	control diet
cDNA	complementary deoxyribonucleic acid
CoA	coenzyme A
CRE	cAMP response element
CREB	cAMP response element binding protein
C_t value	threshold cycle value
DAP	dihydroxyacetone phosphate
DIO	diet induced obesity
DIT	diet induced thermogenesis
DMEM	dulbecco's modified eagle medium
DNA	deoxyribonucleic acid
dsDNA	double-stranded deoxyribonucleic acid
EC_{50}	half maximal effective concentration
ESPA	sodium N-ethyl-N-(3-sulfopropyl) m-anisidine
FBS	fetal bovine serum
FCCP	carbonyl cyanide-p-trifluoromethoxyphenylhydrazone
FGF21	fibroblast growth factor 21
G-1-P	glycerol-1-phosphate

GIP	glucose-dependent insulinotropic polypeptide
GLP-1	glucagon-like peptide-1
GLP-2	glucagon-like peptide-2
GPCR	G-protein coupled receptor
GPO	glycerol phosphate oxidase
GRF/GHRH	growth hormone-releasing hormone/somatoliberin
gWAT	gonadal white adipose tissue
H_2O_2	hydrogen peroxide
HBSS	hank's balanced salt solution
HEK293	human embryonic kidney 293
HFD	high fat diet
HP	heat production
HSL	hormone-sensitive lipase
IBMX	3-isobutyl-1-methylxanthine
i.c.v.	intracerebroventricular
i.p	intraperitoneal
ISO	isoproterenol
iWAT	inguinal white adipose tissue
KO	knockout
MEHA	3-methyl-N-ethyl-N-(β-hydroxyethyl)-aniline
mRNA	messenger ribonucleic acid
NaCl	sodium chloride
NEFA	non-esterified fatty acid
OCR	oxygen consumption rate
oligo	oligomycin
p38 MAPK	p38 mitogen activated protein kinase
PACAP	pituitary adenylate cyclase-activating polypeptide
PBS	phosphate-buffered saline
PCR	polymerase chain reaction
PGC-1α	peroxisome proliferator-activated receptor γ coactivator 1-α
PHM	peptide histidine methionine
PKA	protein kinase A
PLuc	*photinus* luciferase
POD	peroxidase
POMC	proopiomelanocortin
PPARγ	peroxisome proliferator-activated receptor γ
PVN	paraventricular nucleus of hypothalamus
qRT-PCR	quantitative real-time PCR
RER	respiratory exchange ratio
RLuc	*renilla* luciferase
Rosi	rosiglitazone
rpm	rotations per minute
RT	reverse transcriptase
SB	SB203580 (p38 inhibitor)
SCT	secretin

SCT	human gene for secretin
sct	murine gene for secretin
SCTR	secretin receptor
SCTR	human gene or mRNA for secretin receptor
sctr	murine gene or mRNA for secretin receptor
SCTR KO	secretin receptor knockout
SD	standard deviation
SDA	specific dynamic action
T3	triiodothyronine
TFIIB	transcription factor IIB
UCP1	uncoupling protein 1
ucp1	murine gene or mRNA for ucp1
UCP1 KO	uncoupling protein 1 knockout
VIP	vasoactive intestinal polypeptide
WAT	white adipose tissue
WT	wildtype

1. Abstract

In this thesis, the effect of the classical gut hormone secretin on adipose tissue physiology has been investigated *in vitro* and *in vivo*. Secretin is secreted by the first section of the intestine from cells of the duodenum. The release of the hormone is triggered by dropping pH in the intestine following the ingestion of a meal. Secretin is known to mediate functions of digestion, like the stimulation of pancreatic secretion, release of bicarbonate or the inhibition of gastric motility.

The G-protein coupled secretin receptor has been found to be markedly expressed in brown and also in white adipose tissues. Actions of secretin at both types of fat tissues were investigated in this thesis. The mitochondrial respiration in primary brown adipocytes was acutely activated, when cells were stimulated with secretin. In line with cell culture findings, mice intraperitoneally injected with secretin showed an increased energy expenditure measured with indirect calorimetry. For both, the effect was dependent upon the uncoupling protein 1, which is specifically expressed in brown adipose tissue and uncouples the respiratory chain of those cells to generate heat. In an uncoupling protein 1 knockout system, whether cells nor mice increased respiration following a stimulation with secretin. Next to the acute induction of respiration, a stimulation with secretin was furthermore able to increase the expression of the uncoupling protein 1 in white and brown adipocytes.

In further experiments of this thesis it was shown, that the expression, and thereby sensitivity of the secretin receptor at adipose tissues is regulated by environmental factors. Mice adapted to an ambient temperature of 4 °C exhibited a strongly activated brown adipose tissue activity and increased capacity, while the expression of the secretin receptor and thus the sensitivity for stimulation with secretin was strongly decreased. In contrast, when mice were fed a high-fat diet for several weeks, the expression of the secretin receptor was increased.

The regulation of the secretin receptor expression at adipose tissue suggests a regulatory role for secretin, that is not related to its heating function to defend body temperature. Since a transient anorexigenic effect of intraperitoneally injected secretin in mice was found in a further experiment, it is hypothesised that the hormone exhibits a thermoregulatory function for the control of food intake. To check this for hypothesis, further experimental observations will be necessary.

2. Zusammenfassung

In dieser Arbeit wurde der Effekt des Hormones Secretin auf verschiedene Fettgewebe sowohl *in vivo*, als auch *in vitro* untersucht. Secretin wird nach Nahrungszufuhr durch sinkenden pH im ersten Darmabschnitt aus Zellen des Duodenum ausgeschüttet und vermittelt in seiner klassischen Funktion die Stimulation der Pankreas- und Bikarbonatsekretion zur Unterstützung der Verdauung.

Da der G-Protein gekoppelte Rezeptor für Secretin sowohl stark am Braunen (Heizgewebe) als auch etwas schwächer am Weißen Fettgewebe (zur Lagerung von Fetten) exprimiert wird, wurden die Secretin-Wirkungen in verschiedenen Versuchsansätzen an diesen Geweben betrachtet. Die Mitochondrien der Braunen Fettzellen zeigen durch Stimulation mit Secretin eine akute Aktivierung, messbar durch einen gesteigerten Sauerstoffverbrauch, sowohl in isolierten Adipocyten, als auch in lebenden Mäusen. Der Effekt ist abhängig vom transmembranen *uncoupling protein 1* (UCP1), welches im Braunen Fettgewebe die Atmungskette entkoppelt, um Hitze zu erzeugen. In einem UCP1 *knockout*-System konnte durch eine Stimulation mit Secretin weder in Zellkultur, noch in Mäusen, der Sauerstoffverbrauch gesteigert werden. Neben den Effekten am Braunen Fett hat Secretin in der Zellkultur auch eine bräunende Wirkung auf isolierte Weiße Adipozyten, was sich in einer gesteigerten Expression von *ucp1* widerspiegelt.

In weiteren Versuchen konnte im Laufe dieser Arbeit gezeigt werden, dass die Expression des Secretinrezeptors am Fettgewebe, und damit die Sensitivität des Gewebes für die Aktivierung durch Secretin, stark durch Umwelteinflüsse reguliert wird. Werden Mäuse für einige Zeit in Kälte gehalten und das Braune Fettgewebe als Heizgewebe besonders aktiviert, so sinkt sowohl die Expression des Secretinrezeptors am Gewebe, als auch die messbare Stimulierbarkeit des Braunen Fettgewebes nach Secretin-Injektion. Werden die Mäuse hingegen für einige Zeit mit einer Hochfett-Diät gefüttert, so steigert sich die Expression des Secretinrezeptors am Braunen Fettgewebe. Diese Regulation lässt vermuten, dass durch das Dünndarmhormon nicht die klassische Heizfunktion zur Verteidigung der Körpertemperatur des Braunen Fettgewebes, sondern andere Aufgaben gesteuert werden. Da eine periphere Injektion von Secretin auch einen hemmenden Effekt auf die Nahrungsaufnahme verursacht, wäre die Steuerung thermoregulatorischer Nahrungsaufnahme eine mögliche Regulationsfunktion des Braunen Fettgewebes durch Secretin. Zur Überprüfung der Hypothese sind weiterführende experimentelle Untersuchungen notwendig.

3. Introduction

Thermogenesis in brown adipose tissue (BAT) consumes an appreciable amount of energy and is thereby relevant for energy homeostasis in the body. Therefore, the regulation of brown fat thermogenesis is a promising target in the field of obesity research. Known regulators of this tissue are for example mediators of the sympathetic nervous system. So far, signals from the gastrointestinal tract have not been brought in the context. In the present thesis, the role of secretin (SCT) in the regulation of BAT thermogenesis has been investigated.

3.1. Functions and actions of the gut hormone secretin

SCT is the first peptide hormone that has been discovered. It was detected by William Bayliss and Ernest Starling in 1902, who found out that the release of pancreatic secretion after food intake is not mediated by a nervous innervation, but by a chemical substance formed in the mucous membrane of the upper parts of the small intestine. The hormone was named after its secretion stimulating function on the pancreas: secretin (Bayliss & Starling 1902).

3.1.1. Secretin

SCT has been purified by *Erik Jorpes* and *Viktor Mutt* in 1961 (Jorpes & Mutt 1961), which also described the entire amino acid sequence of the porcine SCT (Mutt et al. 1970). The sequence consists of 27 amino acids and the human SCT protein exhibits a molecular weight of 3055 Dalton (Carlquist et al. 1985). SCT is synthesised as a preprohormone, which is processed by enzymes like carboxypeptidase to the mature protein. It has at both ends, N-terminal and C-terminal end, additional peptides that are cleaved before the mature peptide is amidated (Mutt et al. 1965, Bonetto et al. 1995) at the C-terminal (Fig. 1). This amid is not required for biological activity, while a free histidine at the N-terminal is crucial (Gafvelin et al. 1990).

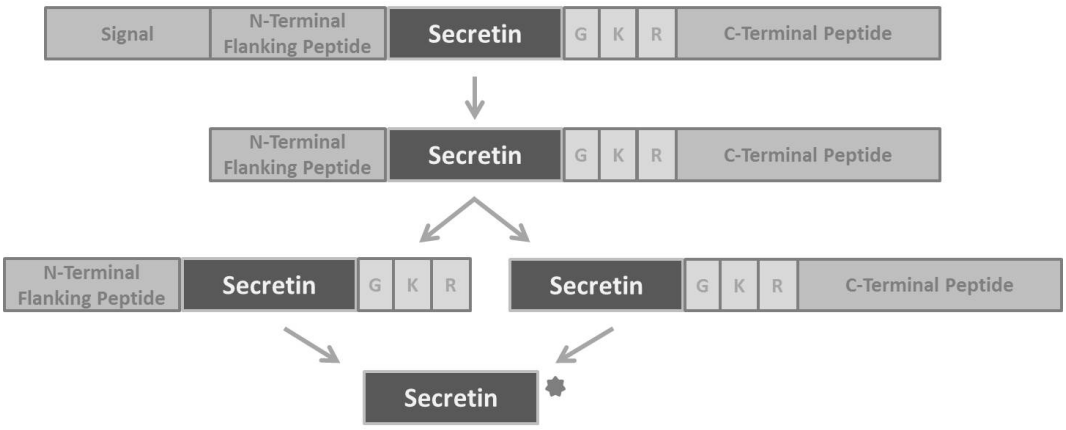

Fig. 1: **Cleavage of SCT Prohormone.** Reproduced from Bonetto et al. 1995
There are two processing pathways for preprosecretin known. The star indicates amidation of the last valin in the mature SCT. G (glycin), K (lysine) and R (arginine) are one-letter codes for amino acids. N-terminally extended forms of this pathway have been shown to exhibit a reduced bioactivity.

The sequence of SCT is highly conserved between species on protein level (Chey & Chang 2003). The human SCT shows 88.9% identity to the murine and also the the rat SCT. The murine and the rat SCT exhibit 92.6% identity among each other (Fig. 2).

Pig, Cow, Sheep	HSD	GTF	TSE	LSR	LRD	SAR	LQR	LLQ	GLV
Dog	HSD	GTF	TSE	LSR	LR**E**	SAR	LQR	LLQ	GLV
Rat	HSD	GTF	TSE	LSR	L**Q**D	SAR	LQR	LLQ	GLV
Human	HSD	GTF	TSE	LSR	LR**E**	**G**AR	LQR	LLQ	GLV
Mouse	HSD	G**M**F	TSE	LSR	LRD	SAR	LQR	LLQ	GLV

Fig. 2: **Alignment for amino acid sequence of SCT for various species.**
Divergent single letter code is marked in bold.

SCT belongs to the pituitary adenylate cyclase-activating polypeptide (PACAP)/glucagon superfamily, which

also contains:

PACAP, glucagon, glucagon-like peptide-1 (GLP-1), glucagon-like peptide-2 (GLP-2), GH-releasing hormone (GRF/Somatoliberin/GHRH), vasoactive intestinal polypeptide (VIP), peptide histidine methionine (PHM) and glucose-dependent insulinotropic polypeptide (GIP). The nine bioactive members of the superfamily are encoded in six genes that have a similar gene organization (Sherwood et al. 2000). All members of the family consist of 22-47 amino acid residues, are synthesised by endocrine cells, neurons and/or immune cells and show structural similarities (Couvineau & Laburthe 2012). The hormones of the family are mostly expressed in the gut and the majority of them stimulate the release of insulin in response to a meal (incretin effect). All hormones of the superfamily except for GIP are furthermore expressed in the brain and several of them in pancreas and testis (Sherwood et al. 2000). In an alignment, SCT shows highest identity to glucagon with an value of 41.1% followed by 37.0% identity with PACAP and PHM and 36.7% identity with GLP-1 (Fig. 3).

```
GIP        YAE GTF ISD YSI AMD KIH QQD FVN WLL AQK GKK NDW KHN ITQ  -
Glucagon   HSQ GTF TSD YSK YLD SRR AQD FVQ WLM NT-  --  --  --  --  -
GLP-2      HAD GSF SDE MNT ILD NLA ARD FIN WLI QTK ITD  --  --  --  -
GLP-1      HAE GTF TSD VSS YLE GQA AKE FIA AWL VKG  R-  --  --  --  -
SCT        HSD GTF TSE LSR LRE GAR LQR LLQ GLV  --  --  --  --  --  -
PACAP      HSD GIF TDS YSR YRK QMA VKK YLA AVL  --  --  --  --  --  -
VIP        HSD AVF TDN YTR LRK QMA VKK YLN SIL  N-  --  --  --  --  -
PHM        HAD GVF TSD FSK LLG QLS AKK YLE SLM  --  --  --  --  --  -
GRH        YAD AIF TNS YRK VLG QLS ARK LLQ DIM SRQ QGE SNQ ERG ARA RL
```

Fig. 3: **Alignment for amino acid sequence of the PACAP-family member proteins** (performed with *workbench.sdsc.edu*)

A conservation of strong groups is marked with a blue box, a conservation of weak groups is marked with a cyan box and a conservation of fully residues is marked with a green box.

On a genetic level *SCT* is located on chromosome 11 in humans and on chromosome 7 in mice. For both species, the gen spans altogether four exons, while the active protein is encoded by a single exon. The hormone-coding region is highly conserved among the *SCT* genes of various species (Whitmore et al. 2000). *SCT* transcript levels were detected in human spleen, testis, brain and small intestine with highest levels found in the duodenum and markedly decline towards jejunum and ileum (Whitmore et al. 2000). In rats, high levels of *SCT* mRNA were also found in lung, heart, and kidney (Ohta et al. 1992). In these organs *SCT* was not detectable in humans.

3.1.2. Secretin receptor

SCT specifically binds to the secretin receptor (SCTR), which was successfully cloned and expressed in 1991 (Fremeau et al. 1983, Robberecht et al. 1988, Ishihara et al. 1991). The SCTR belongs to the Family B or class II of G-protein coupled receptors (GPCRs). Next to the receptors of other PACAP superfamily members, furthermore the receptors for calcitonin, corticotropin releasing factor (CRF), and parathyroid hormone (PTH) belong to this class (Sherwood et al. 2000, Emery et al. 2015, Segre & Goldring 1993). The human SCTR contains 440 amino acids, has a putative hydrophobic leader peptide of 22 amino acids, a hydrophilic amino-terminal extracellular domain with 122 amino acids and 7 transmembrane domains. The

SCTR therefore exhibits 3 exo- and 3 endoloops (254 amino acids). The cytoplasmic tail has 42 amino acids at the carboxyl-terminal end (Fig. 4). The N-terminal extracellular domain and the first exoloop together form the ligand binding site (Siu et al. 2006, Holtmann et al. 1995, Vilardaga et al. 1995, Vilardaga et al. 1996).

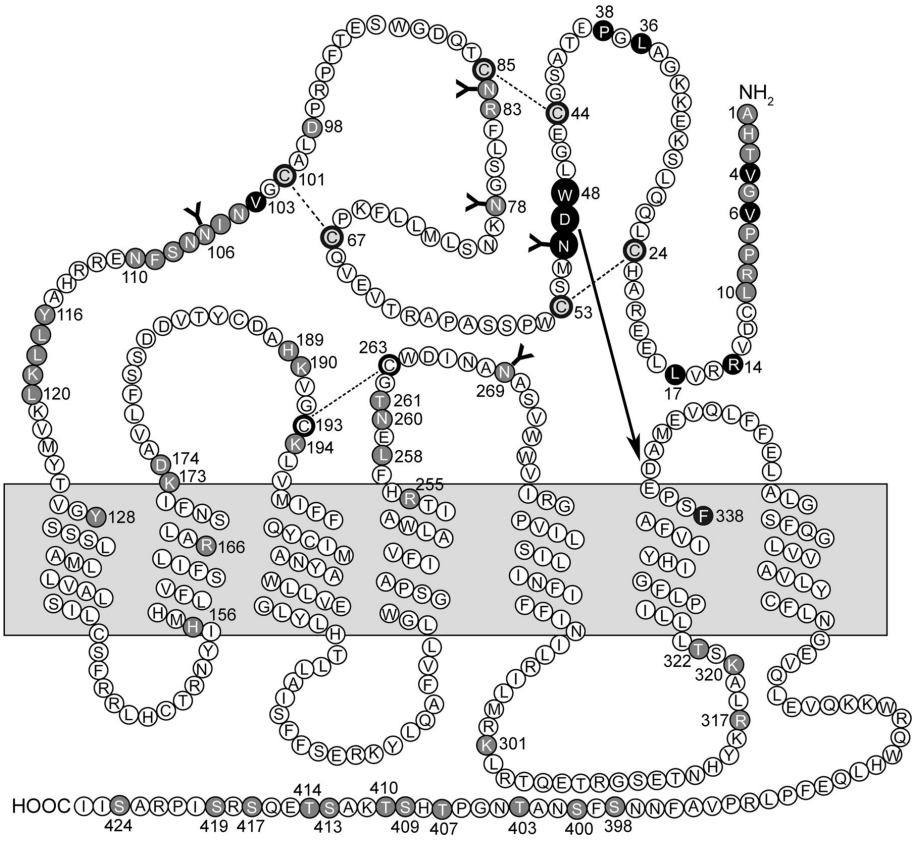

Fig. 4: **Schematic picture of the rat SCTR.** (Miller et al. 2007)
The SCTR has seven transmembrane domains (grey background). The extracellular amino-terminal tail exhibits a glycosylated (forked symbols indicate potential sites of glycosylation) and disulfide bond (dotted lines). Intracellular a carboxyl-terminal tail is found. A disulfide bond linkes cysteines within the first and second extracellular loops, and another site of glycosylation in the second extracellular loop. Potential sites of phosphorylation and residues demonstrated to be functionally important, are illustrated as filled grey circles. The endogenous agonist sequence (WDN) within the N-terminal region is highlighted in large filled black circles (arrow points towards its proposed site of action).

The binding of SCT to its receptor leads to the activation of an intracellular secondary messenger system, which triggers cellular processes (Fig. 5). Like all members of the B family of GPCRs, the SCTR activates the adenylyl cyclase (AC) via the G_s protein. This leads to an accumulation of cyclic adenosine monophosphate (cAMP) (Gether 2000, Chow 1995) and finally the activation of protein kinase A (PKA). Moreover, the SCTR is also coupled to a G_q unit, which is activated when there are high concentrations of SCT. This part of the pathway stimulates inositol triphosphate (IP 3), intracellular calcium and diacylglycerol (DAG) (Trimble et al. 1986, Trimble et al. 1987, Neves et al. 2002).

The SCTR is expressed in pancreatic cells (Ulrich et al. 1998), in cholangiocytes of the liver (Alpini et al. 1994), in parts of the stomach (Gespach et al. 1981, Bawab et al. 1988) and the intestine and colon (Andersson et al. 2000). The SCTR is expressed in several regions of the brain like the cerebellum, the cortex, thalamus, striatum, hippocampus, hypothalamus, nucleus of the solitary tract (NTS) and at moderate levels in midbrain, medulla and pons (Yung et al. 2001, Fremeau et al. 1983, Koves et al. 2002). It can furthermore be detected in other regions of the body like kidney, white adipose tissue, heart and lung (Ishihara et al. 1991, Christophe

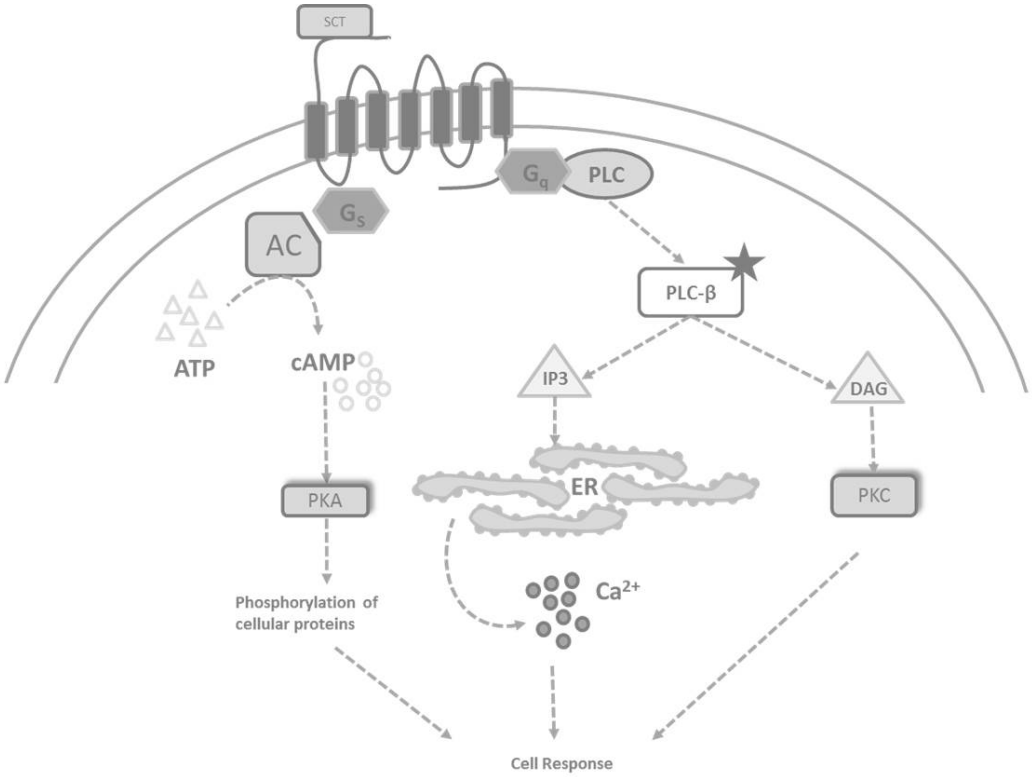

Fig. 5: **Signalling of the SCTR.** Reproduced from Siu et al. 2006
SCT binds extracellularly to the SCTR and activates via the G_s-unit the adenylyl cyclase (AC), which converts ATP into cAMP. The released cAMP activates the protein kinase A (PKA), which leads to the phosphorylation of target proteins. The second subunit of the receptor, the G_q-unit is able to activate the phosphoinositide phospholipase C (PLC), which stimulates inositol triphosphate (IP 3) leading to a cell response via calcium signalling. The PLC can also activate diacyl-glycerol (DAG) leading to a stimulation of protein kinase C (PKC).

et al. 1981, Charlton et al. 1986, Miegueu et al. 2013). The wide distribution of SCTR expression indicates a large spectrum of biological functions of SCT. Further information on *sctr* expression in mice can also be found in the BIO-GPS data in the supplement (Fig. 31).

3.1.3. Functions of SCT

SCT has been discovered as stimulator of pancreatic secretion after food intake (Bayliss & Starling 1902). For decades of research, it has been spotted as a gut hormone with primarily digestion related functions. Not until the last forty years, SCT has also been noticed for its actions as a neuropeptide (Mutt et al. 1979).

3.1.3.1. SCT as a regulator of digestion and gut function

SCT is primarily released by so called S-cells in the duodenum and also in the jejunum of most species (Usellini et al. 1984, Usellini et al. 1990). The most important stimulus for SCT relase in the gut is the decrease in duodenal pH by postprandial exposition to acidified meals and a fatty acid load in the gut (Joffe et al. 1975, Rhodes et al. 1976, Draviam et al. 1991, Shiratori et al. 1989). In general, fasting plasma levels of SCT are considered to be rather low in humans (4-5 pg/ml) with strongest increase when the duodenal pH falls below 4.5 in the postprandial period (7-8 pg/ml) (Chey et al. 1978, Kim et al. 1979). Published plasma

SCT level range from about 10 pg/ml (fasted) to 25-55 pg/ml (fed) in dogs (Kim et al. 1979) and of 3-5 ng/ml (Miegueu et al. 2013) in mice, which is more than 60-fold higher than in other species.
An increase in plasma SCT levels leads to the stimulation of pancreatic secretion (Otsuki et al. 1981, Friedman & Snape 1947, Christodoulopoulos et al. 1961). SCT has been shown to stimulate bile and bicarbonate secretion in the duodenum (Isenberg et al. 1984), in pancreatic (Christodoulopoulos et al. 1961) and in biliary (Jones et al. 1971) ducts, as well as gastric pepsin secretion (Sanders et al. 1983) to neutralise gastric acid and facilitate digestion in the gut (Afroze et al. 2013). Furthermore, SCT inhibits gastric acid secretion (Jin et al. 1994, Walton 2009), food stimulated gastrin release (Straus et al. 1975) as well as motility in gut (Jin et al. 1994, Lu & Owyang 2009, Lu & Owyang 1995, Steiner et al. 1993) and the upper small intestine and reduces lower esophageal sphincter pressure (Andersson et al. 2000, Hubel 1972).
In addition, it is a matter of controversial discussion, if SCT is able to exhibit incretin actions. A reliable conclusion of the effect of SCT on the secretion of insulin can not be drawn from published papers. An incretin effect of SCT seems more likely in mice and rats than in humans suggested by published results (Shima et al. 1978, Ahren & Lundquist 1981, Schaffalitzky de Muckadell 2001, Kraegen et al. 1970, Kofod 1986).

3.1.3.2. SCT actions in the central nervous system

Next to the digestive system SCT and also the SCTR were discovered in wide parts of the brain (O'Donohue et al. 1981, Charlton et al. 1981, Mutt et al. 1979). Four major roles of SCT as a neuropeptide have been explored so far:

Control of social behaviour, spatial learning and autistic disorders
SCT and SCTR expressing cells were detected in the hippocampus (Yamagata et al. 2008, Nishijima et al. 2006), which is well-known to be responsible for social behaviour, memory, and spatial learning. Several years it was discussed that intravenous (i.v.) injections of SCT could improve eye contact, alertness, and expressive language ability in children with autistic spectrum disorders (Horvath et al. 1998). Subsequent studies were not able to confirm these effects (Sandler et al. 1999, Owley et al. 1999, Dunn-Geier et al. 2000, Coniglio et al. 2001).
In animal trials, however, SCTR knockout (KO) mice showed impaired social interaction (Nishijima et al. 2006) and diminished spatial learning (Jukkola et al. 2011).

Motor coordination and motor learning
In mice, that received an intracerebroventricular (i.c.v.) injection of SCT, a reduced open-field activity was observed (Charlton et al. 1983). Additionally, in SCTR KO mice deficits in motor learning on rotarod were reported (Nishijima et al. 2006). A mouse model with a cerebellar Purkinje neuron specific SCT KO revealed that the Purkinje-derived SCT-SCTR axis is essential for motor behavioural controls (Zhang et al. 2014).

Stimulation of water drinking and fluid homeostasis
In 2009, hypothalamic SCT has been found to be released from posterior pituitary following hyperosmolality stress to stimulate vasopressin secretion (Chu et al. 2009). Further studies suggested that the water intake control by angiotensin II is dependent on SCT–SCTR-pathways (Lee et al. 2010).

Suppression of food intake

Since about forty years, possible anorexigenic effects of SCT have been tested in several animal models. There was no suppression of food intake after intraperitoneal (i.p.) injection of SCT found in rats (Glick et al. 1971, Gibbs et al. 1973). However, *Grovum* showed a decreased appetite in fasted sheep after i.v. injection (Grovum 1981).

In 2011, *Cheng* postulated a food intake inhibiting effect for SCT via i.c.v. (1 nm) or i.p. (5 nm) injection in mice that were fasted for 18 hours (Cheng et al. 2011). It was suggested that SCT expression in the appetite-related paraventricular nucleus (PVN) (Chu et al. 2006) and *sct* and *sctr* mRNAs in the area postrema (AP) and the NTS (Tay et al. 2004) are crucial for transmitting peripheral SCT-related satiation signals to the hypothalamus. In a further study, it was shown that a bilateral vagotomy blocks the anorexigenic effect of peripherally injected SCT. Hence, it was hypothesised that the peripheral SCT is mediated via vagal afferences to proopiomelanocortin (POMC) neurons within the hypothalamic arcuate nucleus. The POMC-neurons are activated by the SCTR and release the POMC-product alpha-MSH, which signals downstream to the PVN and is known to trigger an anorexigenic signal (Chu et al. 2013, Cheng et al. 2011).

An additional study by *Sekar* and *Chow* in 2014 showed that SCTR KO mice exhibit a reduced susceptibility towards diet-induced obesity (DIO). This action is conflicting to the anorexigenic effect found for SCT. The DIO-reducing activity of SCT in that paper was not suggested to be mediated centrally, but by a decreased absorption of fat in the intestine caused by reduced transcription levels of cluster of differentiation 36, which is described as a key regulator of fat absorption (Sekar & Chow 2014b).

3.1.3.3. SCT actions on adipocytes and fat tissues

Lipolysis is generally induced by the sympathetic nervous system, which mediates its action by β-adrenergic agonists, particularly in white adipose tissue. However, it has been known for decades that also SCT exhibits lipolytic action (Butcher & Carlson 1970). Especially under conditions of extreme starvation, elevated SCT and also glucagon levels increase the availability of free fatty acids to provide fuel for the metabolism in mice (Sekar & Chow 2013), dogs (Manabe et al. 1987) and humans (Stout et al. 1976). Further functions of SCT have been studied in preadipocytes as well as in differentiating and mature adipocytes, showing that the mitochondrial activity in preadipocytes was increased after incubation with SCT for 25 hours. A chronic treatment with SCT increased free fatty acid uptake and triglyceride accumulation in mature adipocytes as well as the expression of PPARγ (Miegueu et al. 2013).

3.2. Brown adipose tissue and browning of white adipose tissue

3.2.1. BAT and its functions as a part of the adipose organ

The adipose organ in mammals consists of white adipose tissue (WAT) and brown adipose tissue (BAT). The WAT is a storage organ for excess calories in form of fat and is composed of several subcutaneous and visceral depots (Cinti 2005). It has a capacity for buffering nutrient availability, but also the feasibility to communicate to metabolically active organs via adipokines like leptin (Peirce et al. 2014, Scherer 2006, Zhang et al. 1994, Renold et al. 1950).
BAT appears predominantly in the neck region (interscapular) of small rodents and infants, but can be found in all mammals (Cannon & Nedergaard 2004). BAT is a heating organ. The thermoregulatory thermogenesis is generally triggered by cold exposure (Cannon & Nedergaard 2004, Smith 1961). For the execution of its task, BAT cells differ eminently from WAT cells. Brown fat cells, in contrast to white fat cells, are multilocular, exhibit considerably more mitochondria and express uncoupling protein 1 (UCP1), which is located in the inner membrane of mitochondria and uncouples respiration for the generation of heat (Lean et al. 1983, Aquila et al. 1985, Heaton et al. 1978). The thermogenic function is supported by dense innervation and a extensive vascularisation which gives the tissue, together with the high density of mitochondria and thereby cytochrom C, a reddish brown colour.

When adrenergic receptors (AR) in the BAT are stimulated, the activation of cAMP-dependent PKA leads to the induction of lipolysis by phosphorylation of the hormone sensitive lipase (HSL). The free fatty acids released by lipolysis counteract the UCP1-inhibitory cytosolic purine nucleotides. Activated UCP1 uncouples the adenosine triphosphate (ATP) synthesis from the respiratory chain and produces heat (Klingenspor 2003). The acute activation of BAT for the production of heat and also the recruitment process to increase heating capacity are under the control of norepinergic regulation of the sympathetic nervous system. There are three subtypes of ARs (α1-, α2- and β-ARs). For the mediation of effects in BAT the most important subtype is the β-AR (especially β3-AR), which couples to G proteins of the G_s subtype (Cannon & Nedergaard 2004).

Next to its main task as a heating organ for thermoregulatory thermogenesis, further functions and adaptive actions are discussed for BAT. Another important scope of duties is the metaboloregulatory thermogenesis. The activity of BAT causes a decreased metabolic efficiency. *Rothwell and Stock* postulated the paradigm of “cafeteria feeding”, which suggests that the reduced metabolic efficiency observed under a high-fat diet is due to increased BAT activity (Rothwell & Stock 1979). Indeed a raised sympathetic activity in BAT has been found during the early stages of over-eating (Levin & Sullivan 1984). This metabolical activation is supposed to have beneficial effects in preventing the onset of obesity, but is rather thought to occur unintentional as a consequence of a defect in the adipostat (Cannon & Nedergaard 2004, Kozak 2010).
A further component of metaboloregulatory thermogenesis is represented in the acute thermal effects of eating, also called specific dynamic action (SDA). After the intake of a single meal an increase in the metabolic activity of BAT (measured by oxygen consumption) can be found in animals and humans (Bryant et al. 1984, Glick et al. 1989, Closa et al. 1992, Vosselman et al. 2013). The mechanisms of postprandial BAT activation is not sufficiently elucidated so far, but suggested to be mediated sympathetically. Also a

participation of leptin in the BAT activation has been assumed, but considered unlikely since leptin responses to a meal are too slow compared to the appearance of SDA (Cannon & Nedergaard 2004). The functional cause of the BAT activation following food intake is not clear so far.
Moreover, in states of starvation the activity of BAT and also the amount of UCP1 in BAT is decreased. This could be a secondary effect due to the absence of the meal-induced stimulation that would occur regularly in an *ad libitum* fed animal. In any case, the reduced BAT activity leads to a decreased energy expenditure in starved animals (Cannon & Nedergaard 2004, Closa et al. 1992, Garcia-Palmer et al. 1997).

Since the eighties also UCP1-expressing brown adipocyte-like cells were found in typical WAT depots (Young et al. 1984). These cells are called brite (brown-in-white; also beige) adipocytes and develop in WAT depots in response to cold exposure, β-adrenergic stimulation or during a pre- and postnatal development process called "browning" (Young et al. 1984, Cousin et al. 1992, Himms-Hagen et al. 2000, Lasar et al. 2013). Since metabolically active brown and brite adipocytes were detected in healthy adult humans (Cypess et al. 2009) the relevance of BAT activation and brite recruitment is discussed as therapeutic target for the treatment of obesity (Chechi et al. 2014, Nedergaard & Cannon 2010). This is especially relevant in the context of recent findings showing that the abundance of brite adipocytes is associated with obesity-resistance, increased energy expenditure and improved insulin sensitivity (Seale et al. 2011).

3.2.2. Origin and recruitment of brite fat cells

The divergent WAT depots exhibit varying abundance of brite adipocytes. Subcutaneous inguinal WAT (iWAT) depots show a stronger induction of thermogenic gene expression than visceral mesenteric or epididymal depots (Li et al. 2014c, Kozak & Koza 2010, Seale et al. 2011, Cohen et al. 2014, Okamatsu-Ogura et al. 2013). Originally the brown-like multilocular cells were found in WAT depots of mice following a cold exposure challenge (Young et al. 1984). This phenotypic effect was shown to be reversible when mice were returned to a warmer environment (Cousin et al. 1992, Loncar 1991). Although brite adipocytes are known for decades the origin is still largely unknown. Classical brown adipocytes are derived from myogenic factor 5 (myf-5) positive muscule like cells, while brite cells in WAT depots are myf-5 negative (Seale et al. 2008). There are two hypothesis discussed how brite adipocytes derive (Fig. 6). The fist one assumes a transdifferentiation of mature white adipocytes into brites (Kozak 2010, Barbatelli et al. 2010). The other one supposes a *de novo* differentiation from progenitor cells in the tissue (Wu et al. 2012). For both theories of origin for brites there is experimental evidence available and both processes seem to occur dependent on location of WAT depot (Seale et al. 2008, Sanchez-Gurmaches et al. 2012).

In general the strongest browning effect of WAT in various species occurs after a cold-exposure challenge, which also increases the size of the BAT depot. The recruitment may be mediated via the sympathetic nervous system through β3-ARs (Jimenez et al. 2003) and can thereby also be induced by treatment with β-AR agonists (Cousin et al. 1992). In response to receptor activation, the signalling pathway of the G-protein coupled receptor leads to a cAMP-dependent activation of PKA and a following phosphorylation of its target p38 MAPK (p38 mitogen-activated protein kinase). This induces the induction of transcription factors like PGC-1α (peroxisome proliferator-activated receptor γ coactivator 1-α) (Lowell & Spiegelman 2000).

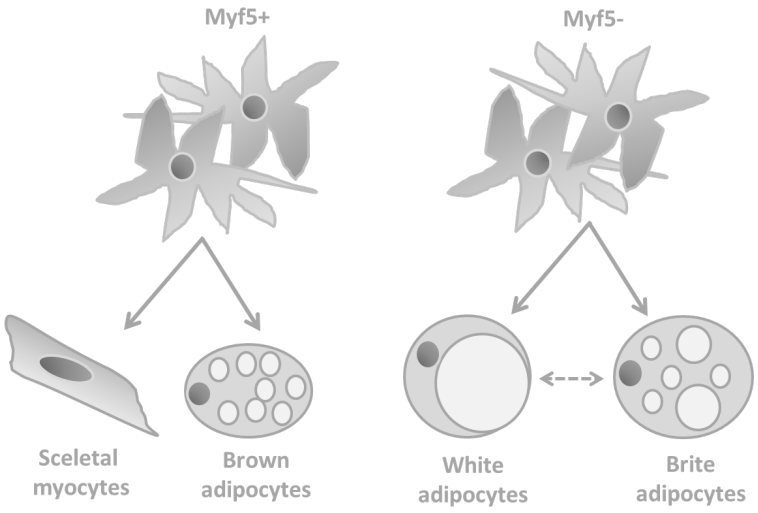

Fig. 6: **Differentiation from progenitor cells into different forms of adipocytes**. Reproduced from Merlin et al. 2015

Myf5-positive cells give rise to sceletal myocytes and brown adipocytes. Myf5-negative progenitors are the origin for white and brite adipocytes. Also transdifferentiation from mature white adipocytes towards brites has been shown.

Brite adipocytes can be activated by β-adrenergic stimulation to increase oxygen consumption (Li et al. 2014b). However, the functional significance of brite adipocytes contributing to a thermogenic function of WAT is still to be determined. So far it is not clear whether brites contribute to the systemic thermogenesis. However some beneficial metabolical effects associated with obesity have been linked with the abundance of brite cells in WAT. Some publications showed improved glucose tolerance and insulin sensitivity correlating with intensified browning (Chondronikola et al. 2014, Wang et al. 2015).

3.2.3. Abundance and relevance of brite adipocytes in humans

For decades BAT has not been considered to be existent in adult humans. Recent studies using positron emission tomographie (PET) have proven metabolically active BAT in supraclavicular, suprarenal, paravertebral and the neck region of adult man (Cypess et al. 2009, Nedergaard et al. 2007, Virtanen et al. 2009, van Marken Lichtenbelt et al. 2009). Supraclavicular BAT depots possess an estimated weight of about 60 g. Being fully activated a brown fat depot of that size could burn an energy equivalent to about 4.0 kg of adipose tissue in one year (Virtanen et al. 2009). Such calculation shed another light on the relevance of BAT in the regulation of energy homeostasis in adult humans which has previously been assumed not to be relevant. The abundance of detected BAT is correlated with the factors age, obesity, sex and season. In scans the tissue was mostly found in young, lean females in winter (van den Beukel et al. 2015, Wang et al. 2015, Saito et al. 2009, Kern et al. 2014, Saito 2013, Saito 2014). As well cold exposure as also food intake can acutely activate BAT in subjects (Chondronikola et al. 2014, Vosselman et al. 2013). The inverse relationship between body fat mass and abundance/activity of BAT in individuals suggests a protective effect of active human BAT against obesity because of its energy dissipation. This makes the recruitment and activation of BAT a promising therapeutic target for counteracting obesity and related metabolic disorders (Saito 2013). One way for this activation is the acute or chronically exposure of subjects to the mild cold, which has been shown to lead to induction of energy expenditure, activation of BAT and over time to a decrease in body fat mass (Yoneshiro et al. 2013). A further option to activate BAT is the stimulation of β3-ARs with agonists. In the past,

candidates for such an activation failed due to adverse effects or lack in selectivity for the receptor subtype (Sidossis & Kajimura 2015, Cannon & Nedergaard 2004). A pharmaceutical activation and recruitment of BAT without stimulation of adrenergic receptors in the body would be of great significance for combating obesity.

3.3. Aims of the thesis

In the last decades some activating effects of PACAP-family members upon stimulation of BAT have been shown. Most of this effects are mediated centrally, which means that the peptides were injected into the brain and BAT was activated via sympathetic innervation. Such effects have been shown for GLP-1 (Kooijman et al. 2015, Lockie et al. 2012, Lopez et al. 2015, Beiroa et al. 2014), PACAP (Diane et al. 2014) and oxyntomodulin (Lockie et al. 2013). For some further hormones, like glucagon (Lockie et al. 2013, Kinoshita et al. 2014) and cholecystokinin (Flo et al. 1998), also stimulating effects at BAT have been detected following peripheral administration.

In 1998 a direct stimulation of oxygen consumption in isolated brown adipocytes has been postulated for glucagon and SCT by *Dicker* (Dicker et al. 1998). In the publication, this induction after stimulation with glucagon was shown to be species specific and not mediated through β-ARs. However, the effect could not be reproduced *in vivo*. The thermogenic action of SCT was demonstrated in isolated BAT cells, but not further investigated (Dicker et al. 1998). Given the well-known lipolytic actions of SCT and first hints towards thermogenic properties, the aim of this thesis was the investigation of several functions of SCT concerning adipose tissues. *Sctr* expressions at fat tissues as well as acute BAT activation *in vivo* and *in vitro* and browning abilities were determined in the course of this thesis. Possible effects were evaluated considering the classical functions of SCT as a food-intake related gut hormone.

For the investigations mostly the mouse strain 129/SvJ and for feeding experiments furthermore the strain C57BL/6 was used. This was motivated by the fact that the 129/SvJ-mice show a significantly higher amount of BAT and browning capacity (Kozak 2010, Vitali et al. 2012, Li et al. 2014a) compared to other mouse strains. It was thus considered to be the most appropriate mouse strain for analysing the topics of interest in this thesis.

4. Material and Methods

4.1. *In vitro* experiments

The *in vitro* experiments in this thesis were mostly conducted using cell culture systems. For the characterisation of the SCTR activity conventional human embryonic kidney 293 (HEK293) cells were used. HEK293 cells were generated from human embryonic tumor tissue of the kidney (Graham et al. 1977). Since this cells do not express the SCTR under standard conditions this setting is called heterologous expression system, because exogenous proteins are produced in the cell. For all other experiments, like the induction of *ucp1* expression, seahorse measurements or the lipolysis assay, differentiated primary adipocytes isolated from mouse fat tissue samples were used. The procedure for obtaining this cells is explained in 4.1.3.

4.1.1. Culturing and transient transfection of HEK293 cells

4.1.1.1. Maintenance and culturing of cells

Cell culture was conducted under a laminar flow workbench and cell culture media were autoclaved to avoid bacterial contamination. For maintenance, cells were kept in dulbecco's modified eagle medium (DMEM) plus 10% FBS and 1% antibiotics mixture (Gentamycin, Penicillin/Streptomycin) and transferred into an incubator at 37 °C and 5% CO_2, where they exhibited a doubling time of 24 to 30 hours. For splitting the cells were washed once with prewarmed phosphate-buffered saline (PBS) and than detached with trypsin buffer for 2 minutes. Subsequently, cells were distributed to 5-7 new 10 cm culture dishes.

4.1.1.2. Transfection of cells

Cells were transfected when they achieved a confluence of 30-60%. Cells received fresh medium 3 hours prior to transfection. Water, DNA and $CaCl_2$ were mixed and after that dripped into twofold hank's balanced salt solution (HBSS) buffer while shaking on a vortex mixer (Tab. 4.1). For transfection the mixture was dropped slowly from the pipette onto the cells. After carefully swaying the plate, cells were incubated over night in the incubator.

Table 4.1: Production of DNA-precipitates

DNA	2.5-5 μg
$CaCl_2$ (2.5 M)	50 μl
water (partially desalinated)	ad 500 μl
2x HBSS	500 μl

Utilized vectors:

- *Mus musculus sctr* (129Sv WT) in pcDNA3.1 (Kindly provided by Professor *B.K.C. Chow*, School of Biological Sciences at the University of Hong Kong)
- pAD-CRE-PLuc, *Photinus pyralis* luciferase under control of cAMP-response-element (CRE)
- phRG-b, *Renilla reniformis* luciferase (PROMEGA)

4.1.2. Reporter gene assay for determination of SCTR activity

To measure the activation of the SCTR following a stimulation with SCT, a luciferase-reporter gene assay was used. The SCTR is a membrane-bound GPCR, that activates the cAMP signalling cascade in the cell, which leads to a modulation of gene expression by phosphorylation of the transcription factor cAMP response element binding protein (CREB). The *photinus phyralis* luciferase (PLuc) is under the control of CRE, thus activation of the signalling cascade affords expression of the luciferase reporter (Fig. 7). This expression can be quantified via luciferase-assay. The expression of the *renilla reniformis* luciferase is constitutively and thereby constant. The expression of the RLuc is thereby influenced by factors like cell number per well or transfection efficiency and can be used to normalise results for PLuc.

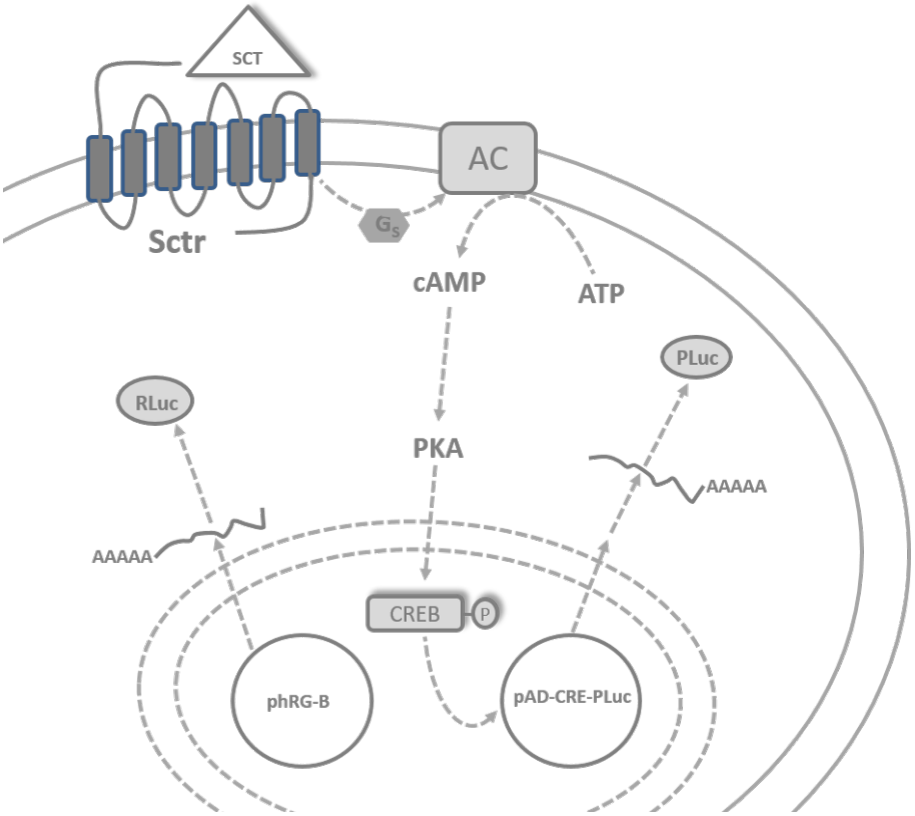

Fig. 7: **Luciferase reportergene-assay to measure activation of SCTR.**
The vectors for the expression of the SCTR, for RLuc expression and for the luciferase reportergene pAD-CRE-PLuc were transiently transfected into HEK293-cells. As result the cells express the SCTR and an activation of the receptor leads via the plotted signalling cascade to expression of the *photinus* luciferase (PLuc) and can be quantified. G_s: G-protein, AC: adenylyl cyclase, PKA: protein kinase A, CREB; cAMP *response element binding protein*.

Preparing a dose-response curve with purchased rat SCT

At about 16 hours after transient transfection the HEK293 cells were seeded to 48-well plates pre-coated with poly-D-lysine. Cells received a serum-free fasting medium over night and were stimulated for six hours with various concentrations of SCT or PASylated SCT in serum-free medium at the following day.

Measurement of bioluminescence

After six hours of stimulation the medium was removed from the cells, they were washed with prewarmed PBS and lysed in 100 μl lysate buffer. After an incubation time of 20 to 30 minutes, cells were mixed and

solved by pipetting up and down. 50 μl of the *photinus* substrate LARII was poured to a luminometer tube and 10 μl of the cell lysate solution was added and pipetted several times up and down to mix. Hereupon the bioluminescence of the *photinus* luciferase was measured using a luminometer after 2 seconds of delay for 10 seconds. The luminometer tube was removed, 50 μl of the Stop&Glow solution was added and after short vortexing the mixture was measured once again in the luminometer to determine bioluminescence of the *renilla* luciferase (2 seconds delay and 10 seconds of measurement).

Data Analysis

The *photinus* luciferase readings, that were induced by SCTR activation, were normalised to the *renilla* luciferase reads, which display constitutive activity, to control for differences in transfection efficiency and cell number.

4.1.3. Culturing primary adipocytes

4.1.3.1. Isolation of stromal vascular fraction from adipose tissues

To isolate tissue samples from inguinal (iWAT) and gonadal (gWAT) white and interscapular BAT depots, mice were killed and directly dissected. The tissues were transferred into small petri dishes filled with prewarmed PBS and 1% antibiotics mixture (Gentamycin, Penicillin/Streptomycin and Fungizone, 2:2:1). To improve cell yields, the same fat depots of two (WAT depots) or three (BAT) mice were pooled. Samples were cut on the dry top of the petri dish and minced into very small pieces using surgical scissors, transferred into a tube and filled up to 7 ml with isolation medium. Digestion took place in an orbital shaker at 37 °C and 120 rpm for 45 minutes and vigorous shaking by hand every 10 minutes until tissue parts were digested and homogenised. Subsequently the fluid was filtered through a sterilised nylon mesh (250 μm pores) and poured with wash medium. After centrifugation (5 minutes, 250 g, mixing and again 5 minutes, 250 g) all of the fluid and mature adipocytes in the supernatant were soaked up and the remaining pellet containing the stromal vascular fraction was resuspended in 7 ml wash medium and filtered with a cell strainer (40 μm pores). The fluid was centrifuged again to seperate phases (5 minutes, 500 g). The pelled with the isolated stromal vascular fraction was resuspended in medium containing 20% FBS and 1% antibiotics (culture medium). Cells were plated on 12-well plates (stimulation experiments) or XF96 V3-PS cell culture microplates (for respirometry measurements) and incubated over night.

4.1.3.2. Culturing and induction of primary adipocytes

At the day after seeding, cells were attached to the plate and the cells from iWAT and gWAT were washed in prewarmed PBS for one to two times to remove the debris. Brown adipocytes only received fresh culture medium to avoid cell loss because of the low cell number. The culture medium was refreshed every second day until the cell layer almost reached confluence, whereupon the medium was switched to induction medium for two days. For the following six days of culturing the cells received differentiation medium that was replaced every second day until the day of stimulation.

Media:

Isolation medium:
1x HBSS w/Mg;Ca
3.5% BSA (0.035 g/ml)
0.55 mM glucose
collagenase A (1 mg/ml)

Wash medium:
1x HBSS w/Mg;Ca
3.5% BSA (0.035 g/ml)

Culture medium:
DEMEM-Medium
20% FBS
1% antibiotics (Gentamycin, Penicilin/Streptomycin, Fugizone; 2:2:1)

Induction medium:
DEMEM-Medium
10% FBS
1% antibiotics (Gentamycin, Penicilin/Streptomycin; 1:1)
850 nM insulin
1 nM T3
500 μM IBMX
1 μM dexamethasone
125 μM indometacin

Differentiation medium:
DEMEM-Medium
10% FBS
1% antibiotics (Gentamycin, Penicilin/Streptomycin; 1:1)
850 nM insulin
1 nM T3
1 μM rosiglitazone (only for respirometry measurements with chronic rosiglitazone)

4.1.4. Quantitative gene expression in primary adipocytes

Primary adipocytes were stimulated at the seventh day of differentiation for six hours with SCT, PASylated SCT (solved in PBS), isoproterenol (solved in ethanol) (ISO), SB203580, H89 or pure PBS in fresh medium. Gene expression levels were measured by quantitative real-time PCR (qRT-PCR) after extraction of mRNA

and synthesis of cDNA.

4.1.4.1. Extraction of mRNA from cells and synthesis of cDNA

For the extraction of mRNA, cells were disrupted with TRIsure and subsequently filtered via silica columns to abstract mRNA. Subsequent to the stimulation of the cells, the medium was soaked up and each of the 12 wells were filled with 500 μl of TRIsure to stabilise the mRNA. Cells were solved from the plate surface by pipetting up and down and transferred to tubes. The tubes can be stored at -80 °C for several days or weeks or be further processed immediately.

After 2 minutes of incubation at room temperature, 100 μl of chloroform were added to the cell-TRIsure mixture and the tubes were vigorously shaken by hand for 15 seconds. The tubes were afterwards centrifuged for 15 minutes at 12,000 g and 4 °C to obtain phase separation. The aqueous supernatant contained solved mRNA and was transferred to columns of the RNA isolation system prestuffed with 75% ethanol in diethylpyrocarbonate (DEPC) water. The subsequent steps of washing, DNAse digestion and elution in RNAse-free water were carried out following the RNA isolation kit instructions (SV total RNA isolation system, Promega). The mRNA was eluted from the column in 40 μl of water and concentration was measured using the microplate reader (TECAN) at a wavelength of 260 nm.

To transfer single-stranded mRNA into the complementary cDNA strain, the retroviral enzyme reverse transcriptase (RT) and an oligo-dT primermix of a kit (Quantitect reverse transcription, Quiagen) were used. A calculated volume of the mRNA extract containing 500 ng of mRNA was filled with RNAse-free water up to a volume of 7 μl. Remaining gDNA contaminations were digested by a wipeout buffer and for reverse transcription a transcriptase and a primermix was added (Tab. 4.2). The attained cDNA can be stored for several months at -20 °C.

Table 4.2: Reverse Transciption

Components	Volume (μl)	
RNA (500 ng)	x	
gDNA wipeout buffer	1	
Nuclease-free water	ad 7	
		3 min, 42 °C
Reverse trascriptase	0.5	
5x RT buffer	2	
Primermix	0.5	
		30 min, 42 °C
		3 min, 95 °C

4.1.4.2. Quantitative real-time PCR

The quantification of mRNA-expression was performed by a qRT-PCR with the complementary cDNA. With this method relative differences in the amount of transcripts of various samples can be detected. The qRT-PCR is performed by a light cycler (light cycler 480, Roche) with an optical detection system. The generation of PCR products can be detected by measurement of the SYBR Green fluorescence signal. SYBR

Green intercalates into the double-stranded DNA (dsDNA) helix. In solution, the unbound dye exhibits very little fluorescence (measured at 530 nm), but is greatly enhanced upon binding to DNA due to conformational changes. Therefore, during qRT-PCR, the increase in SYBR Green fluorescence is directly proportional to the amount of dsDNA generated and is measured in every cycle.

Quantification

The quantification of complementary cDNA is based on cyclic threshold-measures (C_t values), which means that the first cycle gives a signal where fluorescence rises for the first time above background threshold. The higher the kick-off concentration of the target cDNA, the earlier the C_t values is reached in the course of amplification. For assigning a relative concentration out of the displayed C_t values, a standard curve needs to be generated. Therefore a 7-ary 2^n dilution series (1 to 1:64) from undiluted cDNA samples was prepared. The unknown test samples were used in a 1:10 dilution in water and their concentration was calculated out of the slope of the standard curve. The utilised primers were designed with an ideal annealing temperature of 52 °C. To get rid of technical variation, next to the genes of interest a house keeping gene was measured. For the reported experiments the constitutively expressed general transcription factor II B (TFIIB) that is localised in the nucleus was used. The abundance of the house keeping gene should not be influenced by stimulations or treatments. Differences in the expression are thereby considered to be due to technical variation.

Specificity

To check for specificity of the primers an *in silico* PCR for primer blasting was conducted (http://genome.ucsc.edu/). Furthermore, the products of a conventional PCR were loaded on an agarose gel to confirm product size and sharpness of the band.

To ensure the correctness of the RT-qPCR products, melting curves were examined. Therefore the temperature of the cycler was raised from 60 °C to 95 °C. In the course of heating the dsDNA products of the PCR were separated due to the high ambient temperature, which led to an sudden decrease of fluorescence caused by the release of the SYBR Green dye. The temperature needed for double-strain separation is specific for certain PCR-amplificates due to length and nucleic acid composition.

Practical Procedure

The wells of the light cycler plate were prefilled with the qPCR-master mix, standard samples were added in duplicates and measurement samples were added in triplicates in a 1:10 dilution (Tab 4.3). The SensiMix™ SYBR No-ROX Kit (bioline) that was used, contains SYBR Green I dye, deoxynucleoside triphosphates, stabilisers and enhancers.

After pipetting the plate was closed with an adhesive foil and centrifuged for 1 minute at 500 g. Hereupon the plate was transferred to the light cycler and further processed with the cycler program (Tab. 4.4).

Data analysis

Out of the C_t values measured by the light cycler, absolute concentration values for each sample were automatically calculated by the software. For data analysis these values for the genes of interest were divided by the values for the housekeeping gene for each sample to achieve normalisation. Afterwards the mean of

Table 4.3: Mastermix for RT qPCR

Components	Volume(μl)
2x SensiMix	6.25
nuclease-free water	3.25
cDNA	1
Primer for (10 μM)	1
Primer rev (10 μM)	1

Table 4.4: Cycler program for qRT-PCR

Step	temperature (°C)	time (s)	loop
initial denaturation	95	420	
denaturation	95	10	
annealing	52	10	40 x
elongation	72	20	
denaturation	95	15	
melting curve	60-95	1200	

the technical triplicates of one sample was used to calculated mean values for the biological triplicates. The results for each group were statistically analysed for significant differences via t-test analysis in Graph Pad Prism 4.0 for testings with one parameter and via two-way ANOVA in Sigma Plot 12.0 (Systat Software Inc.) for two parameters, if biological replicates were N >2.

Primer:

UCP1	for	5'-GTACACCAAGGAAGGACCGA-3'
	rev	5'-TTTATTCGTGGTCTCCCAGC-3'
SCTR	for	5'-ATGCACCTGTTTGTGTCCTT-3'
	rev	5'-TAGTTGGCCATGATGCAGTA-3'
TFIIB	for	5'-TGGAGATTTGTCCACCATGA-3'
	rev	5'-GAATTGCCAAACTCATCAAAACT-3'

4.1.5. Lipolysis assay

Lipolysis is defined as the hydrolytic cleavage of ester bonds in triglycerides, resulting in the generation of fatty acids and glycerol. In this assay lipolysis is determined by measuring glycerol and non-esterified fatty acids (NEFA) released into medium by the cells.

Stimulation of cells

For the experiment fully differentiated primary adipocytes out of the stromal vascular fraction of adipose tissues on 12-well plates were used (see section 4.1.3).

Cells were washed with prewarmed PBS and received afterwards 500 μl incubation medium per well with

either SCT or ISO for stimulation or without a stimulant as control. Cells were incubated for 1 hour whereupon medium was refreshed once and left on the cells for another hour. Afterwards the medium was removed and collected, stored on ice and frozen at -80 °C.

Detection of glycerol

The quantitative determination of glycerol was measured by coupled enzyme reactions (free glycerol reagent, Sigma-Aldrich). Initially, the phosphorylation of glycerol, which was catalysed by glycerol kinase, generated glycerol-1-phosphate (G-1-P) and adenosine diphosphate (ADP). G-1-P was then oxidised by glycerol phosphate oxidase (GPO) forming dihydroxyacetone phosphate (DAP) and hydrogen peroxide (H_2O_2). In the final step peroxidase (POD) catalysed the coupling of H_2O_2 with 4-aminoantipyrine (4-AAP) and sodium N-ethyl-N-(3-sulfopropyl) m-anisidine (ESPA), which led to the production of a quinoneimine dye with an absorbance maximum at 540 nm (see equations 4.1 to 4.3).

$$\mathrm{glycerol} + \mathrm{ATP} \xrightarrow{\text{glycerol kinase}} \mathrm{glycerol{-}1\text{-}P} + \mathrm{ADP} \tag{4.1}$$

$$\mathrm{glycerol{-}1\text{-}P} + \mathrm{O_2} \xrightarrow{\text{glycerol phosphate oxidase}} \mathrm{DAP} + \mathrm{H_2O_2} \tag{4.2}$$

$$\mathrm{H_2O_2} + \mathrm{4\text{-}AAP} + \mathrm{ESPA} \xrightarrow{\text{peroxidase}} \text{Quinoneimine Dye} + \mathrm{H_2O} \tag{4.3}$$

The increased absorption is directly proportional to the free glycerol concentration in the sample. For the calculation of relative values a standard curve was generated (glycerol standard solution, Sigma-Aldrich).
For the measurement, 10 μl were pipetted into the wells of a 96-well plate (samples in triplicates, water (blank) or standard concentrations in duplicates). Subsequently, 100 μl of glycerol reagent of the kit was added. The plate was protected from light by a lid and incubated for 15 minutes at room temperature while swinging it gently on a vertical shaker. The determination of the absorption at 540 nm was conducted using a microplate reader (TECAN).
Finally, the concentrations in the samples were calculated out of the slope of the standard curve.

Detection of NEFAs

For the determination of NEFA levels also coupled enzymatic reactions were used (NEFA-HR (2), Wako Chemicals). First, coenzyme A (CoA) was acylated by the fatty acids, which was catalysed by acyl-CoA-sythetase (ACS). The produced acyl-CoA was further oxidised by an acyl-CoA-oxidase (ACOD) which produced H_2O_2. The peroxidase (POD) catalysed the oxidative condensation of H_2O_2 with 3-methyl-N-ethyl-N-(β-hydroxyethyl)-aniline (MEHA) and 4-aminoantipyrin to a purple coloured product that could be measured at 550 nm (see equations 4.4 to 4.6).

$$\mathrm{RCOOH} + \mathrm{ATP} + \mathrm{CoA} \xrightarrow{\text{ACS}} \mathrm{acyl{-}CoA} + \mathrm{AMP} + \mathrm{PPi} \tag{4.4}$$

$$\mathrm{acyl{-}CoA} + \mathrm{O_2} \xrightarrow{\text{ACOD}} \mathrm{2{,}3{-}trans{-}enoyl{-}CoA} + \mathrm{H_2O_2} \tag{4.5}$$

$$\mathrm{H_2O_2} + \mathrm{4\text{-}aminoantipyrin} + \mathrm{MEHA} \xrightarrow{\text{POD}} \text{purple pigment} + 3\,\mathrm{H_2O} \tag{4.6}$$

To perform the assay, firstly a standard curve of twelve concentrations was prepared using the supplied palmitate solutions (NEFA standard solutions, Wako Chemicals). Standards as well as each sample were pipetted to the wells of a 96-well plate in duplicates, before transferring the plate into the microplate reader (TECAN). In the TECAN reagent 1 (ACS, CoA, ATP, 4-AA, AOD, sodium azide and phosphate buffer) was added automatically and after 3 minutes the plate was measured at 546 nm (main) and 660 nm (sub) (measurement point 1) to receive blank values. Hereinafter reagent 2 (ACOD, POD, MEHA) was added to each well of the plate and after further 4.5 minutes the wells were measured again (546 nm and 660 nm; measurement point 2).

To calculate the originally sample concentrations, firstly the difference between the two wavelengths was computed for both measurement points (546 nm- 660 nm) for all measured wells. Afterwards, the blank values were subtracted from the results (measurement point 2 - measurement point 1). Finally, the sample concentrations were calculated out of the slope of the standard curve.

Media:

Incubation medium:

DMEM no pyruvate, no glucose

glucose, 1 g/l

2% BSA

$\pm$ ISO 0.5 μM, $\pm$ SCT, several concentrations

4.1.6. Respirometry measurements

The respirometry measurements were performed using an XF96 extracellular flux analyzer (Seahorse Bioscience) to determine oxygen consumption rates (OCR) in differentiated primary adipocytes.
The Seahorse Bioscience XF96 instrument measures the rates of changing analytes, dissolved oxygen and pH in the media surrounding living cells in a repeated manner. The measurement was performed using 96 optical fluorescent biosensors embedded in a sterile disposable cartridge that is placed onto the XF96 V3-PS cell culture microplates, where primary adipocytes were seeded. The measured values were used to determine rates of the cellular metabolism.

Table 4.5: Protocol of the XF96 analyzer for measurement of UCP1 activity

Step	Action	Duration	Loop
1	Calibrate probes		
2	Equilibrate	12 min	
3	Mix	2 min	
4	Delay	2 min	3
5	Measure	3 min	
6	Inject A (20 μl) **Oligomycin**		
7	Mix	2 min	
8	Delay	2 min	3
9	Measure	3 min	
10	Inject B (22 μl) **Iso/Sct**		
11	Mix	2 min	
12	Delay	2 min	5
13	Measure	3 min	
14	Inject C (24 μl) **FCCP**		
15	Mix	2 min	
16	Delay	2 min	3
17	Measure	3 min	
18	Inject D (26 μl) **Antimycin A**		
19	Mix	2 min	
20	Delay	2 min	3
21	Measure	3 min	
22	Program end		

The measurement was conducted at the seventh day of differentiation with cells that were plated on XF96 V3-PS cell culture microplates. The cells were washed with prewarmed, unbuffered measurement medium

(basal assay medium) once and than received basal assay medium containing 2% BSA (fatty acid free). The BSA buffers free fatty acids released by lipolysis to inhibit fully uncoupling by ISO or SCT (Li et al. 2014b). Cells were incubated in a room air incubator at 37 °C.
The sensor cartridge was pre-incubated with 200 μl of XF96 calibrant buffer at 37 °C in the room air incubator over night before measurement. At the next day the sensor cartridge was loaded with the assay reagents diluted in basal assay medium (no BSA).

In the assay protocol (Tab. 4.5), firstly basal respiration was measured in untreated cells, followed by an oligomycin treatment (5 μM, injection of port A) to measure the OCR after inhibition of coupled respiration. Next, the cells were stimulated with SCT or ISO (0.5 μM, injection of port B) and the UCP1 mediated uncoupled respiration was measured. Maximum respiratory capacity was assessed with carbonyl cyanide-p-trifluoromethoxyphenylhydrazone (FCCP) stimulation (1 μM, injection of port C) and finally mitochondrial respiration was blocked by antimycin A (5 μM, injection of port D). The residual OCR was considered as non-mitochondrial respiration.
The oxygen consumption rates were displayed automatically by the Seahorse XF-96 device and raw data were exported and analysed using Graph Pad Prism 4.0 (GraphPad Software Inc.). In the results part for each respiratory data set one complete representative measurement is shown as OCR normalised to basal respiration (following oligomycin injection) as 100%. For the presentation of the respiratory fold increase, compared to basal and maximal uncoupled oxygen consumption values were calculated as follows:
For each condition 8-16 wells were measured as technical replicates. Wells with apoptotic cells were excluded manually and means for all other technical replicates for each measurement point were calculated. Afterwards for each condition the lowest OCR after antimycin A addition was taken and defined as leak respiration. This value was subtracted from all other used values. To determine basal respiration the third measurement point after oligomycin addition was used. For induction of respiration by ISO, SCT or FCCP, the highest value measured after addition of the respective substance was used. The "OCR % basal OCR" and "OCR % FCCP OCR" were calculated as follows:

$$\text{OCR \% basal OCR} = \frac{100 * (SCT - antiA)}{(basal - antiA)} \text{ or } \frac{100 * (ISO - antiA)}{(basal - antiA)}$$

$$\text{OCR \% FCCP OCR} = \frac{100 * (SCT - antiA)}{(FCCP - antiA)} \text{ or } \frac{100 * (ISO - antiA)}{(FCCP - antiA)}$$

The results of the calculation show the percentaged increase of respiration following the stimulation with ISO or SCT above basal level (which is 100 %) presented as OCR % basal OCR. OCR % FCCP OCR demonstrates to which percentaged extend the stimulation with ISO or SCT can reach the respiratory values for fully uncoupled respiration by FCCP (which is 100 %).

Media:

Basal assay medium:

DMEM basal medium

25 mM glucose

2 mM sodium pyruvate

31 mM NaCl

2 mM GlutaMax

15 mg/l phenol red

pH 7.4

4.2. *In vivo* experiments

4.2.1. Animal housing

The mice (*mus musculus*, 129S6/SvEvTac, 129S1/SvEvTac (UCP1 KO) and C57BL/6J for food intake measurements) were housed at an ambient temperature of 22 °C and a humidity of 50-60%. The mice were sitting in groups of two to five mice in type-II, long cages (360 cm^2) with a light-dark cycle of 12 hours each. As litter wood shavings were used and the mice obtained plastic cottages as enrichment. The cages and litter were replaced once a week. As not stated otherwise mice had *ad libitum* access to water and food. The chow diet (R/M-H Haltungsfutter, Ssniff) for maintenance contained an energy composition of 58% of carbon hydrates, 33% of protein and 9% of fat. The energy content of the food was 18.5 MJ/kg.
Mice fed a high-fat diet (HFD) received the experimental "palm high-fat" diet (S5745-E712, Ssniff) containing 25% (w/w) fat comprising of 20% palm oil and 5% soybean oil (energy content of 22.7 MJ/kg). The control diet (CD) fed mice received experimental "control" (S5745-E702, Ssniff) with 5% (w/w) soybean oil and no further fat source (energy content of 18.2 MJ/kg). All experimental food was sterilised by γ-irridation.
To adapt mice to an ambient temperature of 4 °C, the animals were housed for four days in groups of two in an open system typ II (370 cm^2) cages in climate cabinets (HPP749, Memmert, Schwabach/Germany) at relative humidity of 55-65%.

4.2.2. Generation and delivery of utilised mice

For food intake measurements, mice of the C67BL/6J strain were used. At the age of seven weeks the mice were adapted to special experimental bottles for one week.
For the calorimetric measurements with wiltype mice, animals of the Sv129/J (S6) strain were used. The experiments started when the mice were about 8 weeks of age.
For the experiments with UCP1 KO mice, animals from our in-house KO line were used. The mice are on a Sv129/J (S1) background. The UCP1 KO mice were generated by a homozygous mating. The WT controls were also bred by a homozygous mating where WT-littermates of the KO-couples were used.

4.2.3. Intraperitoneal injections

For all *in vivo* experiments it was necessary to treat the mice with i.p. injections. The volumes used for injection were not exceeding 10 ml/kg bodyweight. The C57BL/6J animals that were used for food intake measurements got adapted to injections by daily handling for four days ahead of the start of the experiment. The Sv129/J mice did not have to be trained. For injection, mice were kept in one hand fixed at neck and tail and bowed slightly with the head to the ground to slip the intestine up. The i.p. injections were applied with an average velocity and a penetration angle of 30° into the right lower side of the abdomen.

4.2.4. Food intake measurements

For the measurement of food intake a feeding-drinking-activity (FDA, TSE Systems, Bad Homburg/Germany) device with type-III cages was used where the mice were kept in single-housing. Mice were habituated to the cages and daily i.p. PBS-injections (at 10 a.m.) for four days ahead of the experiment start. The body weight

of the mice was measured every day to check for their health status.

After four days of habituation the food was removed from the cages at 5 pm, and the mice were food deprived over night with *ad libitum* access to water. In the next morning, mice were i.p. injected with either PBS as control or with SCT solved in PBS in the treatment groups. The latter was given in different doses. Subsequently, the mice received the respective food back and food intake was monitored during the following 72 hours. Mice were only disturbed for daily body weight measurements.

The values for food intake were cropped in intervals of 5 minutes by automatic weighing the feeder (TSE LabMaster software). The food intake was calculated with the alterations in feeder weight caused by food consumption. The results were exported into a spreadsheet calculation table (Excel, Microsoft) and analysed with Graph Pad Prism 4.0 (GraphPad Software Inc.).

4.2.5. Indirect calorimetric measurements

Indirect calorimetric measurements in mice were performed using an open flow respirometry system (Phenomaster, TSE Systems, Bad Homburg/Germany), which determined oxygen consumption and carbon dioxide production. For the measurement mice were placed individually in metabolic cages (type I, 3 liter volume) without food and water. The cages were transferred to a climate cabinet (TPK 600, Feutron, Greiz/Germany) and the air was pulled continuously with a flow rate of 33 l/h through the cages. For gas analysis a subsample was dried in a cooling trap and analysed for gas exchange. Values were set off against samples from an empty reference cage, which was also located in the climate chamber. For antemeridian determination of the basal metabolic rates (BMR) in the post-absorptive state, the cages were measured in line for four hours at 30 °C ambient temperature. Every cage (also the reference cage) was measured for one minute in each circle (every five minutes). BMR [ml O_2/h] was defined as the lowest mean of three consecutive oxygen consumption values. In the afternoon the mice were consecutively i.p. injected with 0.5 mg/kg SCT (or PBS for the control group) and singularly measured in the calorimetry chamber for about one hour at an ambient temperature of 27 °C. Each mouse was recorded for 45–60 min with a high-resolution recording of 10 second intervals.

The table of results was exported by the TSE LabMaster software to an excel-sheet and subsequently analysed in Graph Pad Prism 4.0 (GraphPad Software Inc.). For all determinations of the area under the curve (AUC) of the HP, the basal metabolic HP was subtracted for each mouse individually.

Respiratory exchange ratios (RER) and heat production (HP) were calculated as follows:

RER = CO_2 production / O_2 consumption

HP[mW] = (4.44 + 1.43 * RER) * O_2 consumption [ml/h]).

4.2.6. Dissection of various tissues

All mice used for dissection were killed via gasifying with CO_2 to prevent damage of BAT depots caused by cervical dislocation. For opening abdomen and neck and dissection of the different adipose tissue depots surgical instruments were used. Tissue samples were snap-frozen in liquid nitrogen and stored at -80 °C until further processing.

4.3. Statistical analysis

Graphs were generated with GraphPad Prism 4.0 or 6.0 (GraphPad Software Inc., La Jolla CA/USA). The values are presented as means ±SD as not stated otherwise. Normal distribution was tested with the Shapiro-Wilk normality test. Significant differences between two groups was assessed by two-tailed Student's t-test with Graph Pad Prism 4.0 (GraphPad Software), when distributed normally. Three groups were tested with one-way analysis of variance (ANOVA) and Holm-Sidak post-test. When normal distribution failed, three groups were compared by Kruskal-Wallis one-way ANOVA on Ranks (Sigma Plot 12.0, Systat Software Inc., San Jose CA/USA). Two-way ANOVA (Simga Plot 12.0, Systat Software Inc.) and Holm-Sidak post-test was used to compare two or more groups with respect two or more variables. Two-way repeated ANOVA and Holm-Sidak post-test (S Plus, SPlus software, TIBICO Spotfire Analytics, Boston MA/USA) was used to compare food intake in repeated measures over time.

Which test was used is stated at the single experiments.

A p-value <0.05 was considered a statistically significant difference. It is depicted in graphics with *.

A p-value <0.01 is illustrated with **

and a p-value <0.001 is depicted with ***.

4.4. Chemicals, equipment and kits

4.4.1. Chemicals and reagents

The chemicals and reagents used in this thesis are listed in table 4.6.

4.4.2. Equipment and devices

The equipment and devices that have been used for the thesis are listed in table 4.7.

4.4.3. Kits

The commercial kits that have been used for the thesis are listed in table 4.8.

Table 4.6: Chemicals and reagents

labelling	Supplier	Catalogue Nr
3,3',5.triiodo-L-thyronine sodium salt (T3)	Sigma-Aldrich	T6397
3-isobutyl-1-methylxanthine (IBMX)	Sigma-Aldrich	I5879
Antimycin A	Sigma-Aldrich	A8674
Bovine Serum albumin (BSA) fraction V	Carl Roth	8076
Bovine serum albumin (BSA), fatty acid free	Sigma-Aldrich	A3803-100G
Chloroform p.a.	Carl Roth	Y015.1
Collagenase A	Biochrom	C 1-22
Control diet	S5745-E702	Ssniff
Dexamethason	Sigma-Aldrich	D1159
Dulbecco's modified eagle medium (DMEM) high gluc	Sigma-Aldrich	D5796
DMEM, no pyruvate, no glucose	GIBCO	11966-025
DMEM for XF96 Flux Analyzer	Sigma-Aldrich	D5030-10X1L
Dimethyl sulfoxide (DMSO)	Carl Roth	4720
Ethanol 70%, denaturated	Carl Roth	T913
Ethanol 99.8% p.a.	Carl Roth	9065
FCCP	Sigma-Aldrich	C2920-10MG
Fetal bovine serum (FBS)	Biochrom	S0615
Fungizone (Amphotericin B)	Biochrom	A2612
Gentamycin	Biochrom	A2712
Glutamax	Life Technologies	35050-061
Glucose	Biochrom	HN06
H89 dihydrochloride	Tocris	2910
Hank's balanced salt solution (HBSS) w/Mg; Ca	Invitrogen	14025-050
High-fat diet	S5745-E712	Ssniff
Indomethacin	Sigma-Aldrich	I7378
Insulin solution, human	Sigma-Aldrich	I9278-5ML
Isoproterenol (ISO)	Sigma-Aldrich	I6504-100MG
Nuclease-free water	Quiagen	129114
Oligomycin	Sigma-Aldrich	O4876-5mg
PASylated secretin	Prof. Skerra	
Penicillin/Streptomycin	Biochrom	A2212
Phosphate Buffered Saline (PBS) Tablets	Gibco	18912-014
Poly-D-Lysin	Sigma Aldrich	P6407
SB203580	Sigma-Aldrich	S8307
Secretin (SCT) (rat)	Tocris	1919
Sodium pyruvate solution 100nM	Gibco	11360-070
Rosiglitazone (Rosi)	Cayman Chemical	71740
Sodium Chloride	Carl Roth	3957
SensiMix SYBR no Rox	Bioline	QT650-20
TRIsure	Bioline	BIO-38033
Trypsin/EDTA, 100ml	Biochrom	L2163
XF calibrant buffer	Seahorse Bioscience	100840-000

Table 4.7: Equipment and devices

labelling	Supplier	Catalogue Nr
Indirect calorimetry	TSE-Systems	
Cellculture plates, 12 well	Sarstedt	83.3921
Cellculture plates, 48 well	Sarstedt	83.3923
Cell strainer, 40 μM	BD Bioscience	352340
Climate cabinet	Memmert	HPP749
Eppendorf Research plus 10-100, 8-channel	Eppendorf	3122000035
Eppendorf Research plus 30-300, 8-channel	Eppendorf	3122000051
Feeding-drinking-activity device	TSE-Systems	
Infinite M200 Microplate reader	TECAN	30016056
Light Cycler 480 (384 well)	Roche Applied Science	5015243001
Sirius (Luminometer)	Berthold Detection Systems	
Nylon mesh	SFT	250 μm
Seahorse XF extracellular flux analyzer	Seahorse Bioscience	
XF96 V3-PS cell culture microplate	Seahorse Bioscience	Part 101085-004

Table 4.8: Kits

labelling	Supplier	Catalogue Nr
Dual-Luciferse Reporter Assay System	Promega	E1960
Free glycerol reagent	Sigma-Aldrich	F6428
Glycerol standard solution	Sigma-Aldrich	G7793
NEFA-HR (2)	Wako Chemicals	999-34691
NEFA standard solutions	Wako Chemicals	995-3479, 991-34891
		993-35191, 276-76491
Quantitect Reverse Transcription	Quiagen	205313
SensiMix, SYBR No-ROX Kit	bioline	SM599-B031190
SV Total RNA Isolation System	Promega	Z3105

5. Results

SCT is predominantly known for its postprandial contribution to functions of digestion by stimulating the pancreas and its neuroactive properties in the brain. The analysis using the BIO-GPS tool revealed a high expression of *sctr* in BAT of mice (supplement, Fig. 31). Taking into account the lipolytic activity (Butcher & Carlson 1970, Stout et al. 1976) of the hormone in adipocytes, the action of SCT on BAT and WAT depots was investigated in this thesis in *in vitro* and *in vivo* approaches.

5.1. Adipose *sctr* expression *in vivo* and *in vitro*

Since the SCTR is the only known targeted receptor of SCT, its expression at various adipose tissue depots is required for the mediation of a potential effect of the hormone. Therefore the abundance of *sctr* mRNA was determined by quantitative real-time PCR in murine adipose tissue depots as well as in isolated and fully differentiated primary adipocytes.

Wildtype 129/S6-mice were killed and interscapular BAT, inguinal WAT (iWAT) and gonadal WAT (gWAT) depots were sampled. The *sctr* expression was measured by qPCR . The expression of the receptor was significantly higher in BAT compared to iWAT. Furthermore, the expression was also higher in BAT compared to gWAT, but the difference was not statistically significant (Fig. 8, A). These results are in line with data from BIO-GPS (supplement, Fig. 31), showing highest *sctr* expression in BAT directly after placenta and brain among all analysed tissues.

Various functional assays in this thesis concerning the regulatory role of SCT in adipose tissues were conducted in *in vitro* systems. The expression of the *sctr* was also analysed in primary adipocytes. Cells isolated from the stromal vascular fraction of three different mouse adipose tissues (BAT, iWAT and gWAT) were cultured and fully differentiated. The quantification of the *sctr* by qPCR revealed a pattern consistent with the tissue findings. Also in differentiated primary adipocytes the expression was much higher in cells from BAT depots compared to cells from iWAT or gWAT (Fig. 8, B).

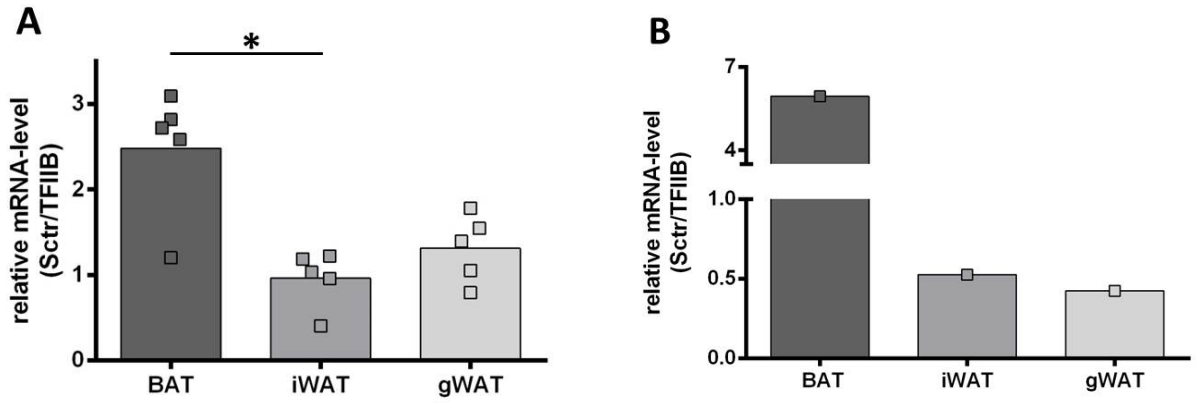

(a) mouse adipose tissues (b) primary adipocytes

Fig. 8: ***sctr* expression in mouse adipose tissues (A) and in differentiated primary adipocytes (B).** Data show relative expression of *sctr* in mouse fat depots (A) normalised to transcription factor TFIIB for N=5. Statistics were conducted using one-way ANOVA and since normality test (Shapiro-Wilk) failed ($P < 0.050$) a Kruskal-Wallis one-way analysis of variance on ranks was performed ($p=0.021$). The * indicates $p<0.05$. The expression of the *sctr* in primary adipocytes (B) was also normalised by TFIIB-expression. Data are presented as mean of technical triplicates of N=1.

5.2. SCT effects on lipolysis in brown adipocytes

SCT is known for its lipolytic actions in WAT (Sekar & Chow 2014a, Stout et al. 1976, Butcher & Carlson 1970). The investigation of SCT´s lipolytic effects in brown fat cells was the aim of the following experiment. A lipolysis assay was conducted *in vitro* with fully differentiated primary brown adipocytes. Cells were stimulated for 2 hours with SCT or ISO. Free fatty acids and glycerol in the cell medium were analysed after two hours of stimulation.

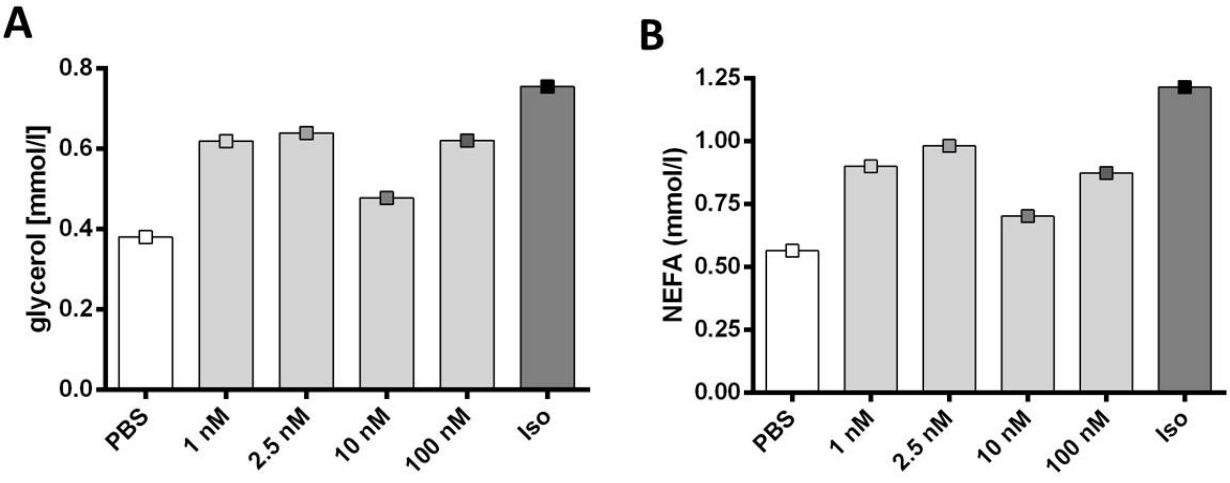

(a) glycerol (b) NEFA

Fig. 9: **Release of glycerol (A) and NEFA (B) induced by stimulation with SCT in brown adipocytes.** Fully differentiated cells were stimulated with increasing concentrations of SCT or with 500 nM of ISO. Glycerol and non-esterified free fatty acids (NEFA), released into the medium during the second hour of stimulation are depicted here. Columns represent the mean of technical replicates.

A lipolytic effect of SCT on brown adipocytes could be shown for all tested concentrations (1 nM to 100 nM) and lipolysis was already fully activated at the lowest concentration of 1 nM SCT (Fig. 9). The amount of released glycerol and NEFAs was similar for both compounds, ISO and SCT. ISO is an agonist of β-ARs and a classical activator of lipolysis. The used concentration of ISO was fivefold higher (500 nM) than the highest concentration of SCT (100 nM).

In this experiment a lipolytic action for SCT was confirmed in brown adipocytes. A stimulation with 100 nM SCT increased the release of glycerol and NEFA approximately 30% compared to the control. In contrast a publication by *Sekar* stated a sixfold induction of glycerol and NEFA release for the stimulation with 100 nM SCT in white adipocytes (Sekar & Chow 2014a). Results for brown adipocytes, which were used in own experiments here, were not published so far.

5.3. *In vitro* stimulation of respiration by SCT

The main function of BAT is the production of heat by uncoupled respiration. Since the *sctr* is expressed in brown adipocytes, we investigated the effects of the hormone on the typical thermogenic BAT function by indirect measurement of oxygen consumption rates (OCR). The adipocytes were treated with oligomycin (OCR during inhibition of coupled respiration), SCT/ISO, FCCP (OCR for fully uncoupled cells) and antimycin A (residual OCR during blocking of mitochondrial respiration) in all respiratory experiments of this section.

5.3.1. SCT induced oxygen consumption in primary brown adipocytes

Fully differentiated brown adipocytes were measured in the XF-96 flux analyzer to determine stimulated respiration. The induction of oxygen consumption was similarly stimulated by SCT and the β-adrenergic agonist ISO, which is a common activator of uncoupled respiration mediated by UCP1 (Fig. 10, A). Applied to the basal respiration, as well SCT and ISO were able to increase oxygen consumption by about 200% (Fig. 10, B). With both compounds the uncoupled respiration reached an extent of about 75% of maximum uncoupled respiration induced by FCCP (Fig. 10, C). There was no statistical difference observed for the respiratory activation by SCT compared to ISO for basal ($p=0.712$) or maximum respiration ($p=0.946$). Both compounds were used in the same concentration. The ability of SCT to induce mitochondrial respiration *in vitro* can be considered equal as by typical β-adrenergic activation (ISO). This suggests a physiological role for SCT in the regulation of BAT.

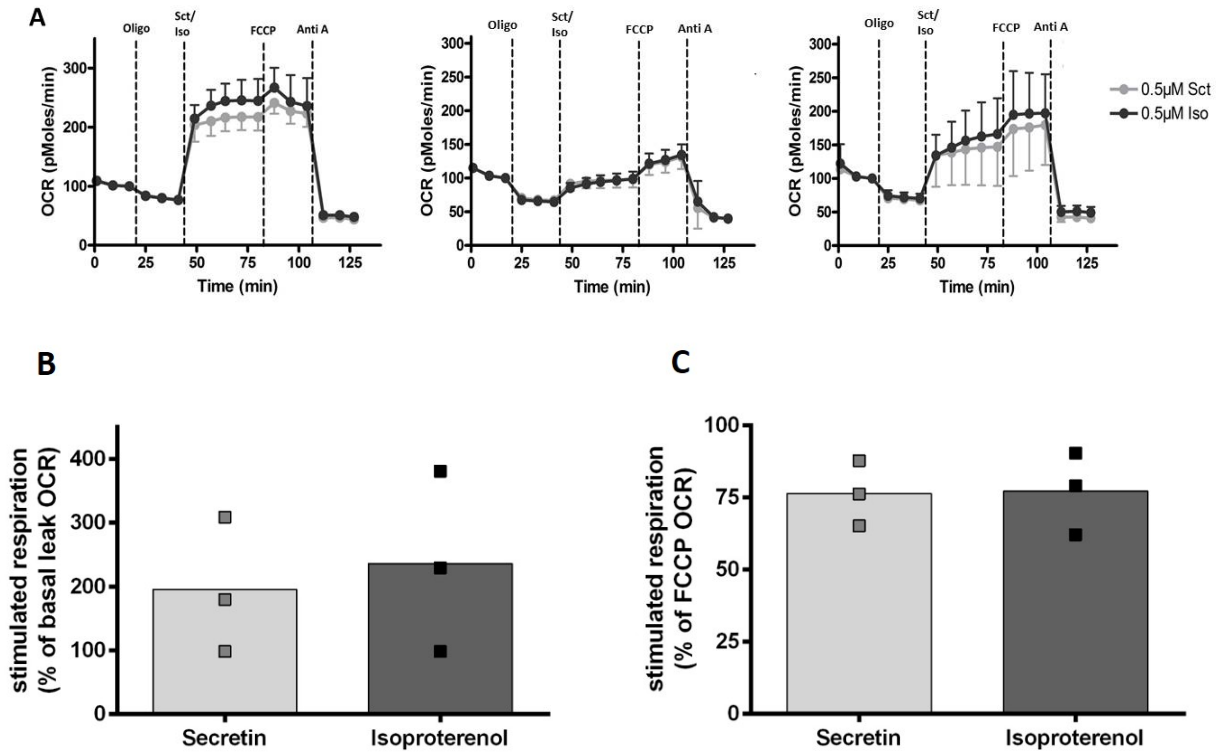

Fig. 10: **SCT induced oxygen consumption in brown adipocytes**.
Respiratory measurement was conducted at the seventh day of differentiation. Three measurements are shown (A) in technical replicates of 6-7; Dots represent means $\pm SD$. Cells were treated with oligomycin (Oligo), SCT/ISO, FCCP and antimycin A (Anti A). Percentaged fold increase above basal respiration was calculated (B, p=0.712). Also percentaged attainment of totally uncoupled FCCP respiration was calculated (C, p=0.946). Values of the three individual measurements (shown in A) with technical replicates of 6-8 per group were used and are represented as dots. Testing for significance was conducted using t-test.

5.3.2. SCT induced oxygen consumption in UCP1 KO primary brown adipocytes

SCT is able to induce respiration in brown fat cells (Fig. 10). To investigate the dependency of this induction upon UCP1, the respiratory measurement was repeated with cells from UCP1 KO mice on a 129/S1-background and related WT controls using the same protocol as in 5.3.1. For both, SCT and ISO, an increase in oxygen consumption after stimulation was found in cells from WT mice (Fig. 11), as shown before. At the same time the induction of respiration by both, SCT or ISO was impaired in cells from UCP1 KO mice. It must be mentioned that the cells from UCP1 KO mice also exhibited a much smaller fully uncoupled respiration by FCCP than WT controls.

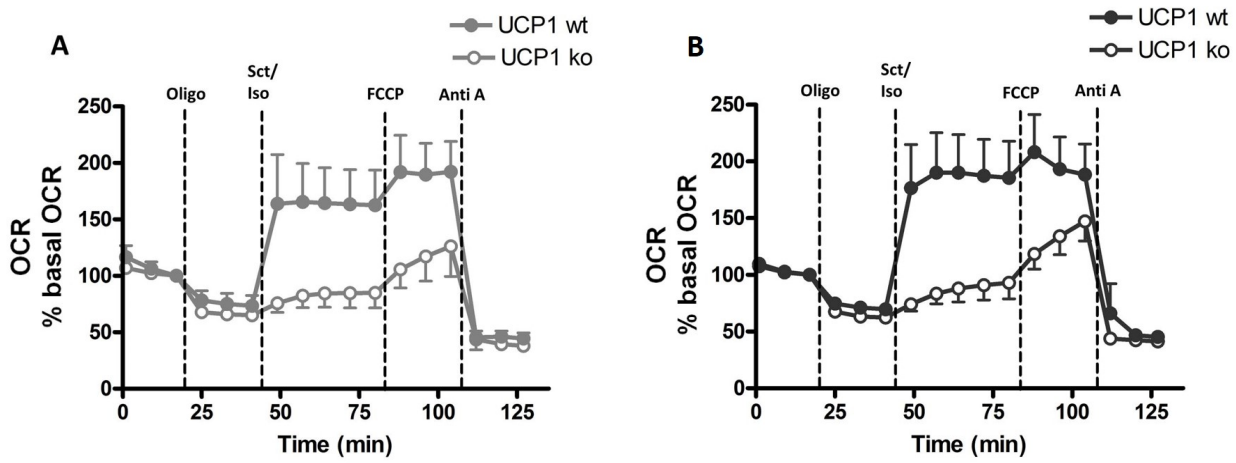

(a) Secretin (b) Isoproterenol

Fig. 11: **SCT induced oxygen consumption in brown adipocytes of UCP1 KO mice**
Measurement was conducted at the seventh day of differentiation. Cells were injected with oligomycin (Oligo), SCT (left)/ISO (right), FCCP and antimycin A (Anti A). Dots represent means $\pm SD$ of 6-16 technical replicates. White cycles indicate UCP1 KO cells and filled cycles indicate UCP1 WT cells.

The results of this experiment clearly point out that the induction of respiration in brown adipocytes by β-adrenergic stimulation or by SCT is dependent on UCP1. The potential for direct activation of UCP1 already is established for ISO. In this experiment it was also confirmed for the peptide hormone SCT.

5.3.3. SCT induced respiration and *sctr* expression after chronic roziglitazone treatment

The PPARγ agonist rosiglitazone increases *ucp1* expression in brown adipocytes during chronic stimulation and thereby enlarges the respiratory capacity of the cells. Primary brown adipocytes were cultured with the PPARγ agonist during the seven days of differentiation. Afterwards, the cells were stimulated with SCT or ISO to induce respiration. Furthermore, the expression of the *sctr* after rosiglitazone treatment was measured by RNA sequencing.

A chronic PPARγ agonistic treatment strongly decreased the induction of respiration induced by SCT (Fig. 12, A). The β-adrenergic agonist ISO was able to increase respiration about 250% compared to basal levels. This is likely to be caused by the higher expression of *ucp1* in the brown adipocytes following chronic rosiglitazone treatment, which is in line with published results. In comparison a stimulation with SCT was not

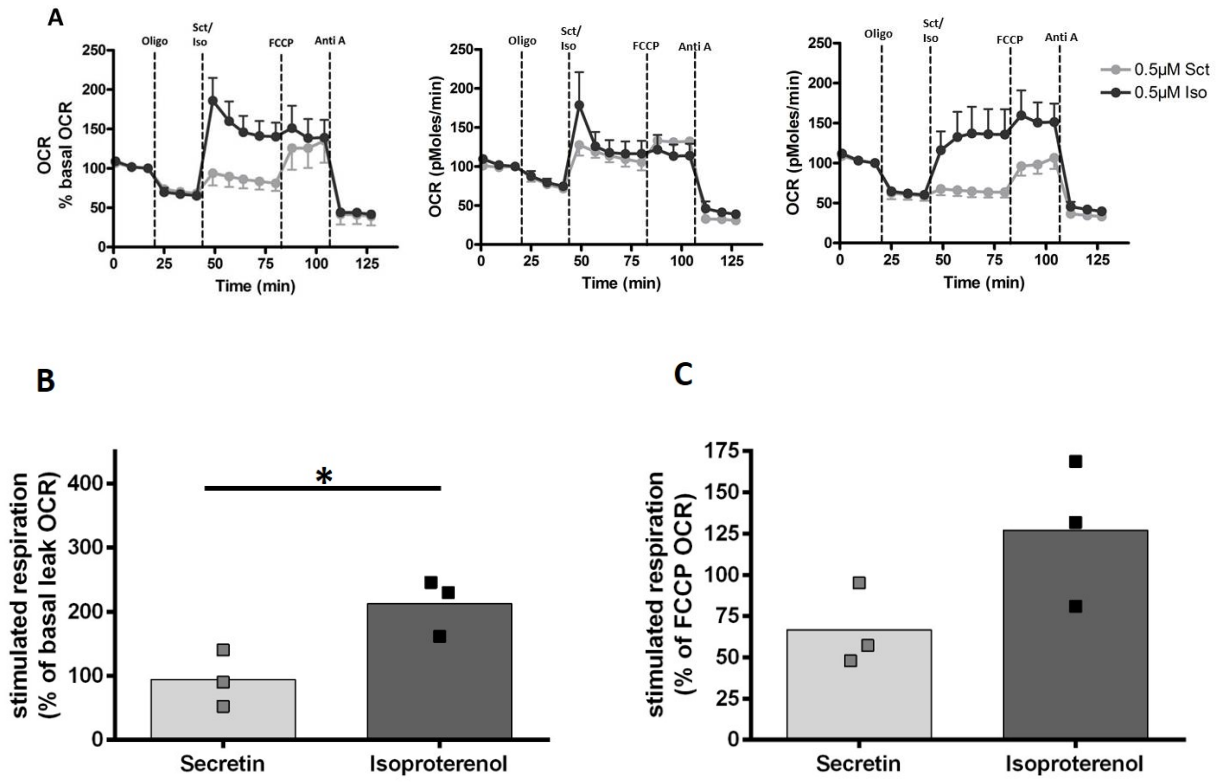

Fig. 12: **SCT induced oxygen consumption in brown adipocytes after chronic rosiglitazone treatment.** Measurement was conducted at the seventh day of differentiation. Cells were treated with oligomycin (Oligo), SCT/ISO, FCCP and antimycin A (Anti A). Three measurement are shown in (A) in technical replicates of 6-8. Dots represent means $\pm SD$. Percentaged fold increase above basal respiration was calculated (B, p=0.031). Also percentaged attainment of totally uncoupled FCCP respiration was calculated (C, p=0.108). Therefore, values of the three individual measurements (shown in A) with technical replicates of 6-8 per group were used and are represented as dots. Statistical analysis was conducted using t-test and * indicates p<0.05.

able to increase oxygen consumption compared to basal OCR levels, which were measured at the beginning of the recording. For the stimulation of respiration above basal OCR the difference between SCT and ISO was significant (p=0.031) (Fig. 12, B). For two of the three measurements the stimulation with ISO led to fully uncoupled cells, which could not be further stimulated by FCCP. The induction of respiration in percentage of fully uncoupling by FCCP induced OCR was not significant between SCT and ISO (p=0.108).

As already shown in a previous experiment (Fig. 10), SCT has been expected to enhance oxygen consumption in a comparable amount as ISO, also in a setting with chronic rosiglitazone treatment, which increases the respiratory potential of brown adipocytes by intensified *ucp1* expression. Since the effects of ISO and SCT are not mediated by the same receptors, the regulation of expression of their respective receptors may provide an explanation for the divergent results in this experiment.

The expression of *sctr* and *β3-ar* following chronic rosiglitazone treatment was analysed by RNA sequencing in primary brown adipocytes and compared to untreated differentiated and also to undifferentiated cells (Fig. 13). For the *sctr* the data revealed a decreased expression by chronic rosiglitazone treatment (A), which was not significant. The cells from the stromal vascular fraction (SVF) did not differ from the two differentiated groups. The expression of the *β3-ar* (B) was significantly increased by differentiation (no Rosi vs. SVF p=0.017; Rosi vs. SVF p=0.023). The effect was independent of rosiglitazone treatment (p=0.549).

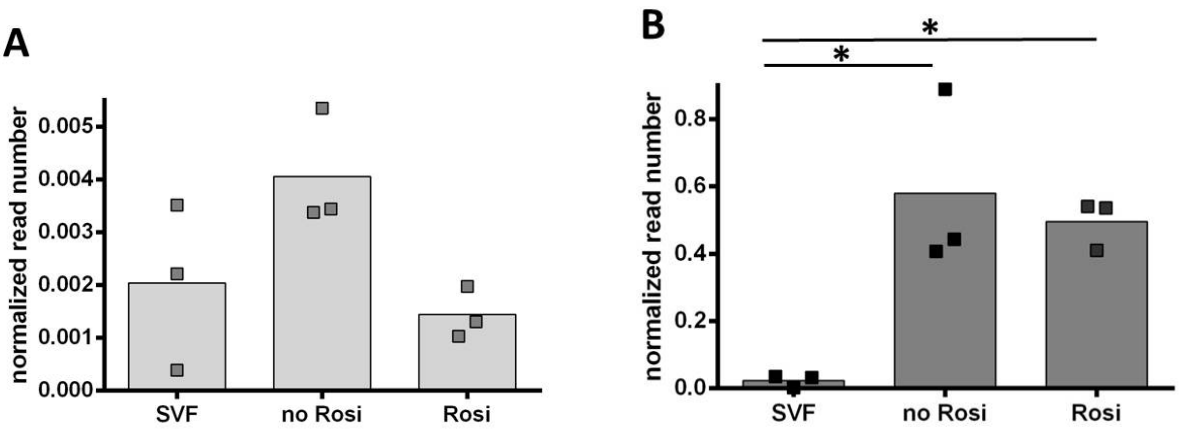

(a) secretin receptor

(b) β3-adrenergic receptor

Fig. 13: ***sctr* and β*3-ar* expression in brown adipocytes following chronic rosiglitazone treatment.** Isolated cells of stromal vascular fraction from brown adipose tissue depots were either analysed directly (SVF) or cultured and differentiated with (Rosi) or without (no Rosi) chronic treatment of 100 nM rosiglitazone for seven days and afterwards analysed by RNA sequencing. The bars represent the mean of N=3, single measurements are depicted as dots. Statistics were conducted using one-way ANOVA and there were no significant differences between the three groups for the expression of the *sctr* ($p=0.070$). For the β*3-ar* expression there was a significant regulation between the groups ($p=0.011$). Pairwise multiple comparison (Holm-Sidak method) showed a significant difference for no Rosi vs. SVF ($p=0.017$) and Rosi vs. SVF ($p=0.023$). The * indicates $p<0.05$.

The reduction in the expression of the *sctr* gives an explanation for the diminished respiratory response of the cells that were stimulated with SCT and chronically treated with rosiglitazone (Fig. 12).

5.4. Impact of SCT stimulation on *ucp1* expression in primary adipocytes

In many cases activators of BAT do not only acutely induce the respiratory activity of the tissue, but also increase the respiratory capacity by increasing the expression of *ucp1*. In the following section, effects of SCT on *ucp1* mRNA expression were tested. An induction of *ucp1* abundance in brown adipocytes indicates BAT recruitment, while in white adipocytes the appearance of brite cells indicates browning of WAT.

5.4.1. *ucp1* expression following stimulation with SCT in differentiated white and brown adipocytes

For the following experiment differentiated inguinal white and interscapular brown primary adipocytes were stimulated with SCT or ISO. Expression of mRNA was determined with qRT-PCR.

SCT was able to increase the expression of *ucp1* in cells from iWAT (Fig. 14, A). The effect was highly significant and comparable to the induction of *ucp1* expression by ISO (PBS vs SCT $p<0.001$; PBS vs ISO $p<0.001$; SCT vs ISO $p=0.066$). It can be concluded that SCT has the potential to induce browning in iWAT adipocytes to a similar degree as ISO.

Likewise, in primary brown adipocytes SCT significantly increased the expression of *ucp1* compared to the unstimulated PBS control (PBS vs SCT $p=0.008$; PBS vs ISO $p=0.018$; SCT vs ISO $p=0.291$). Again, a stimulation with ISO was used as a positive control and induced *ucp1* expression in a similar range as SCT. These results show that SCT does not only acutely activate UCP1 mediated respiration in brown adipocytes. SCT is also able to increase *ucp1* expression in those cells and thereby enhances their thermogenic potential. It has to be mentioned that for this experiment SCT was used in a fivefold lower concentration than ISO. To predict differences in the effectiveness of the two compounds concerning the required minimum concentration further determinations were performed in a next step.

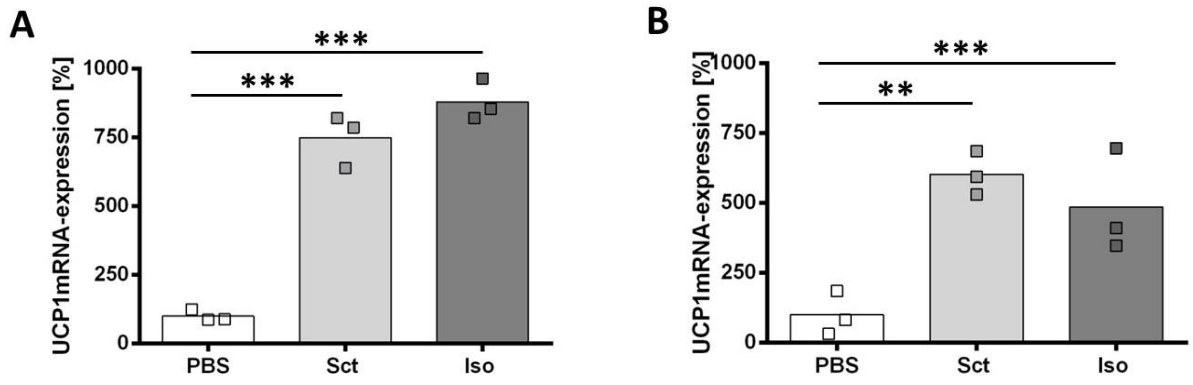

(a) inguinal white adipocytes (b) brown adipocytes

Fig. 14: **SCT induced *ucp1* expression in primary adipocytes.**
Differentiated primary adipocytes from iWAT (A) or BAT (B) were stimulated with 0.1 µM SCT or 0.5 µM ISO for 6 hours. Expression of *ucp1* mRNA was measured by qRT-PCR and normalised to TFIIB expression. Results were standardised to PBS treated condition. Bars represent means (N=3) and dots represent single measurements, each consisting of technical triplicates. For statistical analysis one-way ANOVA was conducted (WAT: PBS vs Sct $p<0.001$; PBS vs Iso $p<0.001$; Sct vs Iso $p=0.066$; BAT: PBS vs Sct $p=0.008$; PBS vs Iso $p=0.018$; Sct vs Iso $p=0.291$).

5.4.2. Dose-dependent induction of *ucp1* expression in adipose tissues

In most experiments examining the effect of a substance, supraphysiological concentrations are used. Therefore, it is reasonable to determine the lowest amount that still induces an effect *in vitro*. This concentration can be compared to physiological levels for further evaluation of the biological relevance. Differentiated primary adipocytes isolated from BAT and iWAT were stimulated for six hours with concentrations from 1 nM to 100 nM, respectively 1 μM of SCT. Dose-dependent effects upon stimulation of *ucp1* expression were elucidated by qRT-PCR. No dose-dependent modulation of *ucp1* expression was detected for the stimulation with various concentrations of SCT (Fig. 15). The lowest concentration of 1 nM was able to provoke the maximum response in both adipose tissues. Statistics were only performed for brown adipocytes (Fig. 15, B). All concentrations of SCT significantly ($p<0.01$) increased *ucp1* expression compared to the negative control (PBS). There were no statistical differences detected between the concentrations.

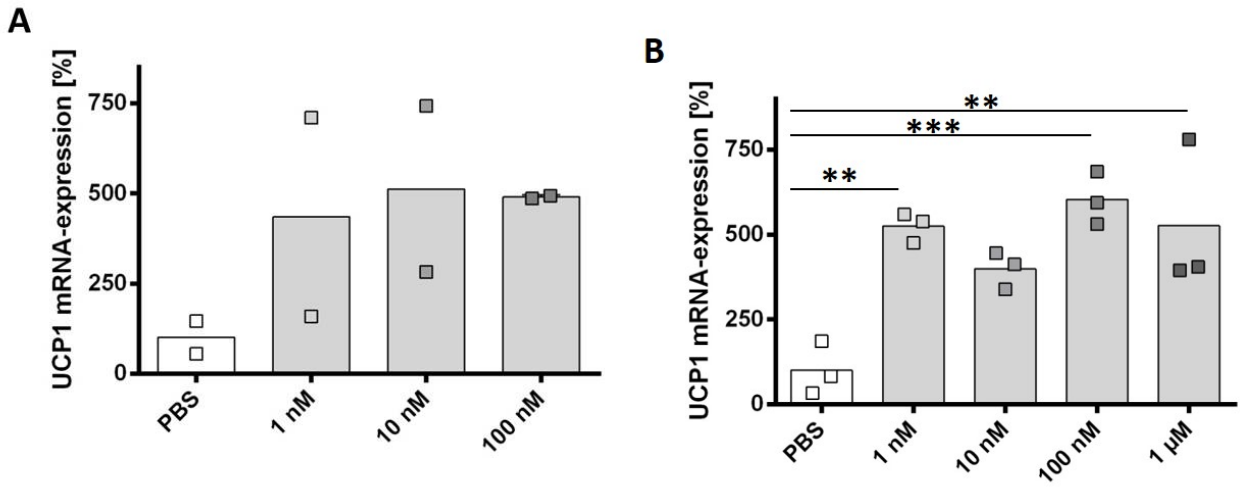

(a) inguinal white adipocytes (b) brown adipocytes

Fig. 15: **Dose-dependent *ucp1* expression following SCT stimulation in primary adipocytes.** Cells were stimulated with various concentrations of SCT for 6 hours. Expression of *ucp1* mRNA was measured by qRT-PCR and normalised to TFIIB-expression. Results were standardised to PBS condition. Bars represent the mean of N=2, single values shown as dots, in cells from iWAT (A) and N=3 from BAT (B) measured in technical triplicates. Statistical analysis for brown adipocytes was conducted using one-way ANOVA (BAT: Pairwise multiple comparison (Holm-Sidak method) for PBS vs 1 nM p=0.008; PBS vs 10 nM p=0.065; PBS vs 100 nM p=0.003; PBS vs 1 μM p=0.009 and no significant differences between the concentrations of SCT).

5.4.3. Signalling pathway of SCT stimulated induction of *ucp1* expression

Since the SCTR is a GPCR like the β-3-AR, both can activate the PKA via cAMP accumulation. To determine the congruency of downstream pathways of both receptors, inhibitors for known signalling mediators of *ucp1* regulation were utilised. On the one hand a commercial inhibitor for PKA (called H89) and on the other hand SB203580 (SB), an inhibitor of p38 mitogen-activated protein kinase (MAPK) were used. The levels of *ucp1* mRNA expression were measured by qRT-PCR and compared to the *ucp1* expression following a stimulation with SCT and ISO alone.

The expression of *ucp1* was increased by SCT and ISO in white and also brown adipocytes as shown before.

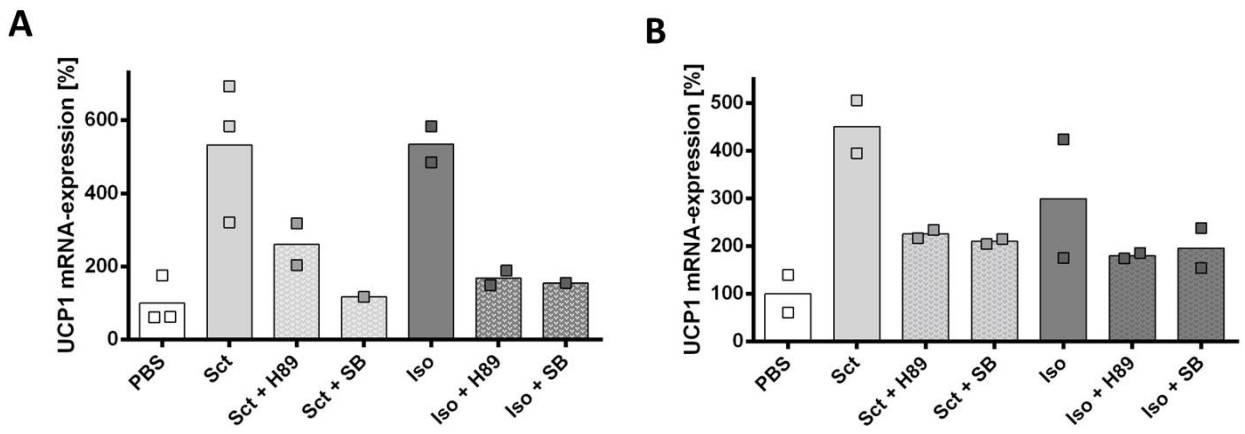

(a) inguinal white adipocytes

(b) brown adipocytes

Fig. 16: **SCT induced *ucp1* expression using PKA- and p38-inhibitors.**
Primary adipocytes of iWAT (A) and BAT (B) depots were stimulated for 6h with SCT and furthermore with inhibitors of PKA (H89) or p38 (SB). Expression of *ucp1* mRNA was measured by qRT-PCR. Results were normalised to TFIIB as housekeeper gene and standardised to gene expression by PBS treatment. Columns represent mean of N=1-3, single values shown as dots.

The inhibition of PKA with H89 markedly reduced the *ucp1* mRNA levels in SCT and ISO stimulated cells (Fig. 16) independent of the fat depot. However, the level of *ucp1* expression in non-stimulated cells (PBS) was not reached. This result indicates that the induction of *ucp1* by SCT as well as ISO, is mediated by PKA. Furthermore, in both types of adipocytes the expression of *ucp1* was also decreased after addition of the p38 MAPK inhibitor SB to the stimulation with SCT or ISO. These results suggest, that the activation of the SCTR in fat tissues leads to an induction of *ucp1* expression, which is mediated by PKA and p38 MAPK signalling, like it is already known for β-adrenergic stimulation.

5.5. SCT induced UCP1 activation in mice

In chapter 5.3 the effect of SCT on acute activation of respiration has been shown in *in vitro* experiments. In this section, the stimulation of respiration is investigated *in vivo*. Therefore, SCT was injected i.p. into 129/S6-mice and oxygen consumption was measured by indirect calorimetry. In addition the impact of SCT injections in UCP1 KO mice, cold adapted mice and also high-fat diet fed mice was investigated.

5.5.1. Acute effect of SCT on respiration in WT mice

For the measurement of oxygen consumption, WT mice were either i.p. injected with PBS or with 0.5 mg/kg of SCT solved in PBS.

The calorimetric determination of basal metabolic respiration (BMR) was performed in advance at 30 °C for 3 hours (results are shown in the supplement, Tab. 6.1). All values were highly comparable between the two groups. Hence, differences between the treatment groups were not due to inappropriate matching.

Independently of the injected substance, mice showed an increased metabolic activity in the first five minutes following injection measured at 27 °C (Fig. 17). This peak is assumed as "arousal" since most mice were woken up for injection and showed a higher level of excitement for the first minutes back in the cage (presumably caused by the disturbance). After ten to fifteen minutes the mice in both groups started to calm down and showed a reduced activity level, which has been observed through a window in the climate chamber. A sedation in the injected mice was also displayed in the declining levels of HP (Fig. 17, A). The PBS group almost reached basal metabolic levels (indicated by grey background) from about 20 minutes after injection until the end of the measurement. Mice injected with SCT showed in opposite a distinct higher HP until the end of recording. The AUC was calculated for the whole 45 minutes of the measurement for both groups (Fig. 17, B). The basal metabolic rates were subtracted for each mouse individually (mean shown in grey in Fig. 17, A). The difference for the AUC was highly significant between the two treatments ($p=0.001$).

In the RER (Fig. 17, C) there was no difference between the groups regarding the whole 45 minutes of measurement (AUC: $p=0.875$). However, the RER showed a deviation between SCT and PBS injection for the first 15 minutes after injection. After the administration of SCT the RER dropped compared to the PBS group. The analysis of the AUC for a selected time frame from minute 0 to 15 of the measurement revealed a significant higher RER for the PBS injected mice ($p=0.031$). A possible explanation for this effect would be that the lipolytic action of SCT lead to the metabolisation of fat as a fuel and thereby reduced the RER as a measure of metabolised nutrients.

It can be concluded that mice show a higher rate of metabolic activity after the injection of SCT compared to PBS. This result is in line with the *in vitro* data shown before (Fig. 10).

5.5.2. Acute effect of SCT on respiration in UCP1 KO mice

Mice show a metabolical activation after SCT injection. So far, it is not clear which tissue is responsible for the increase in oxygen consumption. To check if the effect is dependent on UCP1, like already demonstrated for *in vitro* experiments in 5.3.2, the calorimetric measurements were repeated in UCP1 KO mice. Hence, mice (WT and KO) of the 129/S1-UCP1 KO strain were individually measured at 30 °C to determine BMR (Tab. 5.1).

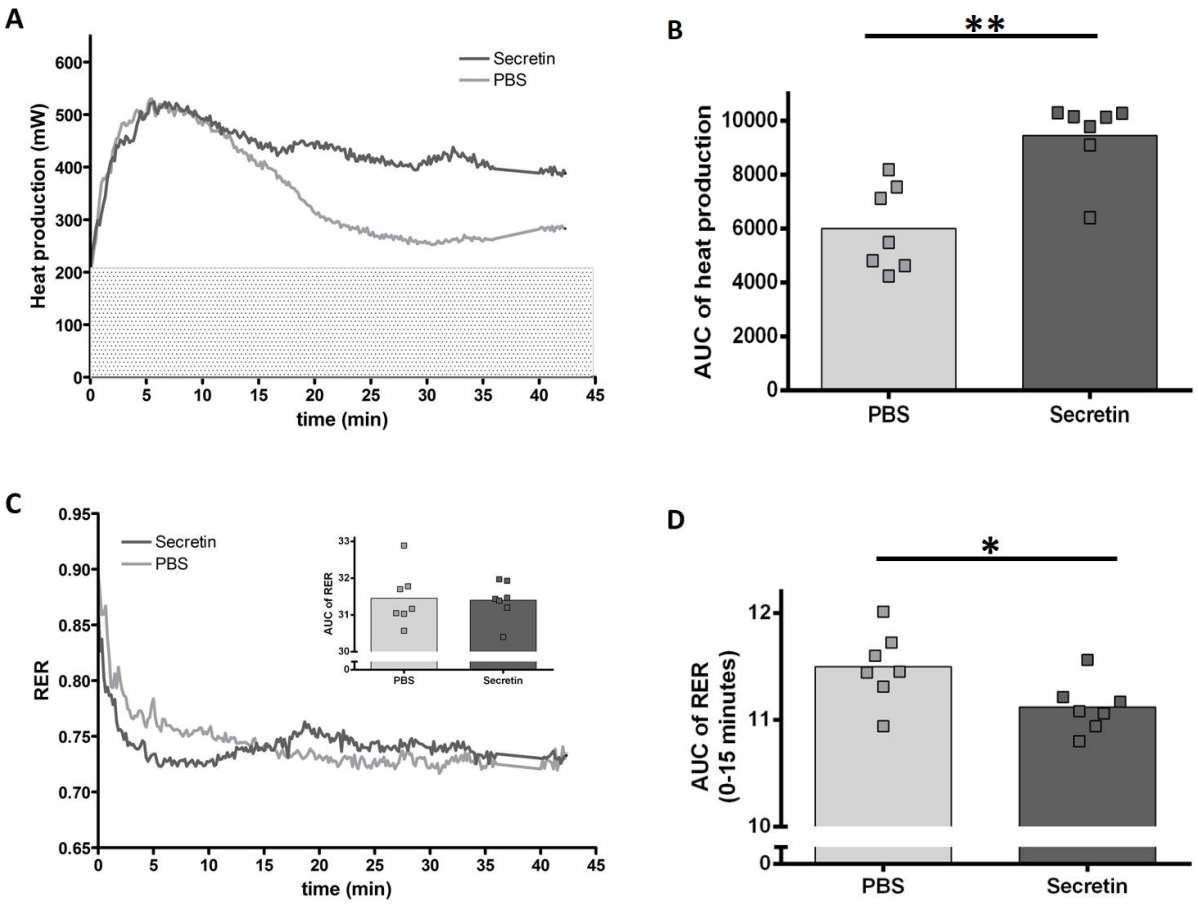

Fig. 17: **SCT induced respiration in WT 129/S6 mice.**
Mice received 0.5 mg/kg SCT solved in PBS or an equal volume of PBS via i.p. injection. Measurement was performed at 27 °C. The mean of N=7 mice per group is shown for HP (A, mean of basal HP measured at 30 °C depicted as grey background). The AUC for HP for 45 minutes of measurement is depicted (B, p=0.001). For this analysis the basal HP was subtracted individually for each mouse. The RER is shown as mean of N=7 mice per group and as AUC for the whole measurement (C, p=0.875). AUC was furthermore calculated for the first 15 minutes of measurement (D, p=0.031). Statistical analysis were performed using t-test.

WT and KO mice showed a comparable bodyweight (p=0.851) for all groups. During BMR measurements KO mice exhibited a slightly increased RER (p=0.295) and HP (p=0.782). There was no difference between the treatment groups within one genotype (Tab. 6.2, supplement). Statistics were conducted using two-way ANOVA.

Table 5.1: Values for body weight (BW) and basal metabolic measures for RER and HP in UCP1 KO and WT mice at 30 °C

	WT		**KO**	
	PBS (N=9)	SCT (N=9)	PBS (N=7)	SCT (N=5)
BW (g)	24.2 ±2.0	24.3 ±1.5	24.4 ±2.4	24.5 ±1.5
RER	0.86 ±0.04	0.84 ±0.03	0.88 ±0.05	0.89 ±0.07
HP (mW)	200.9 ±17.0	208.3 ±24.3	217.0 ±21.7	220.1 ±11.0

In advance to BMR measurements, the respiration following i.p. injection with SCT and PBS was determined by indirect calorimetry (Fig. 18 and Fig. 19). WT mice exhibited, after the first 15 minutes of "arousal", a higher oxygen consumption rate and thereby HP after the i.p. injection of SCT compared to the PBS injected control mice (Fig. 18, A). The AUC for the whole recording was significantly different between the two treatment groups in WT mice (p=0.002, Fig. 18, C). This result confirmed the data for 129/S6-WT mice after i.p. SCT injection (Fig. 17). In the UCP1 KO mice there was no difference observed for HP between SCT and PBS treated mice during the course of recording (Fig. 18, B) or for the AUC (Fig. 18, C; p=0.482).

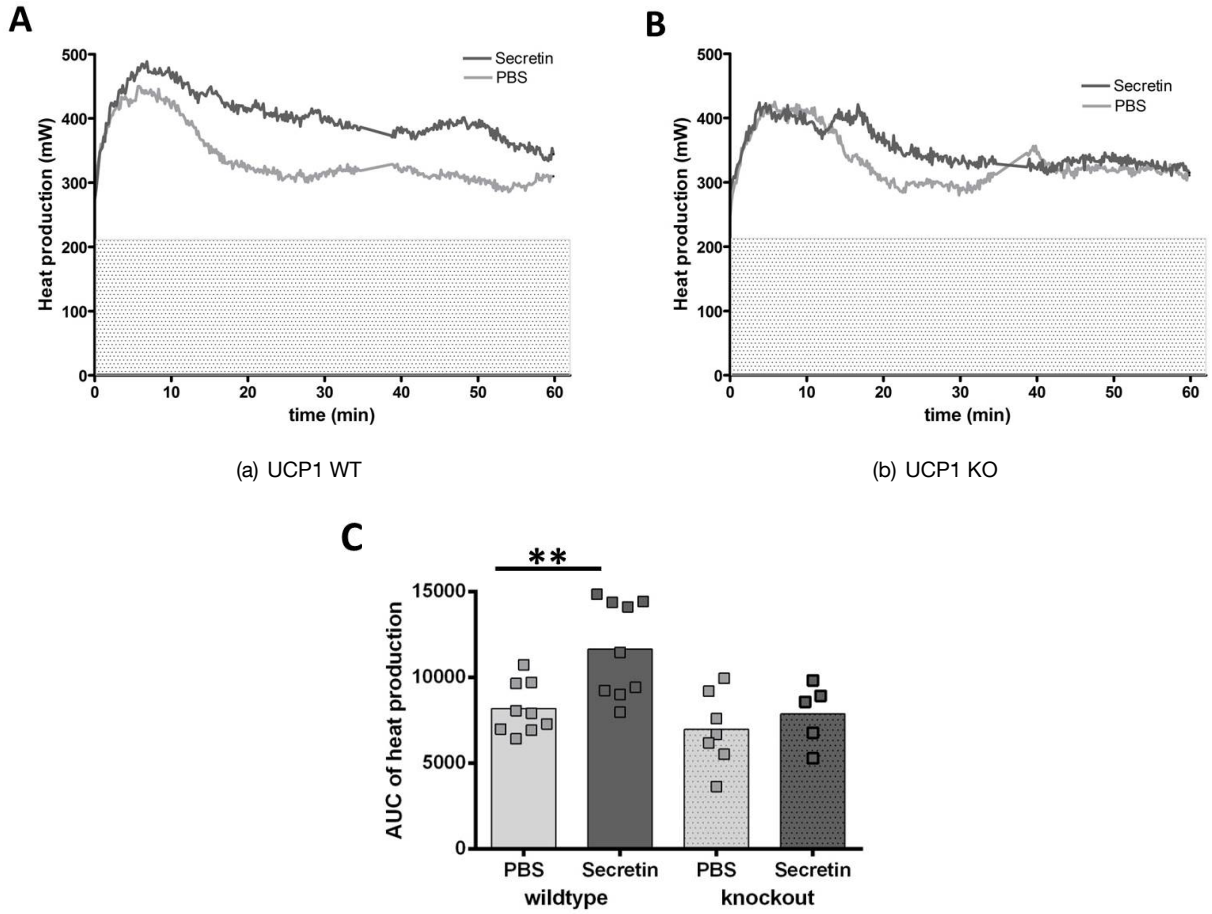

(a) UCP1 WT

(b) UCP1 KO

Fig. 18: **SCT induced HP in UCP1 KO mice.**
Mice received 0.5 mg/kg SCT solved in PBS or equal volume of PBS via i.p. injection. Measurement was performed at 27 °C. In (A) the mean for N=9 WT mice per group and in (B) the mean for N=5-6 KO mice is shown for HP (mean of basal HP measured at 30 °C depicted as grey background). In (C) the AUC for HP for 60 minutes of measurement is depicted. Statistics were conducted using two-way ANOVA. Equal variance test failed (P < 0.050) and therefore a pairwise multiple comparison was conducted using Tukey test (genotype: p=0.005; treatment: p=0.013; genotype x treatment: p=0.128). There was a significant difference for the treatment within WT mice (p=0.002; indicated by **) but not within KO mice (p=0.482) and furthermore a significant difference for the genotype within SCT treatment (p=0.005), but not within PBS treatment (p=0.275), which is not illustrated in the graph.

The drop in the RER during the first 10 minutes following injection, which has already been shown for WT mice in Fig. 17 (C), was reproduced for WT and KO mice (Fig. 19, A and B). If this drop in the RER reflects lipid oxidation by SCT, it is expected that this effect also occurs in UCP1 KO mice since UCP1 does not contribute to the oxidation of lipids. Neither in WT nor in KO mice there is a difference for the RER for both injection groups from minute 15 to the end of the measurement. There was no statistical difference for the AUC of RER for both genotypes after injection of PBS or SCT for the whole measurement (Fig. 19, C)

For the first 15 minutes there was a trend towards a higher AUC for PBS treated mice in both groups, which was not significant (Fig. 19, D; p=0.134).

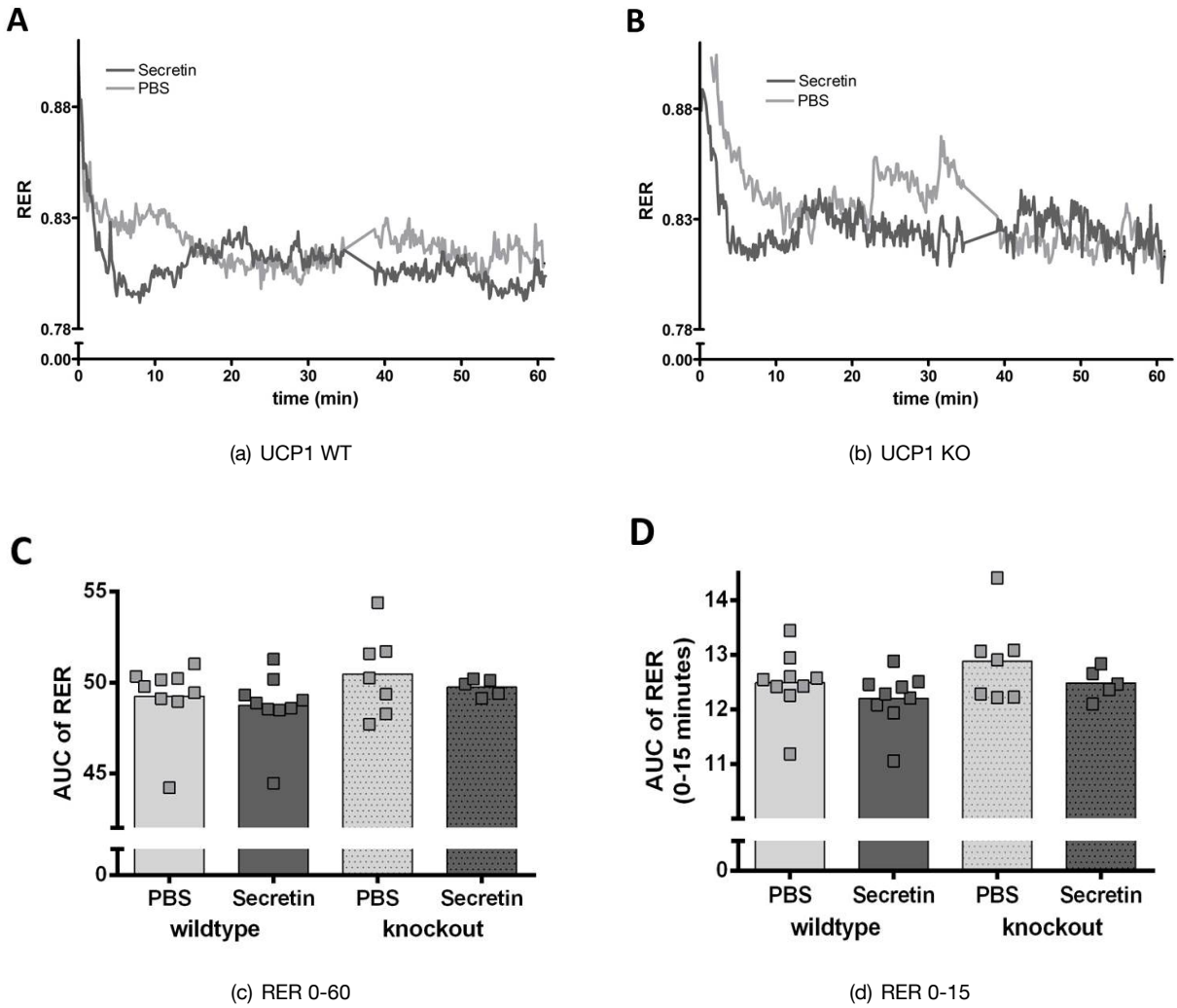

(a) UCP1 WT

(b) UCP1 KO

(c) RER 0-60

(d) RER 0-15

Fig. 19: **SCT effects on respiratory exchange ratio in UCP1 KO mice.**
The RER after i.p. injection of SCT or PBS is shown as mean for N=9 in WT mice (A) and as a mean for N=5-6 in UCP1 KO mice (B). The AUC of the RER was calculated for the whole 60 minutes of recording (C; genotype: p=0.128; treatment: p=0.399; genotype x treatment: p=0.875) and for the first 15 minutes of measurement (D; genotype: p=0.136; treatment: p=0.131; genotype x treatment: p=0.796). Statistical analysis were conducted using two-way ANOVA.

These results lead to the conclusion that the metabolic activation by SCT injection in mice is mediated by an induction of UCP1 and by an activation of BAT.

5.6. The activation of BAT by SCT in different physiological conditions

The role of SCT in the regulation of physiological BAT functions like heating to defend body core temperature, control of energy balance in states of over-feeding and thermoregulatory feeding were investigated in the following section.

5.6.1. Cold-adapted mice

The cold-adaptation of mice to a 4 °C environment strongly increases heating capacity and thereby the body content of BAT. In the following experiment, it was tested, if a higher capacity of BAT by cold-acclimatisation leads to an altered effect of SCT stimulated HP in mice. Furthermore,the expression of the *sctr* in fat tissues of cold-adapted mice was quantified.

5.6.1.1. SCT induced energy expenditure in cold-adapted mice

129/S6 mice were adapted to 4 °C ambient temperature for 4 days at the age of 8 weeks. At the fourth day calorimetric measurements were performed for three hours at 30 °C to identify basal metabolic rates (BMR) for RER and HP (Tab. 5.2). The mice in the two injection groups (PBS vs. SCT) showed a similar bodyweight (p=0.597). During basal metabolic measurements there was no difference between the two treatment groups for RER (p=0.668) or HP (p=0.960) detected, which suggests that the groups were appropriately matched. Statistics were performed using one-way ANOVA. After the basal metabolic measurement the mice received an i.p. injection of SCT or PBS and were individually measured for one hour at 27 °C.

Table 5.2: Values for body weight (BW) and basal metabolic measures for RER and HP in cold-acclimated mice (for 4 days at 4 °C) measured at 30 °C

	PBS (N=7)	SCT (N=7)
BW (g)	25.1 ± 1.2	24.7 ± 1.9
RER	0.79 ± 0.04	0.78 ± 0.04
HP (mW)	207.6 ± 30.7	208.3 ± 19.3

In cold-adapted mice both injection groups showed again a short phase of "arousal" following injection of SCT or PBS indicated by an activated metabolism for about 10 minutes (Fig. 20, A). Afterwards the HP was decreased in the PBS group as already shown for WT mice (Fig. 17, A and Fig. 18, A). However, in this experimental setting also cold-adapted mice injected with SCT decreased their metabolic rate after the short phase of "arousal", which was similar to the PBS group. Although the capacity of BAT was increased by the cold exposure, the activation of BAT respiration by SCT vanished. The AUC of HP for the 45 minutes of recording did not differ between the two treatment groups (Fig. 20, B; p=0.953).

A drop in the RER after injection of SCT could, however, also be found in cold-adapted mice (Fig. 20, C). There was no statistical significant difference observed for the AUC of the RER considering the whole 45 minutes of recording (inserted in Fig. 20, C; p=0.120). For the first 15 minutes following the i.p. injection the difference in the AUC was however significant for the two groups (Fig. 20, D; p=0.030). The adaptation to

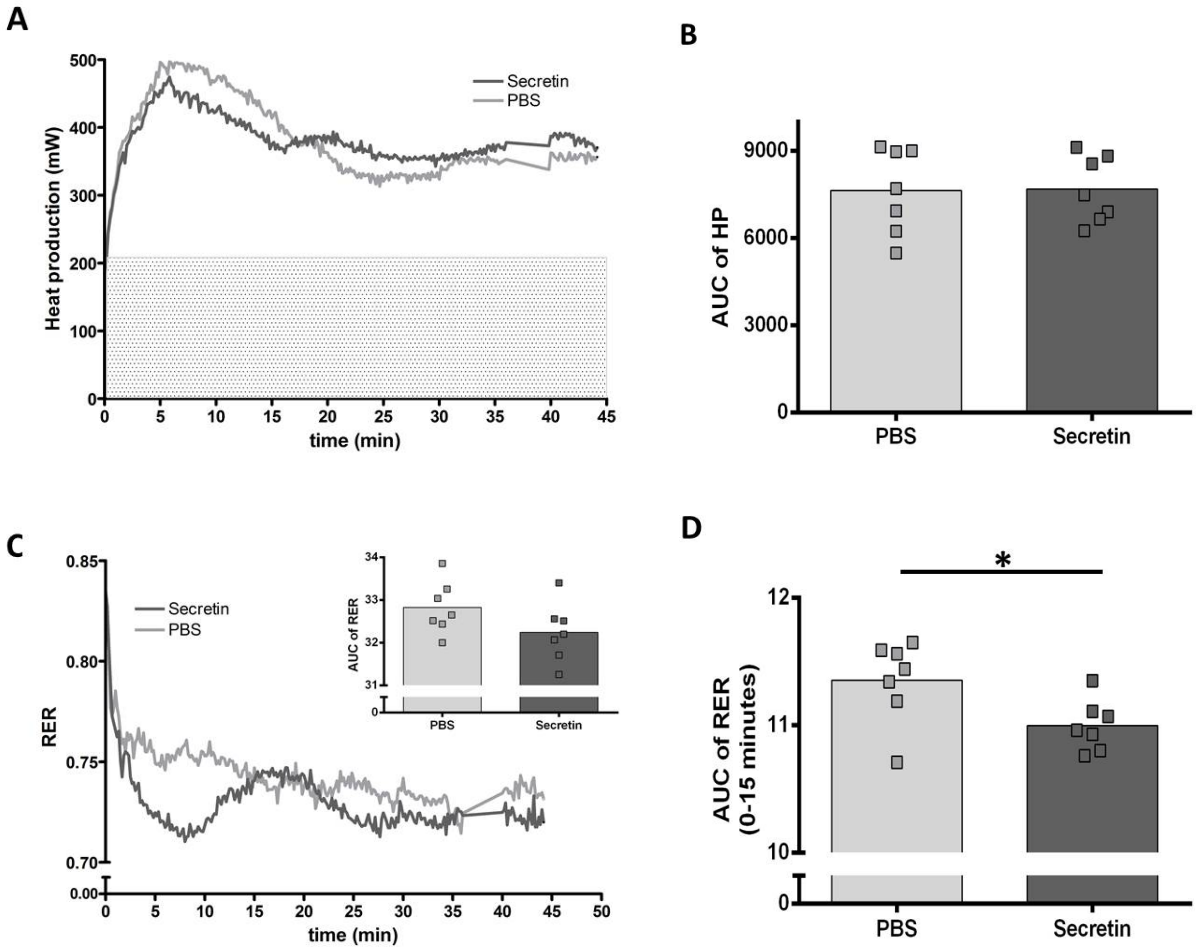

Fig. 20: **SCT effects on metabolic activation in cold-adapted mice.**
Mice were adapted to 4 °C for four days and received than 0.5 mg/kg SCT solved in PBS or PBS via i.p. injection. Measurement was performed at 27 °C. In (A) the mean for N=7 mice per group is shown for HP. The AUC for HP in the first 45 minutes of measurement is depicted in (B) (p=0.953). For this analysis the basal HP was subtracted individually for every mouse. The RER is shown as mean for N=7 mice per group (C). The AUC was calculated for the whole measurement (shown in figure (C), p=0.120) and for the first 15 minutes of measurement (D) (p=0.030; the * indicates p<0.05). Statistical analysis were performed using t-test.

4 °C of ambient temperature did not affect the drop in RER following an injection with SCT.

Taken together, cold acclimation counteracts the thermogenic effect of SCT on BAT. Therefore, it was tested whether the expression of the *sctr* gene in fat tissues is downregulated in response to cold acclimation, which would result in a desensitisation of the tissue towards SCT as it has already been shown for chronic rosiglitazone treatment (see Fig. 12).

5.6.1.2. *sctr* expression in adipose tissues of cold-adapted mice

Subsequent to the calorimetric measurement, distinct fat depots were sampled from cold-acclimated mice and *sctr* as well as *ucp1* gene expression were measured.
Cold-acclimation for 4 days led to significantly increased *ucp1* expression in fat depots of mice, especially in BAT and iWAT, but also in gWAT (Fig. 21, B), which in general exhibits a distinct lower level of *ucp1* expression. This effect is well known from literature, since cold challenges increase the BAT capacity and

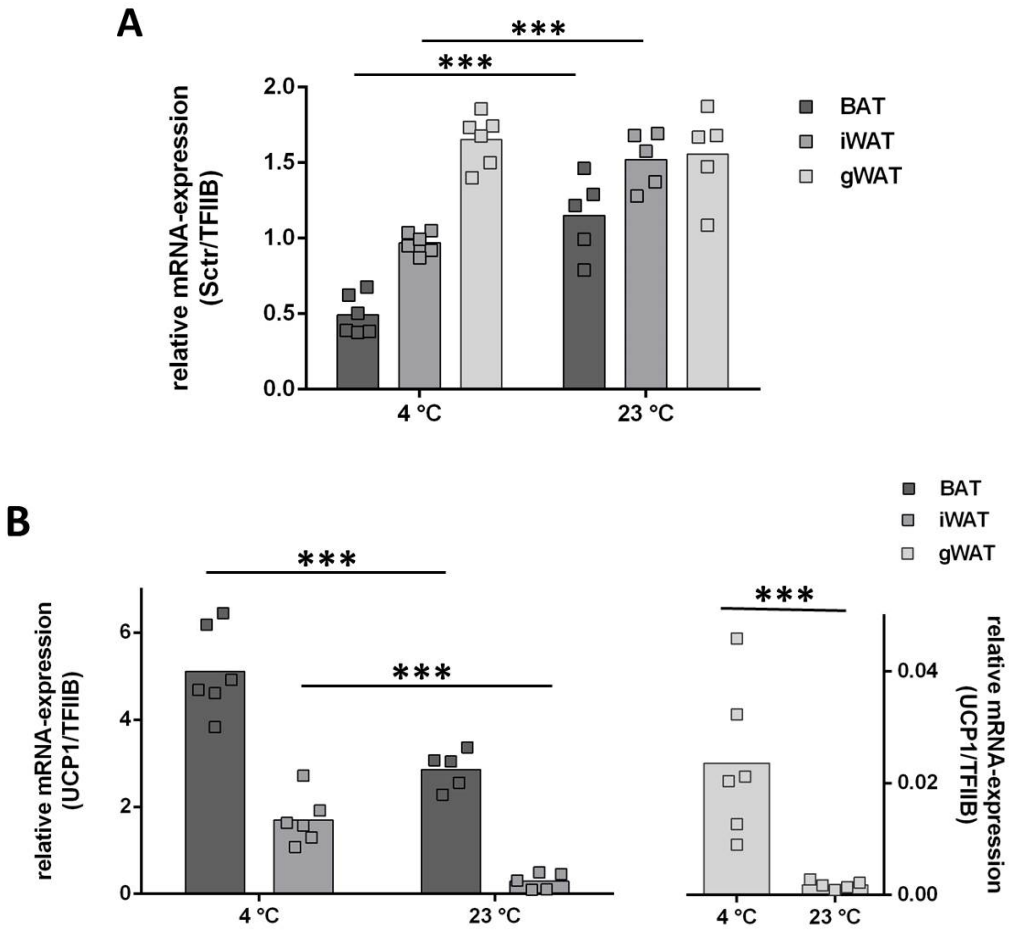

Fig. 21: **Relative mRNA expression of *sctr* and *ucp1* in fat depots of cold-adapted mice.**
Mice were adapted for 4 days to an ambient temperature of 4 °C or were continuously kept at 23 °C as control group. Relative mRNA level were measured via qRT-PCR. Results were normalised to TFIIB as housekeeper gene and represented as mean of N=5-6. Statistical analysis was conducted using two-way ANOVA. There was a significant regulation of *sctr* (fat depot: $p<0.001$; temperature: $p<0.001$; fat depot x temperature: $p<0.001$). For *ucp1* expression data were not distributed normally (Shapiro-Wilk $p<0.05$) and Tukey test was used for pairwise multiple comparison (fat depot: $p<0.001$; temperature: $p<0.001$ and fat depot x temperature: $p=0.174$). The *** indicate a significant difference ($p<0.001$) for the ambient temperature upon gene expression within one fat depot tested by Tukey test.

thereby *ucp1* expression in mice. Notably, *sctr* gene expression was highly significant downregulated by cold exposure in iBAT and also iWAT, whereas the receptor was not altered in gWAT (Fig. 21, A). Taken all together, the results in 5.6.1 indicate that the defence of the body core temperature in a cold challenge, which is the classical task of BAT, is not regulated via a SCT signalling pathway, because the sensitivity of BAT for SCT is strongly decreased in such a condition. SCT is thereby considered to mediate other regulatory issues of BAT.

5.6.2. HFD fed mice

5.6.2.1. SCT induced energy expenditure in HFD fed mice

It is discussed in literature, that besides cold challenge, also a state of excess energy could lead to an amplification of UCP1 expression in BAT and thereby increase its capacity (Fromme & Klingenspor 2011). We fed mice a HFD to determine the role of SCT in adaptation to states of excess energy. The HFD and CD fed mice were i.p. injected with SCT or PBS and measured in a calorimetric device.

Table 5.3: Values for body weight (BW) and basal metabolic rates RER and HP after four and eight days on HFD or CD at 30 °C

After four days of diets

	HFD		**CD**	
	PBS (N=3)	SCT (N=3)	PBS (N=3)	SCT (N=3)
BW (g)	23.7 ± 2.4	24.8 ± 2.3	22. 2 ± 0.1	22.8 ± 0.3
RER	0.73 ± 0.02	0.74 ± 0.02	0.74 ± 0.04	0.8 ± 0.01
HP (mW)	232.0± 30.2	246.9± 33.5	185.7± 10.3	205.4± 12.9

After eight days of diets

	HFD		**CD**	
	PBS (N=3)	SCT (N=3)	PBS (N=3)	SCT (N=3)
BW (g)	25.1 ± 2.2	24.1 ± 1.9	22.9 ± 0.3	22.2 ± 0.3
RER	0.71 ± 0.02	0.72 ± 0.02	0.75 ± 0.02	0.78 ± 0.02
HP (mW)	241.7± 23.6	225.9± 27.0	218.5± 10.7	188.7± 15.3

All mice were continuously kept on their diet (HFD or CD) for the whole eight days of the experiment. The treatment group (PBS or SCT injection) at the measurement day however was switched for every mouse from day four to day eight, thus each mouse was once measured after injection with SCT and once after injection with PBS. At both measurement days basal metabolic rates were determined at 30 °C (Tab. 5.3). The body weight of mice was slightly, but significantly increased after four days, which potentiated after eight days of HFD compared to mice in the CD group (results for statistical analysis are shown in the supplement, Tab. 6.3 and Tab. 6.4). It is well-known that mice fed a HFD increase their energy intake compared to CD fed mice. The values for HP were also marginally higher in the HFD group than in the CD. This is not surprising considering that HP is correlating with body weight. The RER, which reflects the macronutrient consumption in the body, was in a range of 0.71 and 0.8 for all groups. Despite the different diets and thereby main macronutrient sources, there was no obvious difference in RER between the groups, because the measurement took place in a state of fasting during the light phase. The resulting low glucose level favoured a degradation of fat as fuel for cellular respiration in both diet groups.

Subsequent to basal metabolic measurements, mice were i.p. injected with SCT or PBS and measured at 27 °C. CD as well as HFD fed mice showed a phase of "arousal" during measurement of HP for the first 10 minutes after injection (Fig. 22, A and B). Afterwards, the PBS injected mice exhibited a decline in HP, which was less pronounced in the SCT group. This course of the measurement was similar with previous results (Fig. 17). The effect of SCT on respiration in mice was independent of experimental diet. The analysis of the

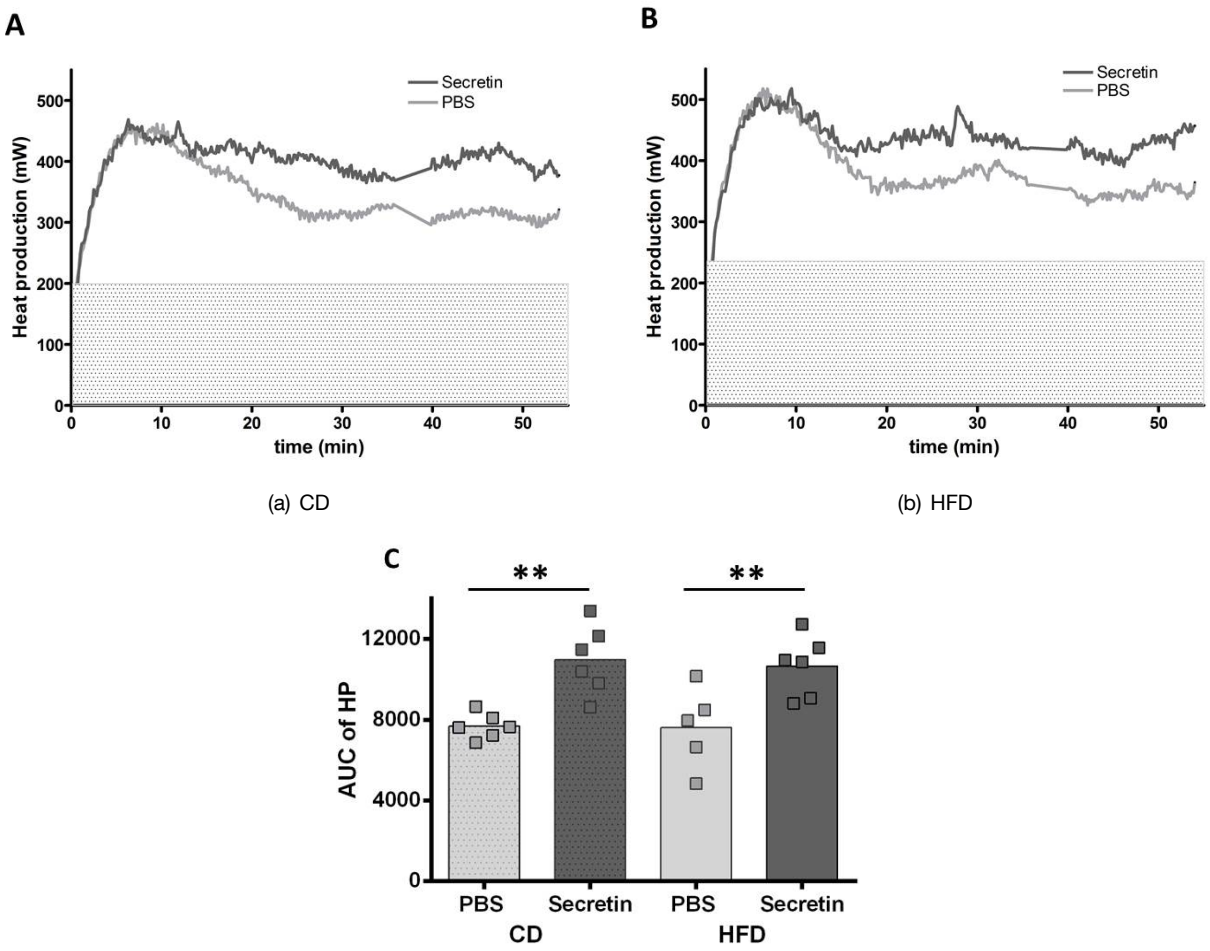

Fig. 22: **SCT induced respiration in HFD fed mice.**
Mice received 0.5 mg/kg SCT solved in PBS or equal volume of PBS via i.p. injection after four or eight days of HFD. Measurement was performed at 27 °C. In (A) the mean of N=6 CD fed mice and in (B) the mean of N=5-6 HFD fed mice are shown for HP (mean of basal HP measured at 30 °C depicted as grey background). In (C) the AUC for HP for the entire recording is depicted. Statistics were conducted using two-way ANOVA (diet: p=0.772; treatment: p<0.001; diet x treatment: p=0.853). ** indicates significance <0.01 within the diets, tested with Tukey test.

AUC revealed a highly significant difference between the injection groups (CD p=0.002 and HFD p=0.004; pairwise multiple comparison procedures by Tukey test), which was not affected by the type of diet (diet p=0.772).

The drop of the RER in the first 10 minutes after SCT injection was not as pronounced as in other experiments, but was observed for both diet groups (Fig. 23, A and B). The AUC for the RER was not statistically significant between SCT and PBS injection (Fig. 23, D) in both diet groups, if analysed for 15 minutes. The reason for the significantly higher RER in the CD group (Fig. 23, C) after injection of SCT compared to PBS group remains unclear.

All in all no difference between HFD and CD was detected regarding the metabolic response to a SCT injection. The results were not dependent on the duration of the feeding period, since mice reacted comparably to a SCT injection after four and eight days of HFD (results not shown). However, a non-transient adaptation to a HFD was not accomplished during a eight day feeding phase. Further experiments with a HFD for several weeks should be conducted in the future.

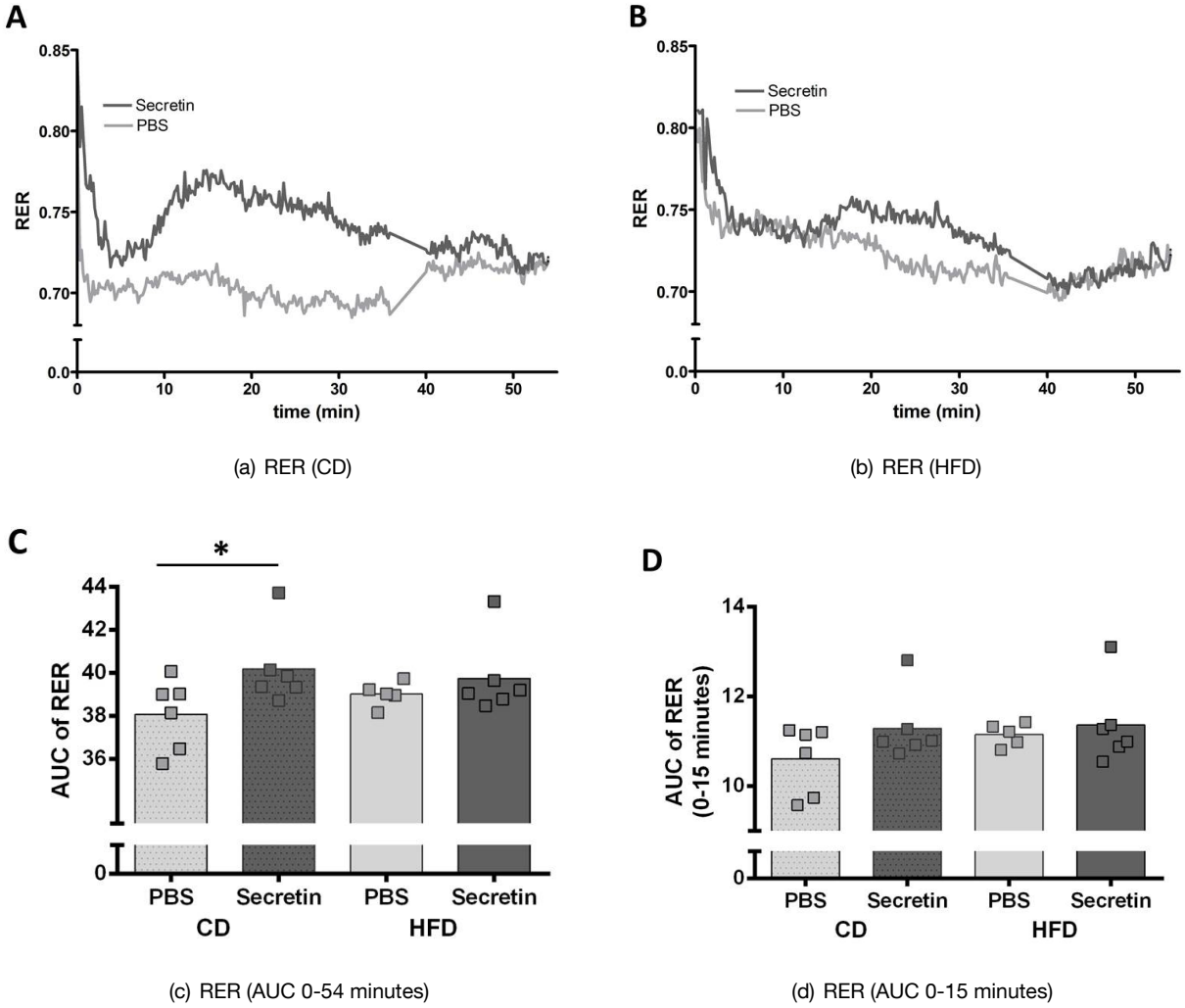

(a) RER (CD)

(b) RER (HFD)

(c) RER (AUC 0-54 minutes)

(d) RER (AUC 0-15 minutes)

Fig. 23: **SCT effect on RER and HP in HFD fed mice.**
Effect of SCT i.p. injection in HFD fed mice and CD fed mice are shown. In figure (C) the RER is shown as mean of N=5-6 for HFD group and N=6 for CD group. Same N-numbers are depicted in figure (D) showing the HP. Statistics were conducted using Two-way ANOVA for 0-15 minutes of RER measurement (diet: p=0.327; treatment:0.162; diet x treatment: 0.453) and 0-54 minutes of RER measurement (diet: p=0.710; treatment:0.045; diet x treatment: 0.308). A pairwise multiple comparison performed using Tukey test showed a significant difference for treatment within the CD (p=0.032) indicated by *.

5.6.2.2. *sctr* expression in adipose tissues of HFD fed mice

In previous experiments it was shown that the expression of the *sctr* is regulated by environmental influences like cold (Fig. 21). In the following part it is furthermore checked if alimentary impacts like HFD would lead to alterations in the *sctr* expression, too. Samples from twelve week old 129/S6-mice fed with a HFD for four weeks were compared to suitable CD fed mice for analysis. Expression of the *sctr* in iWAT and BAT was determined by qRT-PCR (Fig. 24).

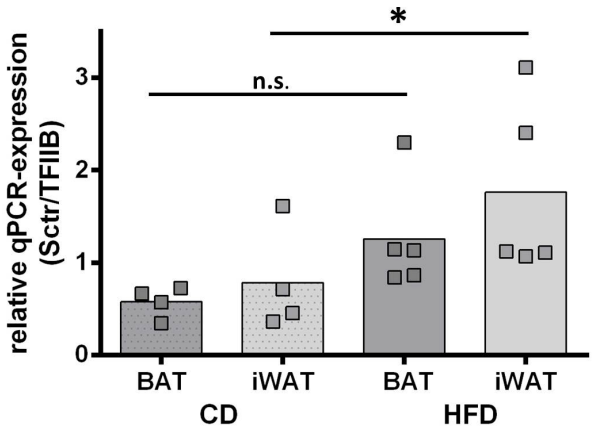

Fig. 24: **Expression of the *sctr* in HFD fed mice in BAT and iWAT.**
Mice were fed a HFD or CD for four weeks. *sctr* expression is shown for iWAT and BAT. Relative mRNA levels were measured via qRT-PCR. Results are normalised to TFIIB as housekeeper gene. Bars represent mean values and single measurements are presented as dots. Statistical analysis was conducted using two-way ANOVA. Since the data were not normally distributed (Shapiro-Wilk test $p<0.05$) a pairwise multiple comparison was performed using Tukey test (diet: $p=0.019$; fat depot: $p=0.271$; diet x fat depot: $p=0.642$). There was a statistical significant difference for the diets within iWAT $p=0.044$ (indicated by *), but not within BAT ($p=0.145$).

In iWAT as well as in BAT a trend towards increased *sctr* expression under HFD compared to CD was observed. The effect was only significant for iWAT ($p=0.044$) and not for BAT ($p=0.145$). The increased expression of *sctr* under HFD did, however, not result in an increased respiration in these mice compared to CD fed mice after stimulation with SCT (Fig. 22 and Fig. 23). Perhaps a difference can only be detected in ranges of very low SCT doses. Maybe the injected amounts of SCT, that were used in this setting, already evoked the maximum response, which could not be further increased by amplified *sctr* expression. In addition it has to be mentioned, that the mice taken for oxygen consumption measurements in the preceding part of 5.6.2.1 were fed a HFD for only four to eight days, whereas the mice that were used for *sctr* expression analysis in the fat tissue depots were fed the HFD for four weeks. Thus a repetition of the calorimetry measurements following HFD feeding for four weeks would be helpful to check for possible stronger effects.

5.6.3. Suppression of food intake in mice following i.p. injection of SCT

In addition to thermogenesis, BAT has been proposed to contribute to the thermoregulatory control of feeding. An increase in body core temperature caused by BAT after initiation of food intake may trigger the termination of a meal (Himms-Hagen 1995). In extension of this hypothesis it is proposed that SCT may be part of a novel endocrine gut - brown fat axis controlling meal patterns. Therefore, the effects of SCT upon food intake in mice fasted overnight for 18 hours were tested. Just before refeeding, mice were i.p. injected with 5 nmol SCT solved in PBS, or PBS as control, and food intake was monitored for the following three

days. Food intake did not vary appreciable between the two injection groups if contemplated for the first 24 hours (Fig. 25). Also for 72 hours after injection (data not shown) no difference between the groups was observed.

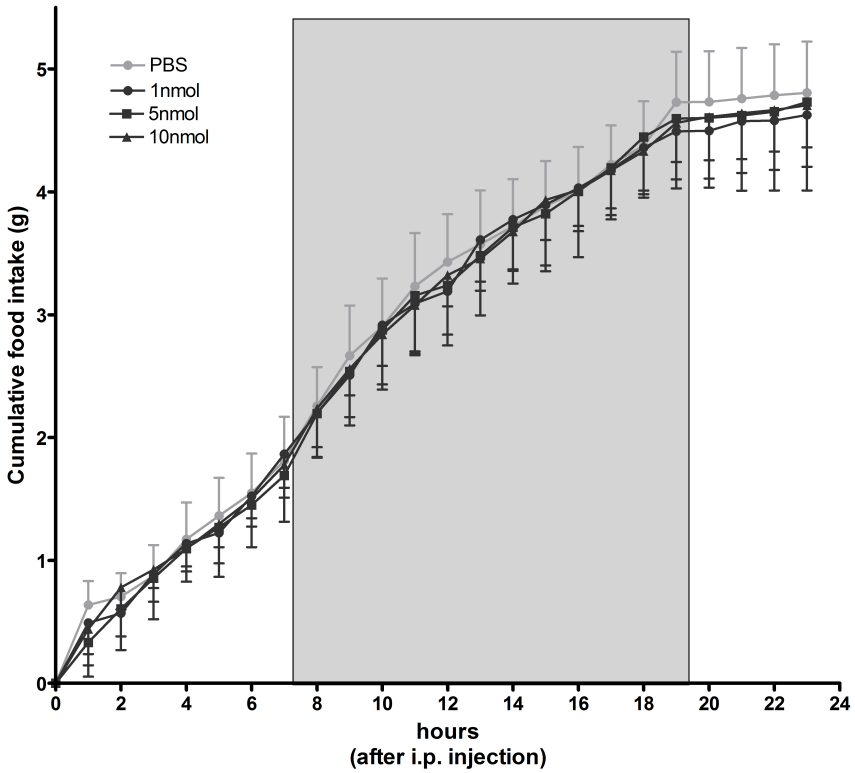

Fig. 25: **Effect of SCT on refeeding in fasted mice over 24 hours.**
Mice were fasted for 18 hours and afterwards .p. injected with 1 nmol, 5 nmol or 10 nmol of SCT solved in PBS. Control mice were injected with PBS. Food intake is shown for 24 hours after injection. Lights off is indicated by grey background. N=11-12 for PBS, 5 nmol and 10 nmol and N=6 for 1 nmol.

Regarding the food intake during the first four hours after injection, there was a slight, significant difference between the SCT group and the PBS injected control mice (Fig. 26). The PBS control group showed a steeper rise in cumulative food intake during the first hour and afterwards a plateau for another hour until they started to ingest regularly. Mice injected with SCT, however, showed a delay in food intake during the first hour, and no plateau once food intake started. SCT induced a significant inhibition of food intake during the first two hours of after injection, suggesting an acute and transient anorexigenic effect of this gut hormone. This effect was independent of the tested SCT concentrations (Statistics with linear mixed effects model were conducted for the first two hours after injection: PBS vs 1 nmol SCT: $p=0.0276$; PBS vs 5 nmol SCT: $p=0.0181$; PBS vs 10 nmol SCT: $p=0.1014$).

Based on the hypothesis of thermoregulatory feeding and in consideration of previously shown results (Fig. 17), it is presumed that the anorexigenic effect of SCT is mediated by the thermogenic activation of BAT. For a more accurate determination of the anorexigenic effect of SCT, experiments with SCT derivates, that show an increased half-life time are desirable. For such a purpose experiments with long-acting PASylated SCT should be carried out.

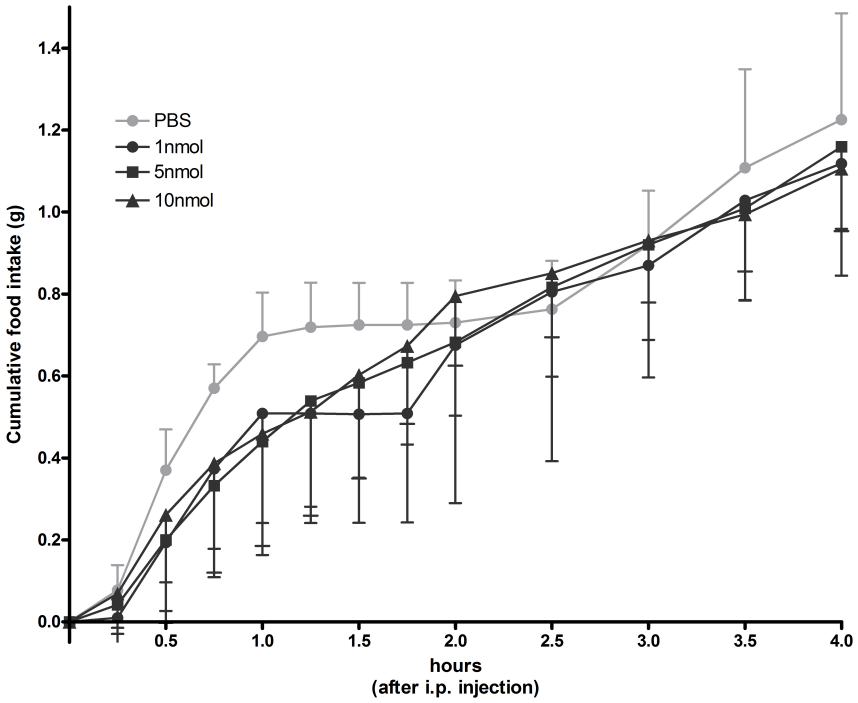

Fig. 26: **Food intake in fasted mice following SCT injection over four hours.**
Mice were fasted for 18 hours and afterwards i.p. injected with 1 nmol, 5 nmol or 10 nmol of SCT. Control mice were injected with PBS. Food intake is shown for four hours after injection. Data are presented as mean of N=11-12 (PBS, 5 and 10 nmol SCT) or N=6 (1 nmol SCT). Statistical analysis were conducted for the first two hours using linear mixed-effects model with TIBICO Spotfire SPlus software (p-values for treatment: PBS vs 1 nmol SCT: p=0.0276; PBS vs 5 nmol SCT: p=0.0181; PBS vs 10 nmol SCT: p=0.1014).

5.7. PASylation of SCT

Since SCT is a hormone with a very short half-life time of only several minutes until it gets eliminated by renal extraction and hepatic degradation (Fahrenkrug et al. 1978) it is very hard to study metabolic effects *in vivo*. In this content, a promising prospect provides the use of PASylated SCT for further experiments, where SCT exhibits an increased plasma half-life. PASylation means the expansion of the target peptide (SCT) by conformationally disordered polypeptide chains comprising the small residues proline, alanine and serine (PAS). This is resulting in an enlargement of the hydrodynamic volume of the bioactive peptide SCT (Schlapschy et al. 2013).

5.7.1. Activation of the SCTR with PASylated SCT

To investigate the general ability of PASylated SCT to agonistically activate its receptor, a luciferase assay system was designed. In the assay the downstream signalling of the SCTR results in an increased expression of *photinus* luciferase. The agonistic activity of PASylated SCT was compared to conventional SCT.

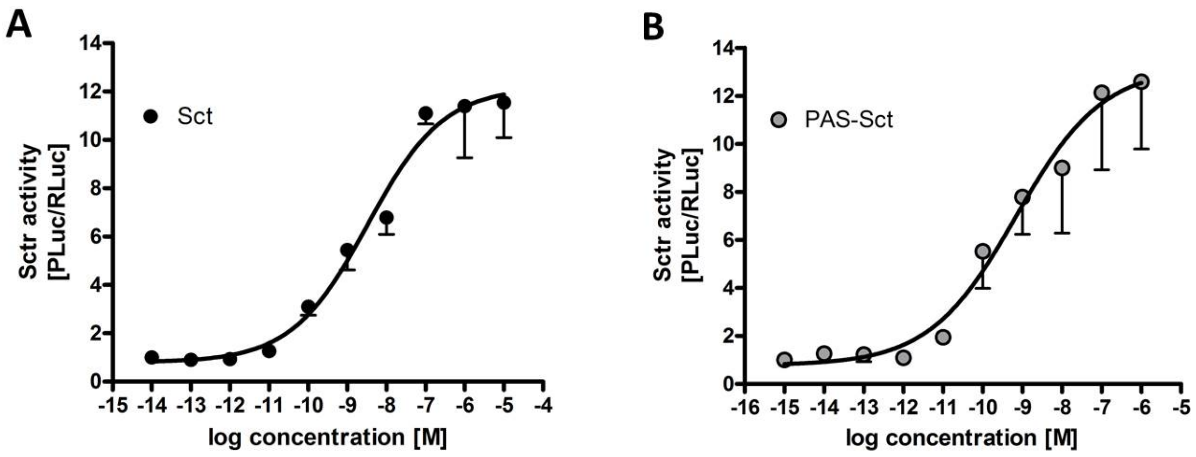

(a) SCT (b) PASylated SCT

Fig. 27: **Agonistic action of PASylated SCT**
Activation of the SCTR by commercially purchased SCT (A) and PASylated SCT (B). For the test system HEK-cells were transiently transfected with SCTR-expression vector, a cAMP-RE regulated *Photinus* luciferase reporter, and a constitutively expressed *Renilla* luciferase for data normalisation.
Results represent the mean $\pm SD$ of N=3, each measured in technical duplicates.

Both the commercial SCT and the PASylated SCT, were able to activate the SCTR (Fig. 27). In both cases the maximum activation reached 12-fold levels above the untreated basal conditions. The potency of both agonists was comparable since the EC_{50} of SCT was 3.28 nM and the EC_{50} of PASylated SCT was 0.56 nM. In summary, the PASylated SCT was, despite of its major modifications, still able to act as an adequate agonist of the SCTR.

5.7.2. Induction of *ucp1* expression in brown adipocytes by PASylated SCT

In section 5.4.1 it has already been shown that SCT is able to induce the expression of *ucp1* in fully differentiated primary brown adipocytes. In a next step, we used PASylated SCT to check, if the actions of SCT on adipocytes maintained by PASylating the peptide (Fig. 28).

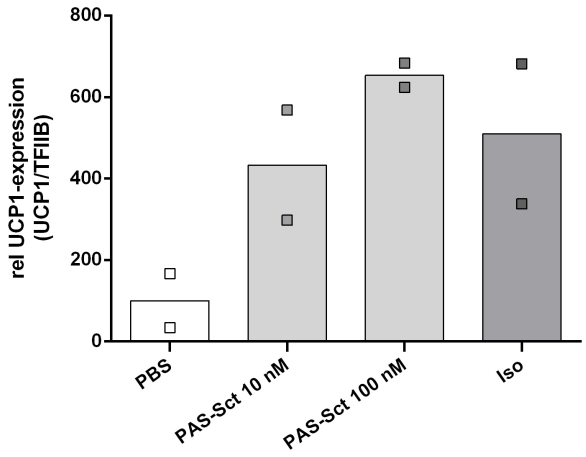

Fig. 28: **Induction of *ucp1* mRNA expression in primary adipocytes by PASylated SCT.**
Differentiated primary brown adipocytes were stimulated with PBS, ISO (500 nmol) or different concentrations of PASylated SCT for 6 hours. Expression of *ucp1* mRNA was measured by qPCR and normalised to TFIIB expression. Results were standardised to PBS conditions. N=2, measurements were performed in technical triplicates. Single measures are indicated as dots.

PASylated SCT was able to strongly increase the expression of UCP1 mRNA in both tested concentrations above the PBS condition as a negative control. The induction was similar to the stimulation with ISO. In the two measurements, there was a trend towards dose-dependency since the higher PASylated SCT concentration (100 nM) induced a stronger *ucp1* expression.

It can be concluded that PASylated SCT is a potent agonist for the SCTR like it is commercial SCT. It also induces *ucp1* expression in brown adipocytes and seems to be an interesting, long-lasting candidate for further investigations.

6. Discussion

6.1. Background and aim of the thesis

Since decades, adiposity is a worldwide pandemic with a high prevalence all over the world and multifactorial reasons (Ng et al. 2014). Under discussion are, amongst others, gene variants, environmental factors and fetal programming (Hebebrand & Hinney 2009, Bessesen 2008, Stout et al. 2015).
Since BAT has been found not only in mammals, but also in healthy adult humans (Cypess et al. 2009), it has become interesting for the treatment of obesity as it is a metabolically highly active tissue. It has for example been found that individuals exhibiting detectable amounts of BAT have lower total cholesterol and low-density lipoprotein cholesterol, which suggests a positive effect on their blood lipid profiles (Ozguven et al. 2015). It has furthermore been shown that the activation of BAT in temperature-acclimated men modulates insulin sensitivity (Lee et al. 2014). In some studies the browning of WAT highly correlated with anti-obesity effects like improved glucose tolerance and insulin sensitivity, which was not depending on BAT function (Liu et al. 2015, Wang et al. 2015). Those positive effects made as well human BAT and also browning in WAT a target for obesity treatment (Chechi et al. 2014, Nedergaard & Cannon 2010).
Considering the positive effects of activated BAT and browning of WAT in humans, it is obvious that activators of both are of great interest in research. The classical and, at the moment, best known activators of brown adipocytes and mammal BAT are β-3-AR agonists.
So far, it has been a challenging task to activate human BAT by its β-3-AR. This is due to the fact that highly selective β-3-AR agonists, working in humans, are hard to find and β-AR agonists used in rodents do not have significant effects in humans (Mund & Frishman 2013, Michel et al. 2010, Weyer et al. 1999). Recently however, human BAT thermogenesis could successfully be activated by oral application of the selective β-3-AR agonist mirabegron (Cypess et al. 2015).
In another study where ISO, a nonselective β-AR agonist was infused to lean adult man, BAT was surprisingly not activated (Vosselman et al. 2012).
Next to the β-3-AR agonists, further activators have been found in the passed years, including adenosin which is a A_{2A} receptor, salsalate via an unknown mechanism, or FGF21 (Gnad et al. 2014, van Dam et al. 2015, Bostrom et al. 2012, Hondares et al. 2010). Further activators that could possibly be used for pharmaceutical treatment of obesity are still of scientific interest.

For some members of the PACAP-family hormones, BAT activating effects have already been reported. Centrally administered GLP-1 analogue exendin-1 activates BAT thermogenesis via sympathetic outflow and increases browning in WAT (Kooijman et al. 2015, Lopez et al. 2015, Beiroa et al. 2014). An increase in interscapular BAT thermogenesis following central administration was furthermore shown for glucagon and oxyntomodulin (Lockie et al. 2012). Another publication postulated that glucagon is essential for adaptive thermogenesis and regulates BAT function, most likely by increasing hepatic FGF21 production (Kinoshita et al. 2014). The KO mouse model for PACAP exhibits impairment in thermoregulation, because appropriate levels of norepinephrine can not be supplied to brown adipocytes during cold-exposure (Diane et al. 2014). In 1998 it has already been published that glucagon and SCT exhibit a thermogenic effect in isolated rat brown fat cells. The thermogenic effect of SCT was identified as artifact in that paper and not pursued

furthermore. For glucagon also an increased oxygen consumption after i.p. injection into rats and hamsters was demonstrated by *Dicker*. Finally it was concluded in the paper that the thermogenic effect of glucagon is not due to a direct action on brown fat cells (Dicker et al. 1998).

In this present thesis a thermogenic effect for SCT *in vivo* and *in vitro* was shown by oxygen consumption measurements. Furthermore the SCT effect upon *ucp1* expression in BAT and also its browning effect in WAT was demonstrated. In the discussion the actions of SCT are compared to well described browning agents. Furthermore the effect of SCT is considered towards biological relevance and function, and finally an outlook on future experiments and therapeutic potential is given.

6.2. *In vitro* effects of SCT

As reported in literature, the lipolytic action (Sekar & Chow 2014a, Stout et al. 1976, Butcher & Carlson 1970) of SCT could be confirmed in own experiments. Lipolytic effects are furthermore known for the β-AR agonist ISO, an activator of BAT. Lipolysis and the activation of BAT generally occur together. This is reasonably, because the extreme energy expenditure in activated brown adipocytes is fuled by the energy stored in fat droplets in the cells, which is in turn mobilised by lipolysis. Furthermore, UCP1 activity is directly activated by free fatty acids resulting from lipolysis. It is thereby assumed that the lipolyitc actions in brown fat, activated by SCT, is triggered to fuel UCP1 activity. A closer look should be taken to the thermogenic and UCP1-regulatory effects of SCT.

Induction of respiratory activity in brown adipocytes by SCT

The respirometry measurements in this thesis have proven that a stimulation with SCT can induce an increase of oxygen consumption in differentiated primary brown adipocytes (shown in 5.3.1) in a similar range as ISO. The thermogenic effect of SCT in isolated brown adipocytes is in line with findings of 1998 (Dicker et al. 1998). The publication by *Dicker* however did not find an explanation for the mode of action of the thermogenic effect of SCT.

The action of SCT is most likely mediated via the SCTR, since its expression could be proven in several adipose depots (BAT, iWAT, gWAT). Due to the fact that the SCTR is a GPCR, like the β-3-ARs mediating the effect of ISO, it is considered, that both stimuli are using the same signalling cascade. Another respiratory experiment with UCP1 KO cells revealed that the SCT effect upon brown fat cell respiration is dependent upon UCP1 activation, which is also true for β-adrenergic stimulation by ISO (shown in 5.3.2). A clear evidence for the dependency of the thermogenic effect of SCT upon the SCTR is however lacking. Further tests with SCTR KO cells or an antagonistically inhibition of the SCTR would be desirable for a final conclusion. Also, further experiments blocking the PKA signalling pathway would strengthen the molecular mechanisms mediating the UCP1 activating effect of SCT in brown fat cells.

In a further experiment of this thesis, the cultured primary brown adipocytes were chronically treated with rosiglitazone during the phase of differentiation. Roziglitazone is a PPARγ agonist, known to increase the mass of interscapular BAT *in vivo* and for the induction of *ucp1* expression in brown fat cells (Tai et al. 1996). As shown before (Festuccia et al. 2010), in our experiments rosiglitazone treatment in BAT cells markedly increased oxygen consumption rate by stimulation with ISO, which was caused by the augmented expression of *ucp1*. In contrast, when stimulated with SCT no increase in cell respiration could be yield by previous rosiglitazone treatment. A quantitative mRNA expression analysis revealed that this was due to decreased *sctr* abundance in the chronically treated cells. Those results lead to the assumption that a continuous PPARγ stimulation causes a negative regulation for the responsiveness of brown fat cells upon activation by SCT. This divergence in the action of SCT, respectively ISO following chronic rosiglitazone treatment is a hint towards different biological functions of the two BAT stimulating routes that are reflected by the agents.

Induction of *ucp1* expression by SCT in primary adipocytes

Activators of BAT, which stimulate energy expenditure, often exhibit additional regulatory effects upon the expression of *ucp1*. It is therefore not surprising that a stimulation of brown adiocytes with SCT for six hours leads to increased mRNA levels of *ucp1*. In this thesis, an induction was detected as well for primary brown, but also for primary white adipocytes, indicating additionally WAT browning potential for the gut hormone. The effect size in both types of fat adipocytes was again comparable to a treatment with ISO. However, it is to be noted that the used concentration of 0.5 μM ISO was adapted to published data and experience in our lab (Li et al. 2014b) and thereby quite higher than the concentrations that were required for similar effects by SCT. For a dose response examination, we used SCT concentrations in a range of 1 μM to 1 nM. Cells stimulated with the lowest concentration of 1 nM SCT showed an increase in *ucp1* mRNA at almost maximum level. This is surprising, taking into account that as well in published data as also in own experiments an EC_{50} for the SCTR was found at a concentration of 0.4-5 nM (Fig. 27) (Shetzline et al. 1998, Ganguli et al. 1998). In cell culture experiments it seems not necessary to use satiating concentrations of SCT to receive a maximum functional reply.

In a further panel of experiments various inhibitors of the classical β-3-AR signalling cascade were used to test whether both, SCT and ISO, signal via the same pathway.

The SCTR is a GPCR like the β-3-ARs, thus both receptors can stimulate the adenylyl cyclase resulting in an accumulation of cAMP. As a consequence the PKA is activated leading to the induction of lipolysis in fat cells (Carmen & Victor 2006). The fatty acids serve as fuel for the heat production via UCP1, which uncouples the respiratory chain in the mitochondria of the fat cells. The PKA can furthermore stimulate the p38 mitogen activated protein kinase (MAPK) in brown adipocytes (Cao et al. 2004), which leads to the transcription of the *ucp1* gene in mice. Also the high amount of free fatty acids that accumulate following the lipolysis, stimulated by SCT and ISO, can influence the expression of *ucp1* mRNA (von Praun et al. 2001). On the one hand the free fatty acids are ligands to PPARs and are considered to mediate browning (Li et al. 2005). On the other hand exogenous fatty acids inhibit cAMP production (Fain & Shepherd 1975).

To check for those signalling cascades inhibitors for PKA (H89 dihydrochloride) and p38 (SB203580) were used.

The induction of *ucp1* expression via SCT stimulation is decreased by inhibition of PKA (H89) or p38 (SB). This effect suggest a mediation role of PKA and p38 in the regulation of the *ucp1* expression. This signalling pathway downstream of the AC activation is in line with published and in this thesis confirmed results for a stimulation with ISO (Fig. 29).

Taken together from the *in vitro* experiments it can be concluded that SCT can activate uncoupled respiration in isolated primary brown adipocytes and increase *ucp1* expression in brown and also in white fat cells, which means that SCT can induce browning. SCT reaches the same maximum impact in all its functions as the classical activator of β-3-ARs ISO, but can be used in lower concentrations, which underlines its biological potential and physiological relevance. SCT is considered to activate the SCTR, which is expressed in varying amounts in all fat depots that were examined. The downstream signalling pathways are suggested to be identical to the β-3-AR cascade by activating PKA via cAMP accumulation.

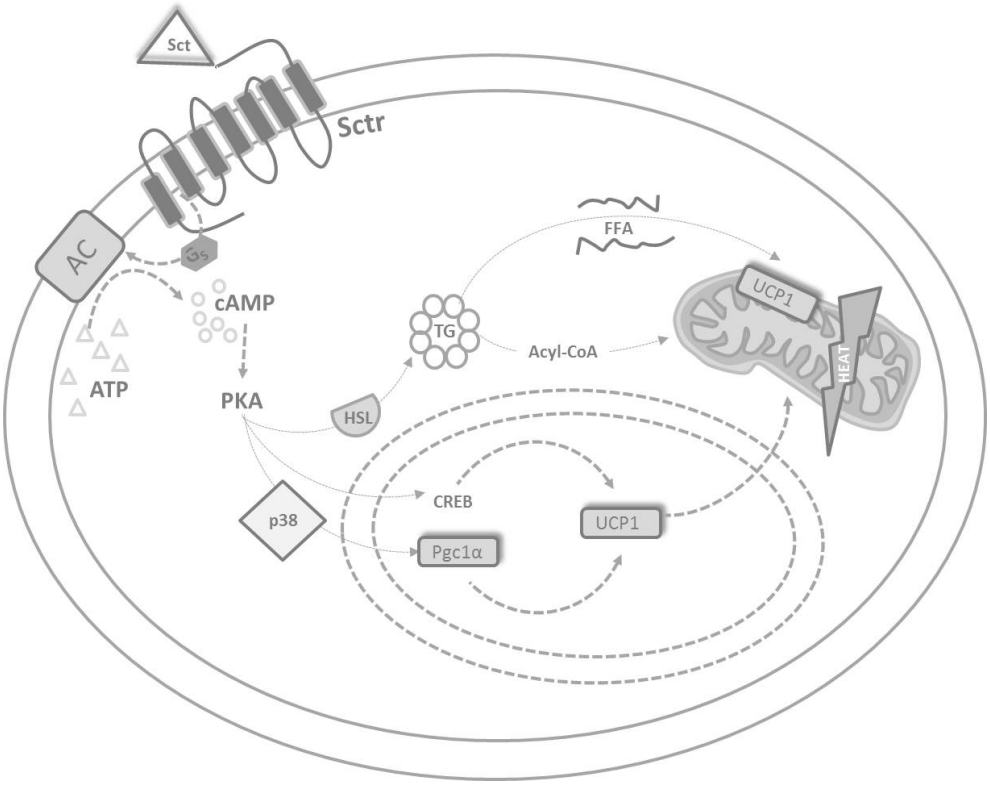

Fig. 29: **Signalling cascade in adipocytes following stimulation with SCT.**
SCT binds to its membrane bound GPCR (SCTR), which hereupon activates the adenylyl cyclase (AC) via its G_s-subunit. The AC converts ATP into cAMP, which furthermore activates the protein kinase A (PKA) triggering lipolysis (i) via hormone-sensitive lipase (HSL) releasing free-fatty acids (FFA) and acyl-coenzyme-A (Acyl-CoA), cAMP response element-binding protein (CREB) (ii) and p38 mitogen-activated protein kinases (p38) (iii) leading to an activation of PPARγ coactivator 1-α (PGC1α), all resulting in an activation of UCP1.

6.3. *In vivo* effects of SCT

Complementary to cell culture data, the actions of SCT were assessed in *in vivo* experiments. The respiratory measurements conducted via indirect calorimetry revealed, that SCT can stimulate oxygen consumption following i.p. injection also in a whole organism. This has already been shown for the PACAP family member glucagon (Dicker et al. 1998, Lockie et al. 2013), too, indicating that SCT and glucagon can directly influence BAT activity in the periphery. For other members of the family an effect could only be demonstrated following central application (Kooijman et al. 2015, Lockie et al. 2012, Lopez et al. 2015, Beiroa et al. 2014). For SCT itself it is the first time that thermogenic and respiratory inducing actions have been shown *in vivo*.

Quantitative mRNA-expression analysis revealed, that there is an abundance of the SCTR in BAT and WAT depots of mice, which could mediate effects of SCT. The *in vitro* experiments discussed before suggested that the SCT mediated respiratory induction is dependent upon direct UCP1 activation. The lack of SCT induced increase of respiration in UCP1 KO mice leads to the suggestion that the effect is as well mediated by UCP1 *in vivo*. This experiment could demonstrate that it is feasible to activate UCP1 via i.p. SCT injection in mice to a measurable amount.

In a further experiment, mice were moreover cold acclimated to increase BAT content, which enhanced respiratory response to ISO stimulation as expected. For the treatment with SCT however, the mice were insensitive after cold exposure. The explanation for that result is found in the downregulation of the SCTR in BAT depots. This regulatory response suggests that under physiological conditions, SCT plays not a role in the classical brown fat function of rescuing body temperature in a cold challenge by non-shivering thermogenesis. SCT rather seems to regulate BAT activity during states of normal ambient temperature. In this occasion BAT is not used to defend body temperature, which is certainly the highest priority task of BAT. It has been shown that BAT is activated in mice by feeding a high fat diet (Rothwell & Stock 1983). SCT could thereby be a regulator of BAT in states of excess energy. In this thesis, the relevance of BAT regulation by SCT under high caloric feeding was determined by checking for *sctr* expression in various adipose tissue depots. The *sctr* mRNA was found to be upregulated under HFD in BAT, but also in iWAT, which has the highest browning capacity. Even tough the receptor expression suggests a regulatory role for the gut hormone in the body adaptation for HFD, in respiratory measurements no alteration of oxygen consumption could be found for a SCT stimulation after four to eight days of HFD. It is to consider that the determination of *sctr* mRNA expression was carried out after four weeks of HFD, while the oxygen consumption measurements were conducted after a considerably shorter HFD of only four to eight days. Maybe this was the reason for the divergent results. In case of a repetition of the oxygen consumption measurements mice should be fed a HFD for four weeks.
There are nonetheless further potential explanations for the BAT regulatory physiological function of SCT that will be discussed in the following section.

6.4. Biological relevance and physiological function of the thermogenic SCT effect

Modulation of SCT sensitivity in BAT

In the described *in vitro* and *in vivo* experiments the sensitivity of brown fat cells for SCT stimulation was highest when the cells were not activated for heating tasks *in vivo* or by chronic rosiglitazone treatment *in vitro*. It was shown that in states of cold exposure or chronically PPARγ stimulation the SCT sensitivity was strongly decreased by downregulation of the *sctr*. This adjustment of the impact strength of SCT leads to the suggestion that the duty fulfilled by the gut hormone is only of relevance if BAT has a capacity for other tasks than heating. A possible function in this context for BAT could be thermoregulatory feeding.

Hypothesis of thermoregulatory feeding

The hypothesis of food intake control via thermogenesis using BAT activity was established by *Himms-Hagen* in 1995. The hypothesis gives a possible explanation for the food intake terminating mechanisms in rats (Himms-Hagen 1995). It is known that rats eat between nine and twelve discrete meals per day. The initiation of a meal is considered as a result of metabolic deficiency after a longer period with no food intake. In rats, there is a periodically fluctuation of body temperature of about 1 °C. It is known that feeding starts 15 minutes after BAT temperature begins to rise (Blessing et al. 2013) and stops when the peak is reached. In BAT the activity is thereby increased via sympathetic stimulation, which raises body temperature. At the same time the sudden metabolic activation of BAT provokes an influx of glucose from the circulation into BAT, which leads to a drop of blood glucose concentration. At the lowest hypoglycemic level, as a counteraction, liver restores blood glucose concentration to its previous level. The drop in blood glucose concentrations evokes the initiation of food intake by action in the brain (Smith & Campfield 1993, Campfield & Smith 1990). The strong BAT thermogenesis persists during food intake, which continuously raises body temperature till it reaches a peak (which means a liver temperature of 39.3 °C) were countermeasures prevent hyperthermia. At this point the rat stops eating and body temperature begins to fall. All in all eating is suggested as the culmination of a thermoregulatory process (Himms-Hagen 1995, Ootsuka et al. 2009, Blessing et al. 2012, Blessing et al. 2013, Adachi et al. 1991, Di Bella et al. 1981, Rampone & Reynolds 1991).

SCT is secreted by dropping in the duodenal pH, which occurs shortly after the initiation of food intake and fulfils plenty of digestion related tasks in pancreas, stomach and gut. It is reasonable that the gut hormone is a further trigger of BAT activation to control thermoregulatory feeding (see Fig. 30). It has already been suggested that termination of meal is controlled by signals arising from the intestine, since satiety occurs long before the meal is digested and absorbed (Himms-Hagen 1995). Furthermore the BIO-GPS data revealed that the *sctr* is, next to the brain, most dominantly expressed in BAT. Hence, it is most likely that SCT plays a relevant physiological role in BAT. In own expression studies (Fig. 8, A and Fig. 31, but not confirmed in Fig. 21, A and Fig. 24) it has also been shown that the *sctr* is stronger expressed in BAT than in WAT depots. Thus, the activation of BAT could be of more physiological relevance than the browning effects in WAT. To further proof the hypothesis of thermoregulatory feeding control by SCT, it would be useful to link SCT to food intake regulation.

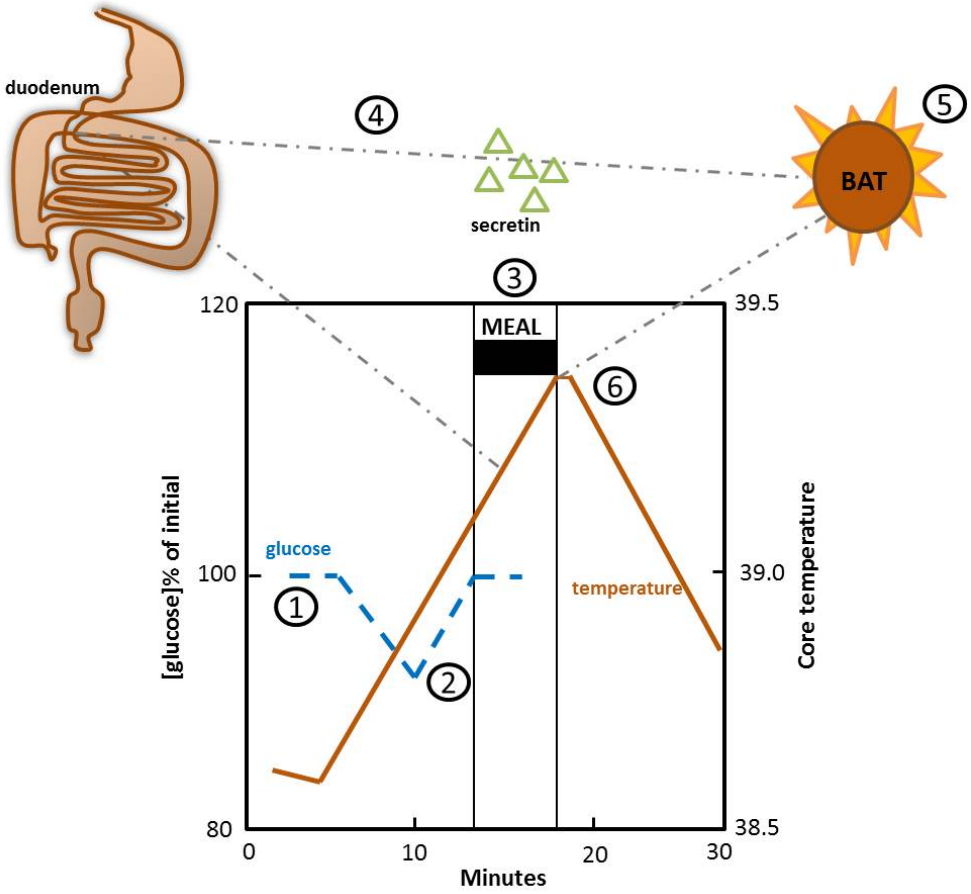

Fig. 30: **SCT and thermoregulatory feeding.** Modified from Himms-Hagen 1995
The initiation of a meal is driven by an increase in body temperature which happens rhythmically several times a day. Since the increase in temperature is generated by BAT, the heating organ consumes glucose, which leads to a drop in blood glucose levels (1), rapidly compensated by glucose provided by the liver (2). As soon as body temperature exceeds a threshold food intake starts (3), which leads to the release of SCT from the duodenum (4). The hormone further stimulates BAT (5) leading to a peak temperature that finally terminates the meal. The body temperature begins to decline again (6).

Anorexigenic effect of peripheral SCT in mice

The action of SCT as an anorexigenic agent has already been of investigative interest for decades. First studies concerning this topic could show an food intake decreasing effect of an intravenous SCT injection in sheep (Grovum 1981), but failed to show similar actions in rats (Glick et al. 1971, Gibbs et al. 1973). A recent publication by *Cheng* postulated an anorexigenic effect of i.c.v and i.p. injections of SCT in fasted mice. It was suggested that the signal is mediated by vagal afferences to the central nervous system and satiety is triggered by POMCnergic neuron populations in the hypothalamic arcuate nucleus (ARC) projecting to the paraventricular nucleus (PVN) (Cheng et al. 2011).

In this thesis, the experiment from the mentioned paper was repeated to verify the central anorexigenic effect of i.p. administered SCT. Comparable concentrations of SCT, as reported by *Cheng*, were injected into fasted mice and food intake was measured subsequently. The evoked decrease in food ingestion could not affirm the published strong anorexigenic effects. Especially the duration of the satiety effect differed markedly since it was only spanning one hour in own experiments compared to more than 24 hours of significant food intake reduction reported by the publication (Cheng et al. 2011).

However, for the first hour after the i.p. injection of SCT, there was a significant decrease in food intake

compared to the PBS treated control group. Considering the hypothesis drawn in this thesis it could be assumed, that SCT has no direct central anorexigenic function but activates BAT leading to a strong increase in body temperature. According to thermoregulatory feeding a decreased food intake after SCT injection is to be expected. Considering its function the anorexigenic action of SCT is thereby likely to evoke an acute termination of food intake, but not to a long-term satiety signal. The quite small, but measurable effect of SCT injection on voluntary food intake fits to that hypothesis.

It should be mentioned that the hypothesis of thermoregulatory feeding is critically doubted, since it has been shown that treatment with propranolol, an inhibitor of β-ARs, failed to increase meal size (Glick et al. 1989). Furthermore UCP1 KO mice do not exhibit abnormal or excessive food intake. However a missing thermoregulatory control by BAT in those mice could also appear in an altered food intake pattern and must not only be displayed in the absolute amount of food intake. It is suggested by detractors that feeding induced activation of BAT is not necessary to regulate meal size and termination of food intake (Cannon & Nedergaard 2004). Given that thermoregulatory feeding is not assumed to be the unique adjusting path for modulation of food intake, counteract regulations are supposed to take place in states of blocked UCP1 pathways.

To further proof the influence of SCT upon thermoreulatory feeding via BAT activation, it makes sense to repeat the food intake measurement after SCT treatment in UCP1 KO mice. Preliminary and unpublished data by *Katharina Braun* demonstrate that the anorexigenic effect of SCT is vanished in those mice. The results corroborate a mediation of the SCT satiety action via increased BAT temperature.

Experimental concentrations and physiological relevance

In the last part of this section, the biological relevance of BAT activation by SCT will be considered. Physiological plasma concentrations of SCT in mice have been reported to range from about 3–5 ng/ml (1–1.7 nmol/l) (Miegueu et al. 2013, Cheng et al. 2011, Sekar & Chow 2014a). Those values should be viewed critically, because all published data were collected from one group and are not in line with investigated plasma concentrations of other species (20–250 pg/ml or 6–82 pmol/l in humans and 4.5–21.7 pmol/l in rats) (Miegueu et al. 2013) that are up to thousand times lower than in mice. Taking into account the published values for mice plasma SCT level, the used experimental concentrations in this thesis were as well in *in vitro* as in *in vivo* approaches in approximately physiological ranges. A further hint towards physiological relevance is given by the fact that the *sctr* is expressed in copious amount in BAT, which makes an appreciable role very likely.

For mice, an activation of BAT after food intake and a contribution of the fat tissue to diet induced thermogenesis is known (Glick et al. 1981, Moss et al. 1985, Glick et al. 1989, Stock & Rothwell 1986). Also for humans an increased glucose uptake in BAT has been shown after the ingestion of a meal (Vosselman et al. 2013). However, the quantitative portion of BAT induction, in comparison to the activation of other tissues like skeletal muscle, for human DIT is not clarified so far (Vosselman et al. 2013).

All in all a physiological role of SCT in the activation of BAT after food intake is very likely. A contribution of this effect to energy expenditure or regulatory duties in rodents or humans needs further investigations.

6.5. Conclusion

The results in this thesis point out the responsiveness of diverse adipose tissues to the functions of the classical gut hormone SCT. Next to its well known induction of lipolysis it also increases oxygen consumption *in vivo* and *in vitro* by activating BAT. It exhibits furthermore a potential for the induction of *ucp1* expression in BAT and for browning of WAT. The results of some physiological experiments lead to the conclusion that the induction of BAT by SCT is not participating in the thermoregulatory heating functions of the organ. The gut hormone is released after food intake and hereupon metabolically activates BAT. Thus, a possible function of SCT would be the regulation of food intake termination, which is called thermoregulatory feeding. Further investigations are needed to confirm BAT dependency of the slight anorexigenic effect of SCT. Since functional BAT can not be detected in remarkable abundance in humans, it is unlikely that the activation of BAT by SCT plays a physiological role in mankind. However the effect is relevant for therapeutical aspects, because activators of BAT are of strong scientific interest to increase energy expenditure in the fight against obesity (Chechi et al. 2014, Kajimura & Saito 2014, Ozguven et al. 2015). SCT could depict a side effect low alternative to the activation of BAT by unspecific β-adrenergic agonists and develop a promising therapeutical future.

List of Figures

Bibliography

Adachi, A., Funahashi, M. & Ohga, J. (1991): Hepatic thermogenesis relation to food intake in the conscious rat, Brain Res Bull **27**(3-4): 529–33.

Afroze, S., Meng, F., Jensen, K., McDaniel, K., Rahal, K., Onori, P., Gaudio, E., Alpini, G. & Glaser, S. S. (2013): The physiological roles of secretin and its receptor, Ann Transl Med **1**(3): 29.

Ahren, B. & Lundquist, I. (1981): Effects of vasoactive intestinal polypeptide (vip), secretin and gastrin on insulin secretion in the mouse, Diabetologia **20**(1): 54–9.

Alpini, G., Ulrich, C. D., 2nd, Phillips, J. O., Pham, L. D., Miller, L. J. & LaRusso, N. F. (1994): Upregulation of secretin receptor gene expression in rat cholangiocytes after bile duct ligation, Am J Physiol **266**(5 Pt 1): G922–8.

Andersson, A., Sundler, F. & Ekblad, E. (2000): Expression and motor effects of secretin in small and large intestine of the rat, Peptides **21**(11): 1687–94.

Aquila, H., Link, T. A. & Klingenberg, M. (1985): The uncoupling protein from brown fat mitochondria is related to the mitochondrial adp/atp carrier. analysis of sequence homologies and of folding of the protein in the membrane, EMBO J **4**(9): 2369–76.

Barbatelli, G., Murano, I., Madsen, L., Hao, Q., Jimenez, M., Kristiansen, K., Giacobino, J. P., De Matteis, R. & Cinti, S. (2010): The emergence of cold-induced brown adipocytes in mouse white fat depots is determined predominantly by white to brown adipocyte transdifferentiation, Am J Physiol Endocrinol Metab **298**(6): E1244–53.

Bawab, W., Gespach, C., Marie, J. C., Chastre, E. & Rosselin, G. (1988): Pharmacology and molecular identification of secretin receptors in rat gastric glands, Life Sci **42**(7): 791–8.

Bayliss, W. M. & Starling, E. H. (1902): The mechanism of pancreatic secretion, J Physiol **28**(5): 325–53.

Beiroa, D., Imbernon, M., Gallego, R., Senra, A., Herranz, D., Villarroya, F., Serrano, M., Ferno, J., Salvador, J., Escalada, J., Dieguez, C., Lopez, M., Fruhbeck, G. & Nogueiras, R. (2014): Glp-1 agonism stimulates brown adipose tissue thermogenesis and browning through hypothalamic ampk, Diabetes **63**(10): 3346–58.

Bessesen, D. H. (2008): Update on obesity, J Clin Endocrinol Metab **93**(6): 2027–34.

Blessing, W., Mohammed, M. & Ootsuka, Y. (2012): Heating and eating: brown adipose tissue thermogenesis precedes food ingestion as part of the ultradian basic rest-activity cycle in rats, Physiol Behav **105**(4): 966–74.

Blessing, W., Mohammed, M. & Ootsuka, Y. (2013): Brown adipose tissue thermogenesis, the basic rest-activity cycle, meal initiation, and bodily homeostasis in rats, Physiol Behav **121**: 61–9.

Bonetto, V., Jornvall, H., Mutt, V. & Sillard, R. (1995): Two alternative processing pathways for a preprohormone: a bioactive form of secretin, Proc Natl Acad Sci U S A **92**(26): 11985–9.

Bostrom, P., Wu, J., Jedrychowski, M. P., Korde, A., Ye, L., Lo, J. C., Rasbach, K. A., Bostrom, E. A., Choi, J. H., Long, J. Z., Kajimura, S., Zingaretti, M. C., Vind, B. F., Tu, H., Cinti, S., Hojlund, K., Gygi, S. P. & Spiegelman, B. M. (2012): A pgc1-alpha-dependent myokine that drives brown-fat-like development of white fat and thermogenesis, Nature **481**(7382): 463–8.

Bryant, K. R., Rothwell, N. J. & Stock, M. J. (1984): Acute influences on the two gdp-binding sites in brown-adipose-tissue mitochondria, Biosci Rep **4**(6): 523–33.

Butcher, R. W. & Carlson, L. A. (1970): Effects of secretin on fat mobilizing lipolysis and cyclic amp levels in rat adipose tissue, Acta Physiol Scand **79**(4): 559–63.

Campfield, L. A. & Smith, F. J. (1990): Transient declines in blood glucose signal meal initiation, Int J Obes **14 Suppl 3**: 15–31; discussion 31–4.

Cannon, B. & Nedergaard, J. (2004): Brown adipose tissue: function and physiological significance, Physiol Rev **84**(1): 277–359.

Cao, W., Daniel, K. W., Robidoux, J., Puigserver, P., Medvedev, A. V., Bai, X., Floering, L. M., Spiegelman, B. M. & Collins, S. (2004): p38 mitogen-activated protein kinase is the central regulator of cyclic amp-dependent transcription of the brown fat uncoupling protein 1 gene, Molecular and Cellular Biology **24**(7): 3057–3067.

Carlquist, M., Jörnvall, H., Forssmann, WG., Thulin, L., Johansson, C. & Mutt, V. (1985): Human secretin is not identical to the porcine/bovine hormone, IRCS Medical Science **13**: 217–218.

Carmen, G. Y. & Victor, S. M. (2006): Signalling mechanisms regulating lipolysis, Cell Signal **18**(4): 401–8.

Charlton, C. G., Miller, R. L., Crawley, J. N., Handelmann, G. E. & O'Donohue, T. L. (1983): Secretin modulation of behavioral and physiological functions in the rat, Peptides **4**(5): 739–42.

Charlton, C. G., O'Donohue, T. L., Miller, R. L. & Jacobowitz, D. M. (1981): Secretin immunoreactivity in rat and pig brain, Peptides **2 Suppl 1**: 45–9.

Charlton, C. G., Quirion, R., Handelmann, G. E., Miller, R. L., Jensen, R. T., Finkel, M. S. & O'Donohue, T. L. (1986): Secretin receptors in the rat kidney: adenylate cyclase activation and renal effects, Peptides **7**(5): 865–71.

Chechi, K., Nedergaard, J. & Richard, D. (2014): Brown adipose tissue as an anti-obesity tissue in humans, Obes Rev **15**(2): 92–106.

Cheng, C. Y., Chu, J. Y. & Chow, B. K. (2011): Central and peripheral administration of secretin inhibits food intake in mice through the activation of the melanocortin system, Neuropsychopharmacology **36**(2): 459–71.

Chey, W. Y. & Chang, T. M. (2003): Secretin, 100 years later, J Gastroenterol **38**(11): 1025–35.

Chey, W. Y., Lee, Y. H., Hendricks, J. G., Rhodes, R. A. & Tai, H. H. (1978): Plasma secretin concentrations in fasting and postprandial state in man, Am J Dig Dis **23**(11): 981–8.

Chondronikola, M., Volpi, E., Borsheim, E., Porter, C., Annamalai, P., Enerback, S., Lidell, M. E., Saraf, M. K., Labbe, S. M., Hurren, N. M., Yfanti, C., Chao, T., Andersen, C. R., Cesani, F., Hawkins, H. & Sidossis, L. S. (2014): Brown adipose tissue improves whole-body glucose homeostasis and insulin sensitivity in humans, Diabetes **63**(12): 4089–99.

Chow, B. K. (1995): Molecular cloning and functional characterization of a human secretin receptor, Biochem Biophys Res Commun **212**(1): 204–11.

Christodoulopoulos, J. B., Jacobs, W. H. & Klotz, A. P. (1961): Action of secretin on pancreatic secretion, Am J Physiol **201**: 1020–4.

Christophe, J., Chatelain, P., Taton, G., Delhaye, M., Waelbroeck, M. & Robberecht, P. (1981): Comparison of vip-secretin receptors in rat and human lung, Peptides **2 Suppl 2**: 253–8.

Chu, J. Y., Cheng, C. Y., Sekar, R. & Chow, B. K. (2013): Vagal afferent mediates the anorectic effect of peripheral secretin, PLoS One **8**(5): e64859.

Chu, J. Y. S., Lee, L. T. O., Lai, C. H., Vaudry, H., Chan, Y. S., Yung, W. H. & Chow, B. K. C. (2009): Secretin as a neurohypophysial factor regulating body water homeostasis, Proc Natl Acad Sci U S A **106**(37): 15961–6.

Chu, J. Y., Yung, W. H. & Chow, B. K. (2006): Endogenous release of secretin from the hypothalamus, Ann N Y Acad Sci **1070**: 196–200.

Cinti, S. (2005): The adipose organ, Prostaglandins Leukot Essent Fatty Acids **73**(1): 9–15.

Closa, D., Alemany, M. & Remesar, X. (1992): Effect of food deprivation and refeeding on rat organ temperatures, Arch Int Physiol Biochim Biophys **100**(3): 207–11.

Cohen, P., Levy, J. D., Zhang, Y., Frontini, A., Kolodin, D. P., Svensson, K. J., Lo, J. C., Zeng, X., Ye, L., Khandekar, M. J., Wu, J., Gunawardana, S. C., Banks, A. S., Camporez, J. P., Jurczak, M. J., Kajimura, S., Piston, D. W., Mathis, D., Cinti, S., Shulman, G. I., Seale, P. & Spiegelman, B. M. (2014): Ablation of prdm16 and beige adipose causes metabolic dysfunction and a subcutaneous to visceral fat switch, Cell **156**(1-2): 304–16.

Coniglio, S. J., Lewis, J. D., Lang, C., Burns, T. G., Subhani-Siddique, R., Weintraub, A., Schub, H. & Holden, E. W. (2001): A randomized, double-blind, placebo-controlled trial of single-dose intravenous secretin as treatment for children with autism, J Pediatr **138**(5): 649–55.

Cousin, B., Cinti, S., Morroni, M., Raimbault, S., Ricquier, D., Penicaud, L. & Casteilla, L. (1992): Occurrence of brown adipocytes in rat white adipose tissue: molecular and morphological characterization, J Cell Sci **103 (Pt 4)**: 931–42.

Couvineau, A. & Laburthe, M. (2012): Vpac receptors: structure, molecular pharmacology and interaction with accessory proteins, Br J Pharmacol **166**(1): 42–50.

Cypess, A. M., Lehman, S., Williams, G., Tal, I., Rodman, D., Goldfine, A. B., Kuo, F. C., Palmer, E. L., Tseng, Y. H., Doria, A., Kolodny, G. M. & Kahn, C. R. (2009): Identification and importance of brown adipose tissue in adult humans, N Engl J Med **360**(15): 1509–17.

Cypess, A. M., Weiner, L. S., Roberts-Toler, C., Franquet Elia, E., Kessler, S. H., Kahn, P. A., English, J., Chatman, K., Trauger, S. A., Doria, A. & Kolodny, G. M. (2015): Activation of human brown adipose tissue by a beta3-adrenergic receptor agonist, Cell Metab **21**(1): 33–8.

Di Bella, L., Tarozzi, G., Rossi, M. T. & Scalera, G. (1981): Effect of liver temperature increase on food intake, Physiol Behav **26**(1): 45–51.

Diane, A., Nikolic, N., Rudecki, A. P., King, S. M., Bowie, D. J. & Gray, S. L. (2014): Pacap is essential for the adaptive thermogenic response of brown adipose tissue to cold exposure, J Endocrinol **222**(3): 327–39.

Dicker, A., Zhao, J., Cannon, B. & Nedergaard, J. (1998): Apparent thermogenic effect of injected glucagon is not due to a direct effect on brown fat cells, Am J Physiol **275**(5 Pt 2): R1674–82.

Draviam, E. J., Gomez, G., Hashimoto, T., Miyashita, T., Hill, F. L., Uchida, T., Singh, P., Greeley, G. H., Jr. & Thompson, J. C. (1991): Characterization of secretin release in response to food and intraduodenal administration of fat and hydrochloric acid, Dig Dis Sci **36**(4): 513–9.

Dunn-Geier, J., Ho, H. H., Auersperg, E., Doyle, D., Eaves, L., Matsuba, C., Orrbine, E., Pham, B. & Whiting, S. (2000): Effect of secretin on children with autism: a randomized controlled trial, Dev Med Child Neurol **42**(12): 796–802.

Emery, A. C., Liu, X. H., Xu, W., Eiden, M. V. & Eiden, L. E. (2015): Cyclic adenosine 3',5'-monophosphate elevation and biological signaling through a secretin family gs-coupled g protein-coupled receptor are restricted to a single adenylate cyclase isoform, Mol Pharmacol **87**(6): 928–35.

Fahrenkrug, J., Schaffalitzky de Muckadell, O. B. & Holst, J. J. (1978): Elimination of porcine secretin in pigs, Clin Sci Mol Med **54**(1): 61–8.

Fain, J. N. & Shepherd, R. E. (1975): Free fatty acids as feedback regulators of adenylate cyclase and cyclic 3':5'-amp accumulation in rat fat cells, J Biol Chem **250**(16): 6586–92.

Festuccia, W. T., Blanchard, P. G., Richard, D. & Deshaies, Y. (2010): Basal adrenergic tone is required for maximal stimulation of rat brown adipose tissue ucp1 expression by chronic ppar-gamma activation, Am J Physiol Regul Integr Comp Physiol **299**(1): R159–67.

Flo, G., Vermaut, S., Van Boven, M., Daenens, P., Buyse, J., Decuypere, E., Kuhn, E. & Cokelaere, M. (1998): Comparison of the effects of simmondsin and cholecystokinin on metabolism, brown adipose tissue and the pancreas in food-restricted rats, Horm Metab Res **30**(8): 504–8.

Fremeau, R. T., Jr., Jensen, R. T., Charlton, C. G., Miller, R. L., O'Donohue, T. L. & Moody, T. W. (1983): Secretin: specific binding to rat brain membranes, J Neurosci **3**(8): 1620–5.

Friedman, M. H. & Snape, W. J. (1947): Pancreatic secretion in man in response to administration of secretin and insulin, Fed Proc **6**(1 Pt 2): 107.

Fromme, T. & Klingenspor, M. (2011): Uncoupling protein 1 expression and high-fat diets, Am J Physiol Regul Integr Comp Physiol **300**(1): R1–8.

Gafvelin, G., Jornvall, H. & Mutt, V. (1990): Processing of prosecretin: isolation of a secretin precursor from porcine intestine, Proc Natl Acad Sci U S A **87**(17): 6781–5.

Ganguli, S. C., Park, C. G., Holtmann, M. H., Hadac, E. M., Kenakin, T. P. & Miller, L. J. (1998): Protean effects of a natural peptide agonist of the g protein-coupled secretin receptor demonstrated by receptor mutagenesis, J Pharmacol Exp Ther **286**(2): 593–8.

Garcia-Palmer, F. J., Pericas, J., Matamala, J. C., Puigserver, P., Bonet, M. L., Palou, A. & Gianotti, M. (1997): Diminished response to food deprivation of the rat brown adipose tissue mitochondrial uncoupling system with age, Biochem Mol Biol Int **42**(6): 1151–61.

Gespach, C., Bataille, D., Vauclin, N., Rosselin, G., Moroder, L. & Wunsch, E. (1981): Secretin binding sites coupled with adenylate cyclase in rat fundic membranes, Peptides **2 Suppl 2**: 247–51.

Gether, U. (2000): Uncovering molecular mechanisms involved in activation of g protein-coupled receptors, Endocr Rev **21**(1): 90–113.

Gibbs, J., Young, R. C. & Smith, G. P. (1973): Cholecystokinin decreases food intake in rats, J Comp Physiol Psychol **84**(3): 488–95.

Glick, Z., Teague, R. J. & Bray, G. A. (1981): Brown adipose tissue: thermic response increased by a single low protein, high carbohydrate meal, Science **213**(4512): 1125–7.

Glick, Z., Thomas, D. W. & Mayer, J. (1971): Absence of effect of injections of the intestinal hormones secretin and choecystokinin-pancreozymin upon feeding behavior, Physiol Behav **6**(1): 5–8.

Glick, Z., Uncyk, A., Lupien, J. & Schmidt, L. (1989): Meal associated changes in brown fat thermogenesis and glycogen, Physiol Behav **45**(2): 243–8.

Gnad, T., Scheibler, S., von Kugelgen, I., Scheele, C., Kilic, A., Glode, A., Hoffmann, L. S., Reverte-Salisa, L., Horn, P., Mutlu, S., El-Tayeb, A., Kranz, M., Deuther-Conrad, W., Brust, P., Lidell, M. E., Betz, M. J., Enerback, S., Schrader, J., Yegutkin, G. G., Muller, C. E. & Pfeifer, A. (2014): Adenosine activates brown adipose tissue and recruits beige adipocytes via a2a receptors, Nature **516**(7531): 395–9.

Graham, F. L., Smiley, J., Russell, W. C. & Nairn, R. (1977): Characteristics of a human cell line transformed by dna from human adenovirus type 5, J Gen Virol **36**(1): 59–74.

Grovum, W. L. (1981): Factors affecting the voluntary intake of food by sheep. 3. the effect of intravenous infusions of gastrin, cholecystokinin and secretin on motility of the reticulo-rumen and intake, Br J Nutr **45**(1): 183–201.

Heaton, G. M., Wagenvoord, R. J., Kemp, A., Jr. & Nicholls, D. G. (1978): Brown-adipose-tissue mitochondria: photoaffinity labelling of the regulatory site of energy dissipation, Eur J Biochem **82**(2): 515–21.

Hebebrand, J. & Hinney, A. (2009): Environmental and genetic risk factors in obesity, Child Adolesc Psychiatr Clin N Am **18**(1): 83–94.

Himms-Hagen, J. (1995): Role of brown adipose tissue thermogenesis in control of thermoregulatory feeding in rats: a new hypothesis that links thermostatic and glucostatic hypotheses for control of food intake, Proc Soc Exp Biol Med **208**(2): 159–69.

Himms-Hagen, J., Melnyk, A., Zingaretti, M. C., Ceresi, E., Barbatelli, G. & Cinti, S. (2000): Multilocular fat cells in wat of cl-316243-treated rats derive directly from white adipocytes, Am J Physiol Cell Physiol **279**(3): C670–81.

Holtmann, M. H., Hadac, E. M. & Miller, L. J. (1995): Critical contributions of amino-terminal extracellular domains in agonist binding and activation of secretin and vasoactive intestinal polypeptide receptors. studies of chimeric receptors, J Biol Chem **270**(24): 14394–8.

Hondares, E., Rosell, M., Gonzalez, F. J., Giralt, M., Iglesias, R. & Villarroya, F. (2010): Hepatic fgf21 expression is induced at birth via pparalpha in response to milk intake and contributes to thermogenic activation of neonatal brown fat, Cell Metab **11**(3): 206–12.

Horvath, K., Stefanatos, G., Sokolski, K. N., Wachtel, R., Nabors, L. & Tildon, J. T. (1998): Improved social and language skills after secretin administration in patients with autistic spectrum disorders, J Assoc Acad Minor Phys **9**(1): 9–15.

Hubel, K. A. (1972): Secretin: a long progress note, Gastroenterology **62**(6): 318–41.

Isenberg, J. I., Wallin, B., Johansson, C., Smedfors, B., Mutt, V., Tatemoto, K. & Emas, S. (1984): Secretin, vip, and phi stimulate rat proximal duodenal surface epithelial bicarbonate secretion in vivo, Regul Pept **8**(4): 315–20.

Ishihara, T., Nakamura, S., Kaziro, Y., Takahashi, T., Takahashi, K. & Nagata, S. (1991): Molecular cloning and expression of a cdna encoding the secretin receptor, EMBO J **10**(7): 1635–41.

Jimenez, M., Barbatelli, G., Allevi, R., Cinti, S., Seydoux, J., Giacobino, J. P., Muzzin, P. & Preitner, F. (2003): Beta 3-adrenoceptor knockout in c57bl/6j mice depresses the occurrence of brown adipocytes in white fat, Eur J Biochem **270**(4): 699–705.

Jin, H. O., Lee, K. Y., Chang, T. M., Chey, W. Y. & Dubois, A. (1994): Secretin: a physiological regulator of gastric emptying and acid output in dogs, Am J Physiol **267**(4 Pt 1): G702–8.

Joffe, S. N., Bloom, S. R., Polak, J. M. & Welbourn, R. B. (1975): Proceedings: Release of secretin for s cells of porcine duodenum and jejunum by acid, Gut **16**(5): 398.

Jones, R. S., Geist, R. E. & Hall, A. D. (1971): The choleretic effects of glucagon and secretin in the dog, Gastroenterology **60**(1): 64–8.

Jorpes, J. E. & Mutt, V. (1961): On the biological activity and amino acid composition of secretin, Acta Chemica Scandinavica **15**: 1790–1791.

Jukkola, P. I., Rogers, J. T., Kaspar, B. K., Weeber, E. J. & Nishijima, I. (2011): Secretin deficiency causes impairment in survival of neural progenitor cells in mice, Hum Mol Genet **20**(5): 1000–7.

Kajimura, S. & Saito, M. (2014): A new era in brown adipose tissue biology: molecular control of brown fat development and energy homeostasis, Annu Rev Physiol **76**: 225–49.

Kern, P. A., Finlin, B. S., Zhu, B., Rasouli, N., McGehee, R. E., Jr., Westgate, P. M. & Dupont-Versteegden, E. E. (2014): The effects of temperature and seasons on subcutaneous white adipose tissue in humans: evidence for thermogenic gene induction, J Clin Endocrinol Metab **99**(12): E2772–9.

Kim, M. S., Lee, K. Y. & Chey, W. Y. (1979): Plasma secretin concentrations in fasting and postprandial states in dog, Am J Physiol **236**(5): E539–44.

Kinoshita, K., Ozaki, N., Takagi, Y., Murata, Y., Oshida, Y. & Hayashi, Y. (2014): Glucagon is essential for adaptive thermogenesis in brown adipose tissue, Endocrinology **155**(9): 3484–92.

Klingenspor, M. (2003): Cold-induced recruitment of brown adipose tissue thermogenesis, Exp Physiol **88**(1): 141–8.

Kofod, H. (1986): Secretin n-terminal hexapeptide potentiates insulin release in mouse islets, Regul Pept **15**(3): 229–37.

Kooijman, S., Wang, Y., Parlevliet, E. T., Boon, M. R., Edelschaap, D., Snaterse, G., Pijl, H., Romijn, J. A. & Rensen, P. C. (2015): Central glp-1 receptor signalling accelerates plasma clearance of triacylglycerol and glucose by activating brown adipose tissue in mice, Diabetologia .

Koves, K., Kausz, M., Reser, D. & Horvath, K. (2002): What may be the anatomical basis that secretin can improve the mental functions in autism?, Regul Pept **109**(1-3): 167–72.

Kozak, L. P. (2010): Brown fat and the myth of diet-induced thermogenesis, Cell Metab **11**(4): 263–7.

Kozak, L. P. & Koza, R. A. (2010): The genetics of brown adipose tissue, Prog Mol Biol Transl Sci **94**: 75–123.

Kraegen, E. W., Chisholm, D. J., Young, J. D. & Lazarus, L. (1970): The gastrointestinal stimulus to insulin release. ii. a dual action of secretin, J Clin Invest **49**(3): 524–9.

Lasar, D., Julius, A., Fromme, T. & Klingenspor, M. (2013): Browning attenuates murine white adipose tissue expansion during postnatal development, Biochim Biophys Acta **1831**(5): 960–8.

Lean, M. E., Branch, W. J., James, W. P., Jennings, G. & Ashwell, M. (1983): Measurement of rat brown-adipose-tissue mitochondrial uncoupling protein by radioimmunoassay: increased concentration after cold acclimation, Biosci Rep **3**(1): 61–71.

Lee, P., Smith, S., Linderman, J., Courville, A. B., Brychta, R. J., Dieckmann, W., Werner, C. D., Chen, K. Y. & Celi, F. S. (2014): Temperature-acclimated brown adipose tissue modulates insulin sensitivity in humans, Diabetes **63**(11): 3686–98.

Lee, V. H. Y., Lee, L. T. O., Chu, J. Y. S., Lam, I. P. Y., Siu, F. K. Y., Vaudry, H. & Chow, B. K. C. (2010): An indispensable role of secretin in mediating the osmoregulatory functions of angiotensin ii, Faseb j **24**(12): 5024–32.

Levin, B. E. & Sullivan, A. C. (1984): Regulation of thermogenesis in obesity, Int J Obes **8 Suppl 1**: 159–80.

Li, P., Zhu, Z., Lu, Y. & Granneman, J. G. (2005): Metabolic and cellular plasticity in white adipose tissue ii: role of peroxisome proliferator-activated receptor-alpha, Am J Physiol Endocrinol Metab **289**(4): E617–26.

Li, Y., Bolze, F., Fromme, T. & Klingenspor, M. (2014a): Intrinsic differences in brite adipogenesis of primary adipocytes from two different mouse strains, Biochim Biophys Acta **1841**(9): 1345–52.

Li, Y., Fromme, T., Schweizer, S., Schottl, T. & Klingenspor, M. (2014b): Taking control over intracellular fatty acid levels is essential for the analysis of thermogenic function in cultured primary brown and brite/beige adipocytes, EMBO Rep **15**(10): 1069–76.

Li, Y., Lasar, D., Fromme, T. & Klingenspor, M. (2014c): White, brite, and brown adipocytes: the evolution and function of a heater organ in mammals, Canadian Journal of Zoology **92**(7): 615–626.

Liu, P. S., Lin, Y. W., Burton, F. H. & Wei, L. N. (2015): Injecting engineered anti-inflammatory macrophages therapeutically induces white adipose tissue browning and improves diet-induced insulin resistance, Adipocyte **4**(2): 123–8.

Lockie, S. H., Heppner, K. M., Chaudhary, N., Chabenne, J. R., Morgan, D. A., Veyrat-Durebex, C., Ananthakrishnan, G., Rohner-Jeanrenaud, F., Drucker, D. J., DiMarchi, R., Rahmouni, K., Oldfield, B. J., Tschop, M. H. & Perez-Tilve, D. (2012): Direct control of brown adipose tissue thermogenesis by central nervous system glucagon-like peptide-1 receptor signaling, Diabetes **61**(11): 2753–62.

Lockie, S. H., Stefanidis, A., Oldfield, B. J. & Perez-Tilve, D. (2013): Brown adipose tissue thermogenesis in the resistance to and reversal of obesity: A potential new mechanism contributing to the metabolic benefits of proglucagon-derived peptides, Adipocyte **2**(4): 196–200.

Loncar, D. (1991): Convertible adipose tissue in mice, Cell Tissue Res **266**(1): 149–61.

Lopez, M., Dieguez, C. & Nogueiras, R. (2015): Hypothalamic glp-1: the control of bat thermogenesis and browning of white fat, Adipocyte **4**(2): 141–5.

Lowell, B. B. & Spiegelman, B. M. (2000): Towards a molecular understanding of adaptive thermogenesis, Nature **404**(6778): 652–60.

Lu, Y. & Owyang, C. (1995): Secretin at physiological doses inhibits gastric motility via a vagal afferent pathway, Am J Physiol **268**(6 Pt 1): G1012–6.

Lu, Y. & Owyang, C. (2009): Secretin-induced gastric relaxation is mediated by vasoactive intestinal polypeptide and prostaglandin pathways, Neurogastroenterol Motil **21**(7): 754–e47.

Manabe, T., Tanaka, Y., Yamaki, K., Asano, N., Nonaka, A., Hirano, T., Nishikawa, H. & Tobe, T. (1987): The role of plasma secretin during starvation in dogs, Gastroenterol Jpn **22**(6): 756–8.

Merlin, J., Evans, B. A., Dehvari, N., Sato, M., Bengtsson, T. & Hutchinson, D. S. (2015): Could burning fat start with a brite spark? pharmacological and nutritional ways to promote thermogenesis, Mol Nutr Food Res .

Michel, M. C., Ochodnicky, P. & Summers, R. J. (2010): Tissue functions mediated by beta(3)-adrenoceptors-findings and challenges, Naunyn Schmiedebergs Arch Pharmacol **382**(2): 103–8.

Miegueu, P., Cianflone, K., Richard, D. & St-Pierre, D. H. (2013): Effect of secretin on preadipocyte, differentiating and mature adipocyte functions, Int J Obes (Lond) **37**(3): 366–74.

Miller, L. J., Dong, M., Harikumar, K. G. & Gao, F. (2007): Structural basis of natural ligand binding and activation of the class ii g-protein-coupled secretin receptor, Biochem Soc Trans **35**(Pt 4): 709–12.

Moss, D., Ma, A. & Cameron, D. P. (1985): Cafeteria feeding promotes diet-induced thermogenesis in monosodium glutamate-treated mice, Metabolism **34**(12): 1094–9.

Mund, R. A. & Frishman, W. H. (2013): Brown adipose tissue thermogenesis: beta3-adrenoreceptors as a potential target for the treatment of obesity in humans, Cardiol Rev **21**(6): 265–9.

Mutt, V., Carlquist, M. & Tatemoto, K. (1979): Secretin-like bioactivity in extracts of porcine brain, Life Sci **25**(20): 1703–7.

Mutt, V., Jorpes, J. E. & Magnusson, S. (1970): Structure of porcine secretin. the amino acid sequence, Eur J Biochem **15**(3): 513–9.

Mutt, V., Magnusson, S., Jorpes, J. E. & Dahl, E. (1965): Structure of porcine secretin. i. degradation with trypsin and thrombin. sequence of the tryptic peptides. the c-terminal residue, Biochemistry .

Nedergaard, J., Bengtsson, T. & Cannon, B. (2007): Unexpected evidence for active brown adipose tissue in adult humans, Am J Physiol Endocrinol Metab **293**(2): E444–52.

Nedergaard, J. & Cannon, B. (2010): The changed metabolic world with human brown adipose tissue: therapeutic visions, Cell Metab **11**(4): 268–72.

Neves, S. R., Ram, P. T. & Iyengar, R. (2002): G protein pathways, Science **296**(5573): 1636–9.

Ng, M., Fleming, T., Robinson, M., Thomson, B., Graetz, N., Margono, C., Mullany, E. C., Biryukov, S., Abbafati, C., Abera, S. F., Abraham, J. P., Abu-Rmeileh, N. M., Achoki, T., AlBuhairan, F. S., Alemu, Z. A., Alfonso, R., Ali, M. K., Ali, R., Guzman, N. A., Ammar, W., Anwari, P., Banerjee, A., Barquera, S., Basu, S., Bennett, D. A., Bhutta, Z., Blore, J., Cabral, N., Nonato, I. C., Chang, J. C., Chowdhury, R., Courville, K. J., Criqui, M. H., Cundiff, D. K., Dabhadkar, K. C., Dandona, L., Davis, A., Dayama, A., Dharmaratne, S. D., Ding, E. L., Durrani, A. M., Esteghamati, A., Farzadfar, F., Fay, D. F., Feigin, V. L., Flaxman, A., Forouzanfar, M. H., Goto, A., Green, M. A., Gupta, R., Hafezi-Nejad, N., Hankey, G. J., Harewood, H. C., Havmoeller, R., Hay, S., Hernandez, L., Husseini, A., Idrisov, B. T., Ikeda, N., Islami, F., Jahangir, E., Jassal, S. K., Jee, S. H., Jeffreys, M., Jonas, J. B., Kabagambe, E. K., Khalifa, S. E., Kengne, A. P., Khader, Y. S., Khang, Y. H., Kim, D., Kimokoti, R. W., Kinge, J. M., Kokubo, Y., Kosen, S., Kwan, G., Lai, T., Leinsalu, M., Li, Y., Liang, X., Liu, S., Logroscino, G., Lotufo, P. A., Lu, Y., Ma, J., Mainoo, N. K., Mensah, G. A., Merriman, T. R., Mokdad, A. H., Moschandreas, J., Naghavi, M., Naheed, A., Nand, D., Narayan, K. M., Nelson, E. L., Neuhouser, M. L., Nisar, M. I., Ohkubo, T., Oti, S. O., Pedroza, A. et al. (2014): Global, regional, and national prevalence of overweight and obesity in children and adults during 1980-2013: a systematic analysis for the global burden of disease study 2013, Lancet **384**(9945): 766–81.

Nishijima, I., Yamagata, T., Spencer, C. M., Weeber, E. J., Alekseyenko, O., Sweatt, J. D., Momoi, M. Y., Ito, M., Armstrong, D. L., Nelson, D. L., Paylor, R. & Bradley, A. (2006): Secretin receptor-deficient mice exhibit impaired synaptic plasticity and social behavior, Hum Mol Genet **15**(21): 3241–50.

O'Donohue, T. L., Charlton, C. G., Miller, R. L., Boden, G. & Jacobowitz, D. M. (1981): Identification, characterization, and distribution of secretin immunoreactivity in rat and pig brain, Proc Natl Acad Sci U S A **78**(8): 5221–4.

Ohta, M., Funakoshi, S., Kawasaki, T. & Itoh, N. (1992): Tissue-specific expression of the rat secretin precursor gene, Biochem Biophys Res Commun **183**(2): 390–5.

Okamatsu-Ogura, Y., Fukano, K., Tsubota, A., Uozumi, A., Terao, A., Kimura, K. & Saito, M. (2013): Thermogenic ability of uncoupling protein 1 in beige adipocytes in mice, PLoS One **8**(12): e84229.

Ootsuka, Y., de Menezes, R. C., Zaretsky, D. V., Alimoradian, A., Hunt, J., Stefanidis, A., Oldfield, B. J. & Blessing, W. W. (2009): Brown adipose tissue thermogenesis heats brain and body as part of the brain-coordinated ultradian basic rest-activity cycle, Neuroscience **164**(2): 849–61.

Otsuki, M., Sakamoto, C., Ohki, A., Yuu, H., Maeda, M. & Baba, S. (1981): Pancreatic exocrine secretion and immunoreactive secretin release after intraduodenal instillation of 1-phenyl-1-hydroxy-n-pentane and hcl in rats, Dig Dis Sci **26**(6): 538–44.

Owley, T., Steele, E., Corsello, C., Risi, S., McKaig, K., Lord, C., Leventhal, B. L. & Cook Jr, E. H. (1999): A double-blind, placebo-controlled trial of secretin for the treatment of autistic disorder, MedGenMed S. E2.

Ozguven, S., Ones, T., Yilmaz, Y., Turoglu, H. T. & Imeryuz, N. (2015): The role of active brown adipose tissue in human metabolism, Eur J Nucl Med Mol Imaging .

Peirce, V., Carobbio, S. & Vidal-Puig, A. (2014): The different shades of fat, Nature **510**(7503): 76–83.

Rampone, A. J. & Reynolds, P. J. (1991): Food intake regulation by diet-induced thermogenesis, Med Hypotheses **34**(1): 7–12.

Renold, A. E., Marble, A. & Fawcett, D. W. (1950): Action of insulin on deposition of glycogen and storage of fat in adipose tissue, Endocrinology **46**(1): 55–66.

Rhodes, R. A., Tai, H. H. & Chey, W. Y. (1976): Observations of plasma secretin levels by radioimmunoassay in response to duodenal acidification and to a meat meal in humans, Am J Dig Dis **21**(10): 873–9.

Robberecht, P., De Neef, P., Waelbroeck, M., Camus, J. C., Scemama, J. L., Fourmy, D., Pradayrol, L., Vaysse, N. & Christophe, J. (1988): Secretin receptors in human pancreatic membranes, Pancreas **3**(5): 529–35.

Rothwell, N. J. & Stock, M. J. (1979): A role for brown adipose tissue in diet-induced thermogenesis, Nature **281**(5726): 31–5.

Rothwell, N. J. & Stock, M. J. (1983): Luxuskonsumption, diet-induced thermogenesis and brown fat: the case in favour, Clin Sci (Lond) **64**(1): 19–23.

Saito, M. (2013): Brown adipose tissue as a therapeutic target for human obesity, Obes Res Clin Pract **7**(6): e432–8.

Saito, M. (2014): Human brown adipose tissue: regulation and anti-obesity potential, Endocr J **61**(5): 409–16.

Saito, M., Okamatsu-Ogura, Y., Matsushita, M., Watanabe, K., Yoneshiro, T., Nio-Kobayashi, J., Iwanaga, T., Miyagawa, M., Kameya, T., Nakada, K., Kawai, Y. & Tsujisaki, M. (2009): High incidence of metabolically active brown adipose tissue in healthy adult humans: effects of cold exposure and adiposity, Diabetes **58**(7): 1526–31.

Sanchez-Gurmaches, J., Hung, C. M., Sparks, C. A., Tang, Y., Li, H. & Guertin, D. A. (2012): Pten loss in the myf5 lineage redistributes body fat and reveals subsets of white adipocytes that arise from myf5 precursors, Cell Metab **16**(3): 348–62.

Sanders, M. J., Amirian, D. A., Ayalon, A. & Soll, A. H. (1983): Regulation of pepsinogen release from canine chief cells in primary monolayer culture, Am J Physiol **245**(5 Pt 1): G641–6.

Sandler, A. D., Sutton, K. A., DeWeese, J., Girardi, M. A., Sheppard, V. & Bodfish, J. W. (1999): Lack of benefit of a single dose of synthetic human secretin in the treatment of autism and pervasive developmental disorder, N Engl J Med **341**(24): 1801–6.

Schaffalitzky de Muckadell, O. B. (2001): Secretin in plasma: ups and downs, Scand J Clin Lab Invest Suppl **234**: 105–8.

Scherer, P. E. (2006): Adipose tissue: from lipid storage compartment to endocrine organ, Diabetes **55**(6): 1537–45.

Schlapschy, M., Binder, U., Borger, C., Theobald, I., Wachinger, K., Kisling, S., Haller, D. & Skerra, A. (2013): Pasylation: a biological alternative to pegylation for extending the plasma half-life of pharmaceutically active proteins, Protein Eng Des Sel **26**(8): 489–501.

Seale, P., Bjork, B., Yang, W., Kajimura, S., Chin, S., Kuang, S., Scime, A., Devarakonda, S., Conroe, H. M., Erdjument-Bromage, H., Tempst, P., Rudnicki, M. A., Beier, D. R. & Spiegelman, B. M. (2008): Prdm16 controls a brown fat/skeletal muscle switch, Nature **454**(7207): 961–7.

Seale, P., Conroe, H. M., Estall, J., Kajimura, S., Frontini, A., Ishibashi, J., Cohen, P., Cinti, S. & Spiegelman, B. M. (2011): Prdm16 determines the thermogenic program of subcutaneous white adipose tissue in mice, J Clin Invest **121**(1): 96–105.

Segre, G. V. & Goldring, S. R. (1993): Receptors for secretin, calcitonin, parathyroid hormone (pth)/pth-related peptide, vasoactive intestinal peptide, glucagonlike peptide 1, growth hormone-releasing hormone, and glucagon belong to a newly discovered g-protein-linked receptor family, Trends Endocrinol Metab **4**(10): 309–14.

Sekar, R. & Chow, B. K. (2013): Metabolic effects of secretin, Gen Comp Endocrinol **181**: 18–24.

Sekar, R. & Chow, B. K. (2014a): Lipolytic actions of secretin in mouse adipocytes, J Lipid Res **55**(2): 190–200.

Sekar, R. & Chow, B. K. (2014b): Secretin receptor-knockout mice are resistant to high-fat diet-induced obesity and exhibit impaired intestinal lipid absorption, FASEB J **28**(8): 3494–505.

Sherwood, N. M., Krueckl, S. L. & McRory, J. E. (2000): The origin and function of the pituitary adenylate cyclase-activating polypeptide (pacap)/glucagon superfamily, Endocr Rev **21**(6): 619–70.

Shetzline, M. A., Premont, R. T., Walker, J. K., Vigna, S. R. & Caron, M. G. (1998): A role for receptor kinases in the regulation of class ii g protein-coupled receptors. phosphorylation and desensitization of the secretin receptor, J Biol Chem **273**(12): 6756–62.

Shima, K., Kurokawa, M., Sawazaki, N., Tanaka, R. & Kumahara, Y. (1978): Effect of secretin on plasma insulin and glucagon in man, Endocrinol Jpn **25**(5): 461–5.

Shiratori, K., Watanabe, S. & Takeuchi, T. (1989): Effect of fatty acid on secretin release and cholinergic dependence of pancreatic secretion in rats, Pancreas **4**(4): 452–8.

Sidossis, L. & Kajimura, S. (2015): Brown and beige fat in humans: thermogenic adipocytes that control energy and glucose homeostasis, J Clin Invest **125**(2): 478–86.

Siu, F. K., Lam, I. P., Chu, J. Y. & Chow, B. K. (2006): Signaling mechanisms of secretin receptor, Regul Pept **137**(1-2): 95–104.

Smith, F. J. & Campfield, L. A. (1993): Meal initiation occurs after experimental induction of transient declines in blood glucose, Am J Physiol **265**(6 Pt 2): R1423–9.

Smith, R.E. (1961): Thermogenic activity of the hibernating gland in the cold-acclimated rat, Physiologist **4**: 113.

Steiner, T. S., Mangel, A. W., McVey, D. C. & Vigna, S. R. (1993): Secretin receptors mediating rat forestomach relaxation, Am J Physiol **264**(5 Pt 1): G863–7.

Stock, M. J. & Rothwell, N. J. (1986): The role of brown fat in diet-induced thermogenesis, Int J Vitam Nutr Res **56**(2): 205–10.

Stout, R. W., Henry, R. W. & Buchanan, K. D. (1976): Triglyceride metabolism in acute starvation: the role of secretin and glucagon, Eur J Clin Invest **6**(2): 179–85.

Stout, S. A., Espel, E. V., Sandman, C. A., Glynn, L. M. & Davis, E. P. (2015): Fetal programming of children's obesity risk, Psychoneuroendocrinology **53**: 29–39.

Straus, E., Greenstein, A. J. & Yalow, R. S. (1975): Effect of secretin on release of heterogeneous forms of gastrin, Gut **16**(12): 999–1005.

Tai, T. A., Jennermann, C., Brown, K. K., Oliver, B. B., MacGinnitie, M. A., Wilkison, W. O., Brown, H. R., Lehmann, J. M., Kliewer, S. A., Morris, D. C. & Graves, R. A. (1996): Activation of the nuclear receptor peroxisome proliferator-activated receptor gamma promotes brown adipocyte differentiation, J Biol Chem **271**(47): 29909–14.

Tay, J., Goulet, M., Rusche, J. & Boismenu, R. (2004): Age-related and regional differences in secretin and secretin receptor mrna levels in the rat brain, Neurosci Lett **366**(2): 176–81.

Trimble, E. R., Bruzzone, R., Biden, T. J. & Farese, R. V. (1986): Secretin induces rapid increases in inositol trisphosphate, cytosolic ca2+ and diacylglycerol as well as cyclic amp in rat pancreatic acini, Biochem J **239**(2): 257–61.

Trimble, E. R., Bruzzone, R., Biden, T. J., Meehan, C. J., Andreu, D. & Merrifield, R. B. (1987): Secretin stimulates cyclic amp and inositol trisphosphate production in rat pancreatic acinar tissue by two fully independent mechanisms, Proc Natl Acad Sci U S A **84**(10): 3146–50.

Ulrich, C. D., 2nd, Holtmann, M. & Miller, L. J. (1998): Secretin and vasoactive intestinal peptide receptors: members of a unique family of g protein-coupled receptors, Gastroenterology **114**(2): 382–97.

Usellini, L., Capella, C., Frigerio, B., Rindi, G. & Solcia, E. (1984): Ultrastructural localization of secretin in endocrine cells of the dog duodenum by the immunogold technique. comparison with ultrastructurally characterized s cells of various mammals, Histochemistry **80**(5): 435–41.

Usellini, L., Finzi, G., Riva, C., Capella, C., Mochizuki, T., Yanaihara, C., Yanaihara, N. & Solcia, E. (1990): Ultrastructural identification of human secretin cells by the immunogold technique. their costorage of chromogranin a and serotonin, Histochemistry **94**(2): 113–20.

van Dam, A. D., Nahon, K. J., Kooijman, S., van den Berg, S. M., Kanhai, A. A., Kikuchi, T., Heemskerk, M. M., van Harmelen, V., Lombes, M., van den Hoek, A. M., de Winther, M. P., Lutgens, E., Guigas, B., Rensen, P. C. & Boon, M. R. (2015): Salsalate activates brown adipose tissue in mice, Diabetes **64**(5): 1544–54.

van den Beukel, J. C., Grefhorst, A., Hoogduijn, M. J., Steenbergen, J., Mastroberardino, P. G., Dor, F. J. & Themmen, A. P. (2015): Women have more potential to induce browning of perirenal adipose tissue than men, Obesity (Silver Spring) **23**(8): 1671–9.

van Marken Lichtenbelt, W. D., Vanhommerig, J. W., Smulders, N. M., Drossaerts, J. M., Kemerink, G. J., Bouvy, N. D., Schrauwen, P. & Teule, G. J. (2009): Cold-activated brown adipose tissue in healthy men, N Engl J Med **360**(15): 1500–8.

Vilardaga, J. P., De Neef, P., Di Paolo, E., Bollen, A., Waelbroeck, M. & Robberecht, P. (1995): Properties of chimeric secretin and vip receptor proteins indicate the importance of the n-terminal domain for ligand discrimination, Biochem Biophys Res Commun **211**(3): 885–91.

Vilardaga, J. P., di Paolo, E., de Neef, P., Waelbroeck, M., Bollen, A. & Robberecht, P. (1996): Lysine 173 residue within the first exoloop of rat secretin receptor is involved in carboxylate moiety recognition of asp 3 in secretin, Biochem Biophys Res Commun **218**(3): 842–6.

Virtanen, K. A., Lidell, M. E., Orava, J., Heglind, M., Westergren, R., Niemi, T., Taittonen, M., Laine, J., Savisto, N. J., Enerback, S. & Nuutila, P. (2009): Functional brown adipose tissue in healthy adults, N Engl J Med **360**(15): 1518–25.

Vitali, A., Murano, I., Zingaretti, M. C., Frontini, A., Ricquier, D. & Cinti, S. (2012): The adipose organ of obesity-prone c57bl/6j mice is composed of mixed white and brown adipocytes, J Lipid Res **53**(4): 619–29.

von Praun, C., Burkert, M., Gessner, M. & Klingenspor, M. (2001): Tissue-specific expression and cold-induced mrna levels of uncoupling proteins in the djungarian hamster, Physiol Biochem Zool **74**(2): 203–11.

Vosselman, M. J., Brans, B., van der Lans, A. A., Wierts, R., van Baak, M. A., Mottaghy, F. M., Schrauwen, P. & van Marken Lichtenbelt, W. D. (2013): Brown adipose tissue activity after a high-calorie meal in humans, Am J Clin Nutr **98**(1): 57–64.

Vosselman, M. J., van der Lans, A. A., Brans, B., Wierts, R., van Baak, M. A., Schrauwen, P. & van Marken Lichtenbelt, W. D. (2012): Systemic beta-adrenergic stimulation of thermogenesis is not accompanied by brown adipose tissue activity in humans, Diabetes **61**(12): 3106–13.

Walton, K. L. (2009): Teaching the role of secretin in the regulation of gastric acid secretion using a classic paper by johnson and grossman, Adv Physiol Educ **33**(3): 165–8.

Wang, T. Y., Liu, C., Wang, A. & Sun, Q. (2015): Intermittent cold exposure improves glucose homeostasis associated with brown and white adipose tissues in mice, Life Sci .

Weyer, C., Gautier, J. F. & Danforth, E., Jr. (1999): Development of beta 3-adrenoceptor agonists for the treatment of obesity and diabetes–an update, Diabetes Metab **25**(1): 11–21.

Whitmore, T. E., Holloway, J. L., Lofton-Day, C. E., Maurer, M. F., Chen, L., Quinton, T. J., Vincent, J. B., Scherer, S. W. & Lok, S. (2000): Human secretin (sct): gene structure, chromosome location, and distribution of mrna, Cytogenet Cell Genet **90**(1-2): 47–52.

Wu, J., Bostrom, P., Sparks, L. M., Ye, L., Choi, J. H., Giang, A. H., Khandekar, M., Virtanen, K. A., Nuutila, P., Schaart, G., Huang, K., Tu, H., van Marken Lichtenbelt, W. D., Hoeks, J., Enerback, S., Schrauwen, P. & Spiegelman, B. M. (2012): Beige adipocytes are a distinct type of thermogenic fat cell in mouse and human, Cell **150**(2): 366–76.

Yamagata, T., Urano, H., Weeber, E. J., Nelson, D. L. & Nishijima, I. (2008): Impaired hippocampal synaptic function in secretin deficient mice, Neuroscience **154**(4): 1417–22.

Yoneshiro, T., Aita, S., Matsushita, M., Kayahara, T., Kameya, T., Kawai, Y., Iwanaga, T. & Saito, M. (2013): Recruited brown adipose tissue as an antiobesity agent in humans, J Clin Invest **123**(8): 3404–8.

Young, P., Arch, J. R. & Ashwell, M. (1984): Brown adipose tissue in the parametrial fat pad of the mouse, FEBS Lett **167**(1): 10–4.

Yung, W. H., Leung, P. S., Ng, S. S., Zhang, J., Chan, S. C. & Chow, B. K. (2001): Secretin facilitates gaba transmission in the cerebellum, J Neurosci **21**(18): 7063–8.

Zhang, L., Chung, S. K. & Chow, B. K. (2014): The knockout of secretin in cerebellar purkinje cells impairs mouse motor coordination and motor learning, Neuropsychopharmacology **39**(6): 1460–8.

Zhang, Y., Proenca, R., Maffei, M., Barone, M., Leopold, L. & Friedman, J. M. (1994): Positional cloning of the mouse obese gene and its human homologue, Nature **372**(6505): 425–32.

Supplement

BIO-GPS data - expression of *sctr* in murine tissues

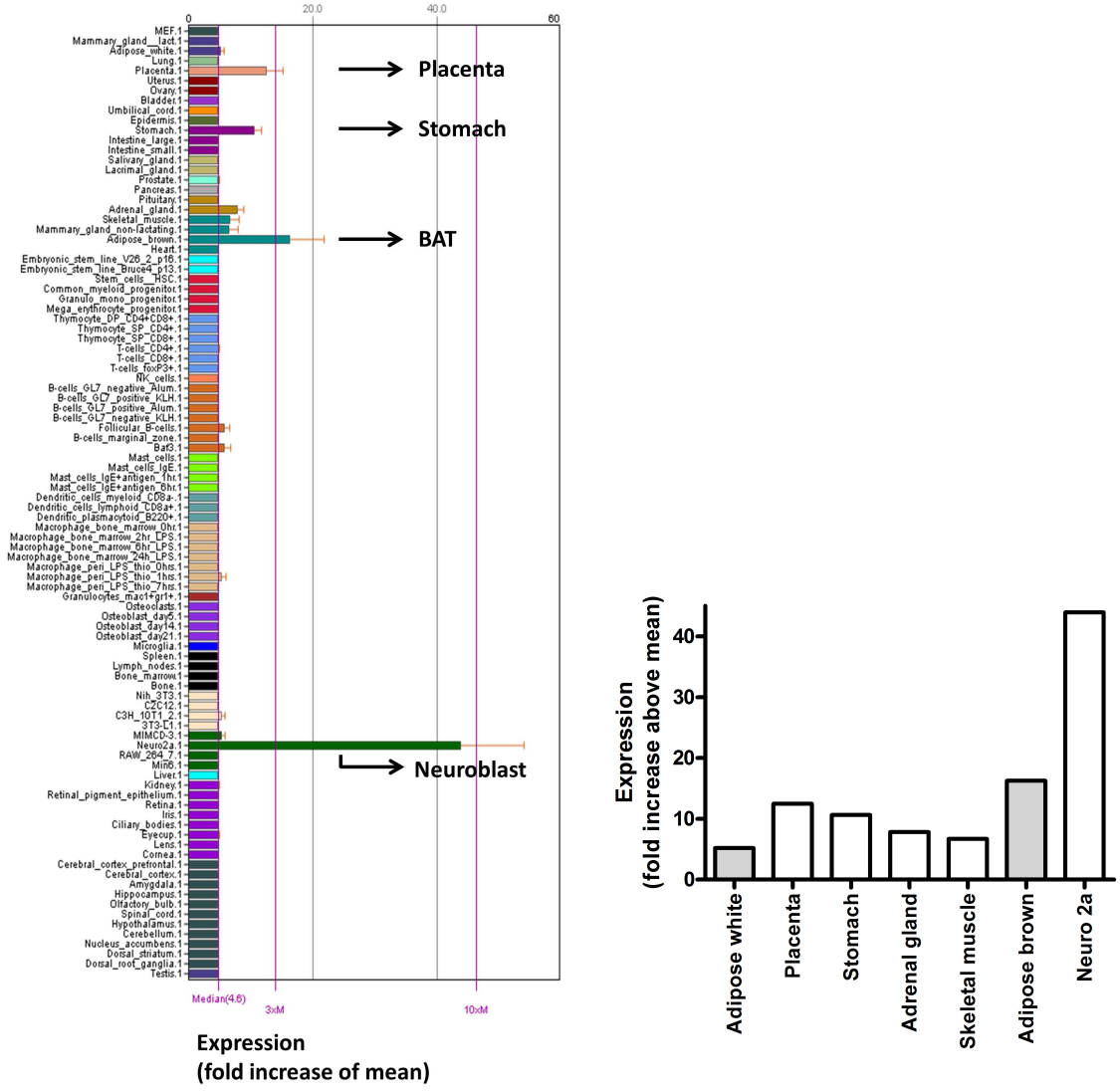

Fig. 31: **Supplement: BIO-GPS data for *sctr* in murine tissues.**
In (A) the orginial data set from biogps.org is presented. In (B) values for certain tissues were selected for an overview. Data can be found in: biogps.org/#goto=genereport&id=319229

Respiratory measurements

Acute effect of SCT on oxygen consumption in WT mice

Calorimetry determination for basal metabolic respiration (BMR) was performed in advance to the measurement at 30 °C for 3 hours.

Table 6.1: Values for body weight (BW) and basal metabolic measures for RER and HP were measured at 30 °C

	PBS (N=7)	SCT (N=7)
BW (g)	25.1 ± 0.6	25.0 ± 1.7
RER	0.80 ± 0.04	0.80 ± 0.04
HP (mW)	208.0 ± 18.8	207.8 ± 17.5

The mean for HP in the injection groups in calorimetry measurements was shown in Fig. 17, A. The curves for all mice individually are presented here.

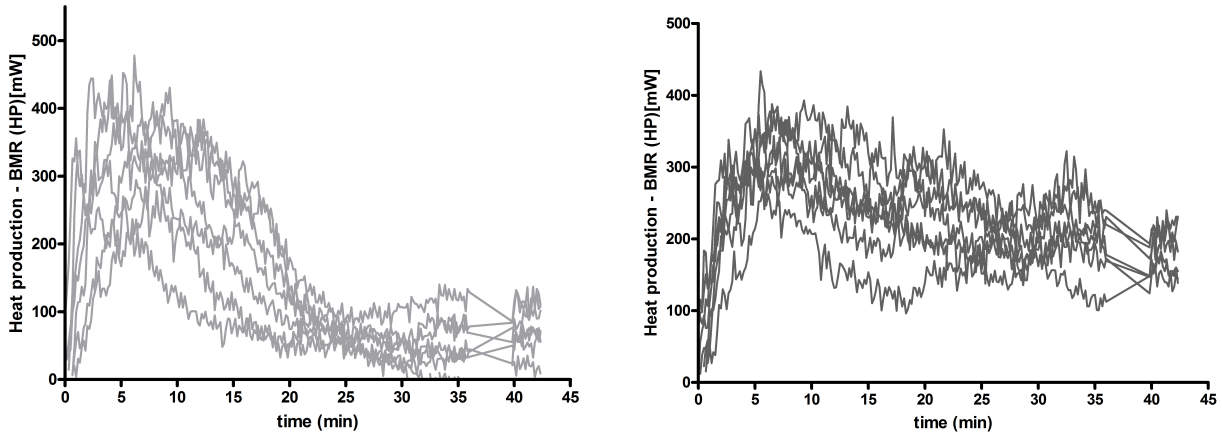

(a) PBS Injection

(b) SCT Injection

Fig. 32: **Supplement: Single values for SCT effects on metabolical activation in mice**
Mice received 0.5 mg/kg SCT solved in PBS or PBS via i.p. injection. Measurement was performed at 27 °C. Single curves of HP for all mice individually are presented (injected with PBS (left) and SCT (right)). The basal HP measured at 30 °C was subtracted for all mice individually for the graph.

Acute effect of SCT on oxygen consumption in cold-adapted mice

The mean for HP for the injection groups in calorimetry measurements was shown in Fig. 20, A. The curves for all mice individually are presented here.

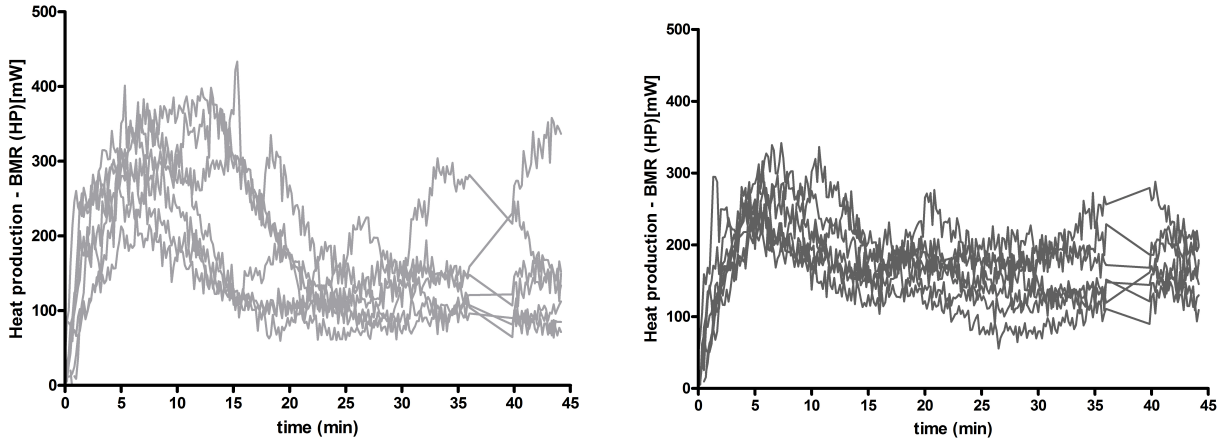

(a) PBS Injection (b) SCT Injection

Fig. 33: **Supplement: Single values for SCT effects in cold-adapted mice**
Mice were adapted to an ambient temperature of 4 °C for 4 days and received for measurement 0.5 mg/kg SCT solved in PBS or PBS via i.p. injection. Measurement was performed at 27 °C. Single curves of HP for all mice individually are presented (injected with PBS (left) and SCT (right)). The basal HP measured at 30 °C was subtracted for all mice individually for the graph.

Acute effect of SCT on respiration in UCP1 KO mice

The results for basal metabolic measurements were shown in Tab. 5.1. Statistical analysis was performed using two-way ANOVA. Results are listed here.

Table 6.2: Statistical analysis (two-way ANOVA) for basal metabolic measurement and body weight in UCP1 KO and WT mice

	Treatment (PBS or SCT)	Genotype (KO or WT)	Treatment x Genotype
BW	p=0.948	p=0.675	p=0.851
RER	p=0.891	p=0.066	p=0.295
HP	p=0.489	p=0.074	P=0.782

The mean for HP for the injection groups in calorimetry measurements was shown in Fig. 18, A and B. The curves for all mice individually are presented here.

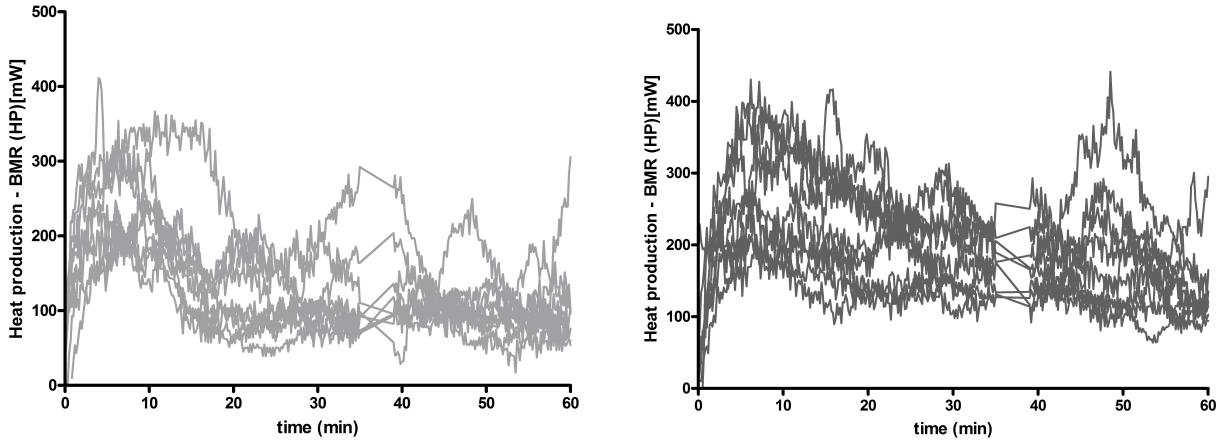

(a) WT (PBS Injection)

(b) WT (SCT Injection)

Fig. 34: **Supplement: Single values for SCT effects in UCP1 WT mice**
Mice were i.p. injected with 0.5 mg/kg SCT solved in PBS or PBS. Measurement was performed at 27 °C. Single curves of HP for all mice individually are presented (injected with PBS (left) and SCT (right)). The basal HP measured at 30 °C was subtracted for all mice individually for the graph.

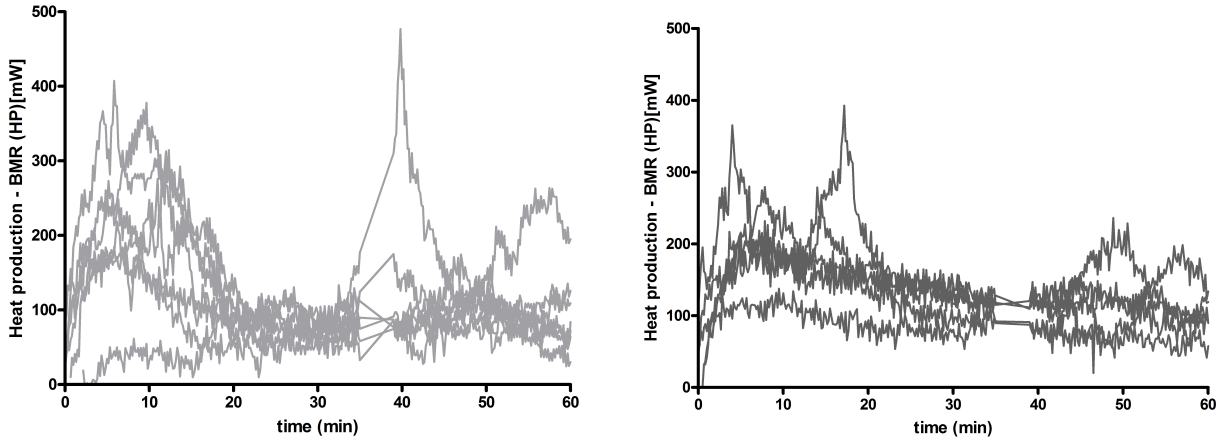

(a) KO (PBS Injection)

(b) KO (SCT Injection)

Fig. 35: **Supplement: Single values for SCT effects in UCP1 KO mice**
Mice were i.p. injected with 0.5 mg/kg SCT solved in PBS or PBS. Measurement was performed at 27 °C. Single curves of HP for all mice individually are presented (injected with PBS (left) and SCT (right)). The basal HP measured at 30 °C was subtracted for all mice individually for the graph.

Most UCP1 WT and KO mice were injected for the measurement in an cross-over design. They received in one run SCT or PBS and in the second run the other substance. In Fig. 36 the AUC of HP for both runs in one individual are compared.

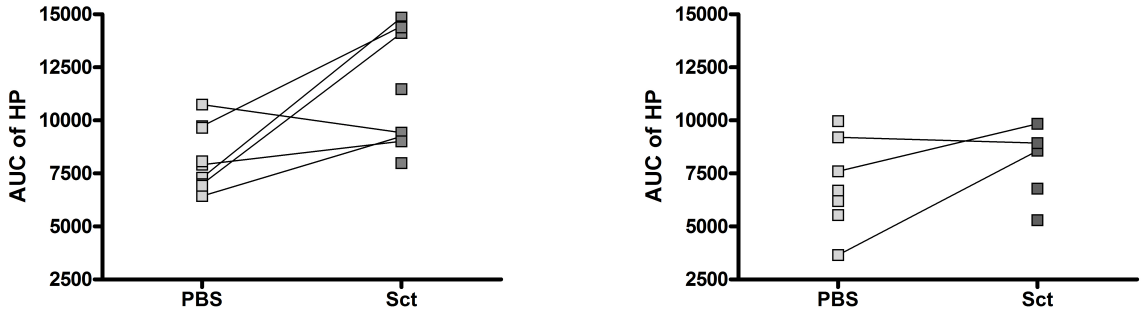

(a) WT (b) KO

Fig. 36: **Supplement: Cross-over design for respirometry measurement in UCP1 KO mice**
The AUC of HP for the calorimetry measurement of UCP1 WT (A) and KO (B) mice after SCT or PBS injeciton is presented for every single mouse as a dot. Repeated measurement of one individual mouse with both compounds is indicated by lines.

Acute effect of SCT on oxygen consumption in HFD fed mice

The results for basal metabolic measurements were presented in Tab. 5.3. Statistical analysis was performed using two-way ANOVA. Results are listed here. Statistical significance is indicated with * for $p<0.05$ and with ** for $p<0.01$.

Table 6.3: Statistical analysis (two-way-ANOVA) for basal metabolic measurement and body weight after four days of HFD

	Treatment (PBS or SCT)	Diet (HFD or CD)	Treatment x Diet
BW	p=0.395	p=0.109	p=0.804
RER	p=0.021 *	p=0.035 *	p=0.114
HP	p=0.247	p=0.013 *	P=0.868

Table 6.4: Statistical analysis (two-way-ANOVA) for basal metabolic measurement and body weight after eight days of HFD

	Treatment (PBS or SCT)	Diet (HFD or CD)	Treatment x Diet
BW	p=0.355	p=0.048 *	p=0.882
RER	p=0.138 *	p=0.003 **	p=0.363
HP	p=0.087	p=0.032 *	P=0.566

The mean for heat production for the injection groups in calorimetry measurements was shown in Fig. 22. The curves for all mice individually are presented here.

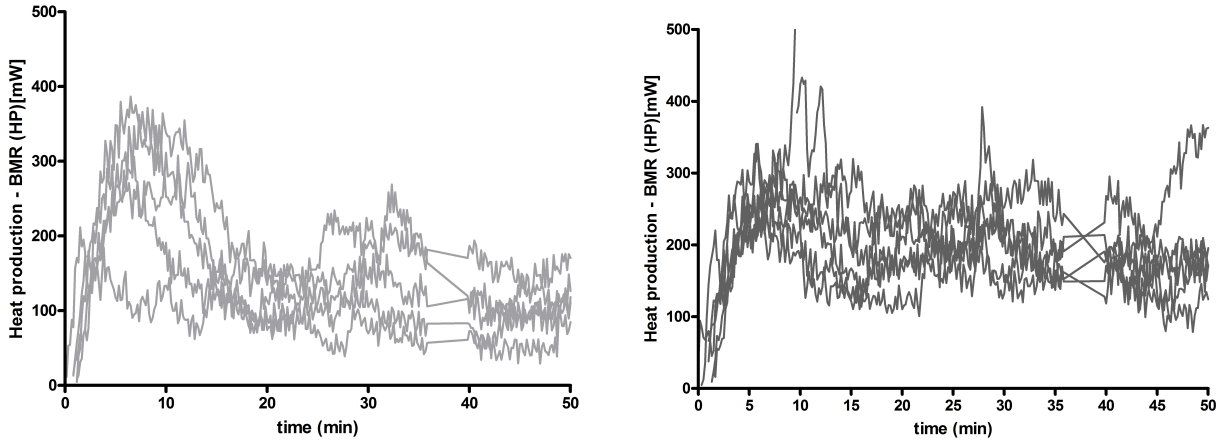

(a) HFD (PBS Injection)

(b) HFD (SCT Injection)

Fig. 37: **Supplement: Single values for SCT effects in HFD fed mice**
Mice were i.p. injected with 0.5 mg/kg SCT solved in PBS or PBS. Measurement was performed at 27 °C. Single curves of HP for all mice individually are presented (injected with PBS (left) and SCT (right)). The basal HP measured at 30 °C was subtracted for all mice individually for the graph.

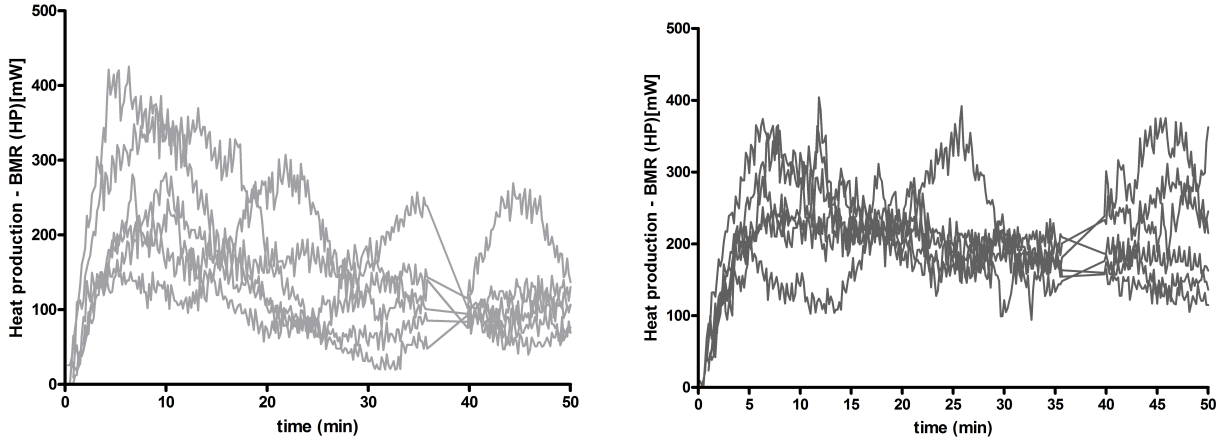

(a) CD (PBS Injection)

(b) CD (SCT Injection)

Fig. 38: **Supplement: Single values for SCT effects in CD fed mice**
Mice were i.p. injected with 0.5 mg/kg SCT solved in PBS or PBS. Measurement was performed at 27 °C. Single curves of HP for all mice individually are presented (injected with PBS (left) and SCT (right)). The basal HP measured at 30 °C was subtracted for all mice individually for the graph.

Acknowledgements

Ich möchte mich zu guter Letzt bei allen bedanken, die durch ihre wissenschaftliche oder moralische Unterstützung dazu beigetragen haben, dass diese Arbeit erstellt werden konnte.

Mein erster Dank gilt Martin für die Bereitstellung des Themas im Rahmen des GRK1482, den unermüdlichen wissenschaftlichen Input, sowie für den Mut mein erstes, aussichtsloses Promotionsthema trotz fortgeschrittener Zeit aufzugeben.

Ebenso möchte ich allen Verantwortlichen und Organisatoren des GRK1482, wie Herrn Haller, Herrn Hauner, Dorothea und natürlich meinem Zweitprüfer Professor Schemann danken. Das Graduiertenkolleg hat für mich eine wunderbare Möglichkeit dargestellt, über den Tellerrand am eigenen Lehrstuhl hinauszusehen und Doktoranden und Themen in einem weiteren Feld kennen zu lernen.

Ich möchte mich bei allen Kollegen am eigenen Lehrstuhl bedanken. Bei Florian, Yongguo, Tobias und Monja für die wissenschaftlichen Ideen und Ratschläge, bei Sabine, Anika, Philipp, Florian, Yongguo und Sabine für ihre Hilfe im Labor, bei Nadine, Florian und Monja für ihre Unterstützung im Tierhaus und bei Sabine, Caroline, Kristina und Florian für ihre wunderbare Freundschaft, Ablenkung und moralischen Aufbauarbeiten. Und bei allen anderen natürlich zudem für die gute Gesellschaft!
Für die gute Laune, unkomplizierte Soforthilfen und Süßigkeiten in unserem Haus, danke ich Jule, Sebastian, Vicky, Bea und Sören. Und natürlich dem gesamten GRK der zweiten Generation mitsamt unseren Assoziierten für Feuerzangebowle auf dem Tollwood und für das Gefühl nicht alleine zu sein mit den Problemen, die eine Promotion mit sich bringt.

Ich danke Herrn Professor Skerra, Volker und Andreas für die Kooperation bei diversen PASylierungen.

Ich danke meinen großartigen Eltern für die jahrzehntelange, bedingungslose Unterstützung bei jeder Entscheidung. Und natürlich danke ich Euch für die zwei besten Brüder, die ich mir jemals hätte wünschen können. Ohne Euch alle, wäre das sicher nicht möglich gewesen.

Vielen lieben Dank an Manu und Cosimo, sowie Gisela, Freya, Kaddl, Inga, Hendrik und Helene für das wunderbare Gefühl, wenn ich nach Hause komme. Für ihre unerschütterliche Freundschaft möchte ich zudem Simona, Steffi, Stephanie, Hjördis, Volker und Anne danken. Ich weiß, dass ich auf euch immer zählen kann!

Ganz besonders dankbar bin ich Florian und Sören für ihre geduldige Hilfe bei den Korrekturen dieses Werkes.

Mein letzter und großer Dank gilt Andreas.